PRODRUG GENE THERAPY VECTORS IN COMBINATION THERAPIES

A THESIS

submitted by

P. GOPINATH

for the award of the degree

of

DOCTOR OF PHILOSOPHY

DEPARTMENT OF BIOTECHNOLOGY

INDIAN INSTITUTE OF TECHNOLOGY GUWAHATI

FEBRUARY 2008

PRODRUG GENE THERAPY VECTORS IN COMBINATION THERAPIES

A THESIS

submitted by

P. GOPINATH

for the award of the degree

of

DOCTOR OF PHILOSOPHY

DEPARTMENT OF BIOTECHNOLOGY

INDIAN INSTITUTE OF TECHNOLOGY GUWAHATI

FEBRUARY 2008

TH-0560_03610605

Dedicated

to my Beloved Parents

TH-0560_03610605

INDIAN INSTITUTE OF TECHNOLOGY GUWAHATI

Department of Biotechnology

STATEMENT

I do hereby declare that the matter embodied in this thesis is the result of investigations carried out by me in the Department of Biotechnology, Indian Institute of Technology Guwahati, India, under the guidance of Dr. Siddhartha Sankar Ghosh.

In keeping with the general practice of reporting scientific observations, due acknowledgements have been made wherever the work described is based on the findings of other investigators.

February, 2008. P.Gopinath

TH-0560_03610605

INDIAN INSTITUTE OF TECHNOLOGY GUWAHATI

Department of Biotechnology

CERTIFICATE

It is certified that the work described in this thesis, entitled "*Prodrug gene therapy vectors in combination therapies*", done by Mr. P.Gopinath for the award of degree of Doctor of Philosophy is an authentic record of the results obtained from the research work carried out under my supervision in the Department of Biotechnology, Indian Institute of Technology Guwahati, India, and this work has not been submitted elsewhere for a degree.

February, 2008.

Dr. Siddhartha Sankar Ghosh
Associate Professor
(Thesis Supervisor)

TH-0560_03610605

ACKNOWLEDGEMENTS

It is with my deepest sense of appreciation that I express my foremost acknowledgement to my research advisor, Dr. Siddhartha Sankar Ghosh for his continuous care, support and encouragement throughout my research work. I am obliged for the ample freedom he allowed me in conducting my work.

I am thankful to the doctoral committee members of my thesis, Prof. A.T. Khan, Dr. A. Ramesh and Dr. L. Sahoo for their constructive criticism and precious suggestions. I owe my gratitude to the Heads of the Department of Biotechnology, Dr. R. Swaminathan and Dr. P. Goswami for providing me the necessary facilities in their respective tenures.

I reserve this paragraph for Prof. Arun Chattopadhayay. I am not only happy but also honored to work with a person like him. With his insightful criticism, comments and suggestions he guided my initiation and progress in the fascinating world of Nanotechnology. Any sort of appreciation or acknowledgement will only demean his deeds towards my thesis work.

I have had the pleasure and privilege of interacting with Dr. Biplab Bose, who apart from being a doctoral committee member, helped me in DNA laddering and mammalian cell cloning experiments.

My research life in Cell and Molecular biology lab has been an association with numerous students and scholars who not only brought about the right milieu but also contributed to my personal growth and enjoyment of this period of my life. It is unfortunate that I cannot mention all of them without risking serious omission. My sincere thanks to our Department Technical Assistants (Mr. Sharan, Mr. Nurul, Mrs. Anita, Ms. Prathana and Mrs. Rashmi) and Central Instrumental Facility,

Scientific Assistants (Mr. Chandan and Mr. Senapathi). I also thank the other staff members Mrs. Bandana and Mr. Krishna of Biotechnology Department.

I cherish my close association with my friends, labmates and colleagues Saravanan, Atul, Satish, Sonit, Aadal, Vijay Kumar Ravi, Shiva, Pallab, Rama, Monash, Muragadoss, Theophilus, Ashok and other friendly faces always abound in my memories.

I take this opportunity to express my love and gratitude to my loving parents, brother and sister for being everything to me all through my career. I would express my humble indebt thanks to all my friends for their suggestions, constant encouragement and moral support throughout my PhD work.

P.Gopinath

February 2008

TH-0560_03610605

ABSTRACT

Prodrug gene therapy, commonly known as suicide gene therapy, provides a selective approach to eradicate tumor cells. Development of efficient suicide gene therapy vectors to improve the therapeutic efficacy is the main theme of this thesis.

Mammalian expression vectors with suicide genes namely; Cytosine Deaminase (CD), Uracil Phosphoribosyl Transferase (UPRT) and CD-UPRT were constructed and their therapeutic efficacies were studied *in vitro*. In the present study, a simple and efficient electroporation technique was used for gene transfer and the Green Fluorescent Protein (GFP) reporter gene in the non-viral plasmid was used to evaluate the gene transfection efficiency. The GFP expression was also used as a noninvasive probe to monitor the therapeutic effect of suicide gene. The transfected cells were treated with the respective prodrug or drug and the therapeutic effect was analyzed by the cell viability and cytotoxicity assay. The IC_{50} value (the concentration of prodrug or drug required to inhibit cell growth by 50% as compared to the control) was estimated.

The therapeutic effect was enhanced with the synergistic application of conventional anticancer compound curcumin and non-conventional compound silver nanoparticles (Ag NPs). The advantages of such combinatorial therapy are, the individual drug could be used below its IC_{50} value, the development of resistance to a particular drug by cancer cells could be reduced, and the individual drug could increase the therapeutic effect by following the same or different molecular mechanism to induce the cell death. Thus, combinatorial therapy attracts much attention for cancer treatment. An important issue, addressed in this study, concerns the cytotoxicity associated with the Ag NPs. The present study explored the molecular

mechanism of Ag NPs induced cell death and laid a new platform that Ag NPs can be used as a new chemosensitization technique.

The complete success of suicide gene therapy depends on its bystander effect, the ability of transfected cells to kill the untransfected neighboring cells in the tumor environment. The bystander effect of CD-UPRT was evidenced by mixed cell culture experiment, where a stable cell line which expressed CD-UPRT was added to parental cell line, which did not express CD-UPRT and treated with prodrug 5-FC (5-Flurocytosine). Understanding the molecular mechanism of suicide gene therapy mediated cell death was very crucial for its long term therapeutic application. The apoptotic mechanism was revealed by combination of several experimental strategies like microscopic analysis, biochemical assays and molecular assays. Apoptotic signaling genes were identified by semi-quantitative RT-PCR analysis.

In summary, the present study demonstrated the therapeutic effect of suicide genes and their enhanced effect in presence curcumin or Ag NPs *in vitro*. This study also revealed the molecular mechanism of cell death induced by suicide genes and Ag NPs.

Keywords: Prodrug gene therapy / Suicide gene therapy, CD, UPRT, CD-UPRT, 5-FC, 5-FU, Apoptosis, Curcumin, Silver nanoparticles (Ag NPs).

CONTENTS

ACKNOWLEDGEMENTS i

ABSTRACT iii

CONTENTS v

LIST OF FIGURES ix

LIST OF TABLES xi

ABBREVIATIONS xii

1. INTRODUCTION **1**

1.1 Objectives 5

1.2 Experimental Approaches 6

1.3 Significance and Salient Features of the Present Study 7

1.4 Organization of Thesis 8

2. LITERATURE REVIEW **9**

2.1 Suicide Genes 9

2.1.1 Thymidine Kinase 9

2.1.2 Cytosine Deaminase 10

2.1.3 Uracil Phosphoribosyl Transferase 12

2.1.4 Cytosine Deaminase-Uracil Phosphoribosyl Transferase 13

2.2 Electrogene Therapy 14

TH-0560_03610605

2.3 Non-invasive Quantification of Transgene Expression ……. 15
2.4 Combination Therapy …… 16
2.5 Anticancer Compound - Curcumin ……..... 18
2.6 Bactericidal and Cytotoxicity of Silver Nanoparticles ……... 19
2.7 Bystander Effects …….……..... 21
2.8 Apoptosis ……... 22

3. MATERIALS AND METHODS 25
3.1 Cell Culture …… 25
3.2 Recombinant Plasmids and Stable Cell Lines …… 25
3.2.1 Construction of Recombinant Plasmid Vector …..... 25
3.2.2 Electroporation ……..... 28
3.2.3 Generation of CD-UPRT::GFP Expressing Cell Lines ……. 28
3.3 Bactericidal Activity of Silver Nanoparticles …… 28
3.3.1 *E. coli* GFP Construct ……... 28
3.3.2 Determination of Minimum Inhibitory Concentration and Minimum Killing Concentration of Ag NPs …… 28
3.3.3 Optical Density Measurement and Bacterial Cell Viability Count ... 29
3.3.4 Plasmid DNA and Protein Gel Electrophoresis ……..... 30
3.4 Microscopic Analysis …….…….... 30
3.4.1 Fluorescence Microscopic Analysis …….…….... 30
3.4.2 Phase-Contrast Microscopic Analysis …….. 30
3.4.3 Confocal Microscopic Analysis …… 31
3.4.4 Scanning Electron Microscopic Analysis ……. 31
3.4.5 Atomic Force Microscopic Analysis …… 31
3.4.6 Transmission Electron Microscopy Analysis ……... 32
3.5 X-Ray Diffraction Measurement ……... 32
3.6 Spectrophotometric and Chromatographic Analysis ……..……... 33
3.6.1 Fluorescence Spectrophotometric Analysis …….. 33
3.6.2 High-Performance Liquid Chromatographic Analysis ……. 33
3.7 Cell Viability and Cytotoxicity Assay ……... 33
3.7.1 Cell Proliferation Assay …… 33
3.7.2 Cytotoxicity Assay …… 34

3.8 Molecular Analysis 35
3.8.1 RNA and DNA Extraction 35
3.8.2 PCR and RT-PCR analysis 36
3.8.3 Semi-quantitative RT-PCR 36
3.8.4 BrdU Cellular DNA Fragmentation ELISA 37
3.8.5 DNA Laddering 39
3.9 Statistical Analysis 40

4. 5-FC/CD GENE THERAPY **41**
4.1 CD-GFP Gene Transfer and its Expression 42
4.2 Comparative Study of Promoter Strength on Cell Viability 43
4.3 Molecular Mechanism of 5-FC/CD Mediated Cell Death 47
4.3.1 Microscopic Observations 47
4.3.2 Effect of Curcumin on Cytotoxicity and Cell Viability 49
4.3.3 Synergistic Apoptosis with 5-FC/CD and Curcumin Treatment 49
4.3.4 Apoptotic DNA Laddering and Gene Expression 52

5. 5-FU/UPRT GENE THERAPY **55**
5.1 GFP Expressing *E. coli* as a Model System to Study Ag NPs Induced Bactericidal Effect 56
5.1.1 MIC and MKC of Ag NPs on GFP Expressing *E. coli* 56
5.1.2 Microscopic Observations 57
5.1.3 Bacterial Count 59
5.1.4 SDS-PAGE Analysis 59
5.1.5 Plasmid DNA Analysis 59
5.2 Synthesis of Ag NPs in Cell Culture Medium 62
5.2.1 TEM and XRD Measurements 62
5.3 Effect of Ag NPs on Mammalian Cells 62
5.3.1 Cytotoxic Effects 62
5.3.2 Microscopic Observations 63
5.3.3 Molecular Analysis 68
5.4 UPRT Expression and Cell Apoptosis 71
5.5 Synergistic Effect in Combination Therapy 71

6. 5-FC/CD-UPRT GENE THERAPY **79**

6.1 CD-UPRT Gene Transfer and its Expression …… 80

6.2 Cytotoxicity and Cell Viability Measurements …….. 80

6.3 Apoptosis Induced with 5-FC/CD-UPRT …….. 82

6.3.1 Microscopic Observations ……. 82

6.3.2 Synergistic Effect of 5-FC/CD-UPRT with Curcumin ……. 84

6.3.3 Apoptotic DNA Laddering and Gene Expression 87

7. COMPARATIVE ANALYSIS OF CD AND CD-UPRT **91**

7.1 CD and CD-UPRT Gene Transfer and Expression ……... 92

7.2 CD and CD-UPRT Enzymatic Activity *in vitro* ……..... 92

7.3 Comparative Analysis of Cell Viability and Cytotoxicity ……. 92

7.4 Synergistic Effect of Curcumin on 5-FC/CD and 5-FC/CD-UPRT …….. 95

8. BYSTANDER EFFECT AND APOPTOSIS **100**

8.1 CD-UPRT Gene Expression and its Functional Activity ……..... 101

8.2 Cell Viability upon 5-FC Treatment ……..... 101

8.3 Bystander Effect …… 103

8.3. Apoptosis Induction with 5-FC Treatment ……... 105

8.3.1 AFM Imaging ……... 105

8.3.2 Apoptosis Signaling Genes …….. 105

9. CONCLUSIONS AND SCOPE FOR FUTURE WORK **110**

9.1 Conclusions ……..... 110

9.2 Scope for Future Work 112

BIBLIOGRAPHY 113

LIST OF PUBLICATIONS 129

I. In Refereed Journals ……. 129

II. In Conferences ……. 130

LIST OF FIGURES

FIGURE	TITLE	PAGE
1.1	Schematic representation of Prodrug gene therapy / Suicide gene therapy ……..	2
1.2	Schematic representation of metabolite pathway of CD and UPRT enzymes ……	4
1.3	Gene therapy vectors currently used in clinical trials ……...	4
2.1	Features of the apoptotic and necrotic cell death process …….	23
3.1	Schematic representation of plasmid vector construction ……	27
3.2	Schematic representation of BrdU labeled DNA fragmentation ELISA ……..	39
3.3	Schematic representation of DNA laddering due to internucleosomal DNA cleavage ……..	39
4.1	GFP expression of BHK21 and HT29 cells observed under confocal microscope at 48 h post transfection …….....	44
4.2	Fluorescence intensity measurement of GFP of the transfected cells at 24 h ……...	44
4.3	Agarose gel picture of PCR and RT-PCR analysis of the transfected cells ……	45
4.4	Fluorescent images of transfected BHK21 (A-E) and HT29 cells (F-J) at varying concentrations (0, 5, 10, 20 and 50 mM) of 5-FC ..	45
4.5	Cell viability by MTS assay …….	46
4.6	Confocal micrographs of AO/EB stained cells …….	48
4.7	Scanning electron micrographs of apoptotic cell morphology …….	48
4.8	Effect of curcumin on membrane leakage and cell viability ……	50
4.9	Confocal micrograph of the transfected cells in presence of 10mM 5-FC and 40 µM curcumin for 72 h …….	51
4.10	Cellular DNA fragmentation ELISA	51
4.11	DNA laddering of 5-FC/CD treated cells …….	53
4.12	Expression of pro-apoptotic caspase and anti-apoptotic bcl-2 gene..	53
5.1	Effect of various concentrations of Ag NPs on the growth of recombinant GFP *E. coli* …….....	58

FIGURE	TITLE	PAGE
5.2	Time-dependent fluorescence micrograph of recombinant GFP *E. coli* …….....	58
5.3	Fluorescence micrographs of GFP *E. coli* at 12 h ……...	60
5.4	TEM micrograph shows perforation on the cell wall of bacteria …	60
5.5	Effect of Ag NPs on the viability of GFP expressing *E. coli* at 0, 3, 6 and 12 h …….	60
5.6	SDS-PAGE of Ag NPs treated *E. coli* whole cell lysate …….	61
5.7	Effect of Ag NPs on the recombinant GFP plasmid DNA migration pattern ……..	61
5.8	Transmission electron microscopy for characterization of Ag NPs.	64
5.9	XRD Analysis of Ag NPs ……	64
5.10	Microscopic observations of Ag NPs treated cells ……..	65
5.11	LDH assay of Ag NPs treated cells …….	66
5.12	MTS assay of Ag NPs treated cells …….	66
5.13	Microscopic observations of Ag^+ ions treated cells …….	67
5.14	MTS assay of Ag^+ ions treated cells ……	67
5.15	SEM analysis of Ag NPs treated cells …….	69
5.16	Time dependent confocal micrographs of AO/EB stained cells …..	70
5.17	Detection of Ag NPs induced apoptosis by cellular DNA fragmentation ELISA, DNA laddering and apoptotic gene expression ……	72
5.18	Construction of UPRT vector and confirmation of UPRT gene transfer and expression by PCR and RT-PCR analysis ……...	74
5.19	MTS assay of 5-FU treated cells …….	75
5.20	Confocal micrographs of AO/EB stained 5-FU treated cells ……..	75
5.21	DNA laddering of 5-FU treated cells ……...	76
5.22	LDH release and synergistic apoptosis due to combine therapy ….	77
6.1	CD-UPRT gene transfer and expression ……..	81
6.2	Effect of 5-FC/CD-UPRT on membrane leakage by LDH assay …	83
6.3	Effect of 5-FC/CD-UPRT on cell proliferation by MTS reduction assay …….	83

TH-0560_03610605

FIGURE	TITLE	PAGE
6.4	Confocal micrographs of AO/EB stained cells	85
6.5	SEM analysis of 5-FC/CD-UPRT treated cells ……...	86
6.6	Quantification of 5-FC/CD-UPRT induced apoptosis by cellular DNA-fragmentation ELISA	86
6.7	5-FC/CD-UPRT treated HEK293 and Hep3B cells ……	88
6.8	DNA laddering of 5-FC/CD-UPRT treated cells …….....	89
6.9	Expression profile of pro-apoptotic and anti-apoptotic genes …….	89
7.1	PCR and RT-PCR analysis of transfected cells ……...	93
7.2	Functional activity measurement by reverse phase HPLC ……..	94
7.3	Cell viability by MTS reduction assay ……	96
7.4	LDH assay to examine the release of LDH leakage ……	97
7.5	Cellular DNA-fragmentation ELISA	98
8.1	CD-UPRT expression in stable BHK21 CD-UPRT::GFP ……..	102
8.2	Cell viability and apoptosis of 5-FC treated BHK21 CD-UPRT::GFP cells ……..	104
8.3	Bystander effects of BHK21 CD-UPRT::GFP cells ……	106
8.4	AFM analysis of 5-FC treated BHK21 CD-UPRT::GFP cells ……	106
8.5	Semi-quantitative RT-PCR analysis of apoptotic signaling genes..	108

LIST OF TABLES

TABLE	TITLE	PAGE
3.1	Linker primers for CD, UPRT and CD-UPRT ……	26
3.2	Primers for apoptotic signaling genes ……..	37

ABBREVIATIONS

5-FC ……..	5-Fluorocytosine
5-FU ……..	5-Fluorouracil
5-FdUMP ……..	5-Flurodeoxyuridine Monophosphate
5-FUMP …….	5-Flurouridine Monophosphate
5-FUTP ……..	5-Flurouridine Triphosphate
ACS ……	American Cancer Society
AFM ……..	Atomic Force Microscope
Ag NPs	Silver Nanoparticles
ANOVA …….	Analysis of Variance
AO ……..	Acridine Orange
BHK21 ……..	Baby Hamster Kidney cells
BrdU ……..	5'-Bromo-2'-Deoxyuridine
CAD ……..	Caspase Activated DNase
CD ……..	Cytosine Deaminase
CD-UPRT ……..	Cytosine Deaminase-Uracil Phosphoribosyl Transferase
CFU	Colony Forming Units
DMEM	Dulbecco's Modified Eagle's Medium
EA ……..	Early Apoptosis
EB ……..	Ethidium Bromide
ELISA ……	Enzyme-Linked Immuno Sorbent Assay
FACS ……..	Fluorescence Activated Cell Sorter
GCV ……..	Ganciclovir
GDEPT ……..	Gene-Directed Enzyme Prodrug Therapy
GFP ……	Green Fluorescent Protein
HEK293 …….	Human Embryonic Kidney cells
Hep3B ……	Human Hepatoma cells
HPLC …….	High-Performance Liquid Chromatography
HSV-TK …….	Herpes Simplex Virus-Thymidine Kinase
HT29 …….....	Human Colon Adenocarcinoma Cells
ICAD ……..	Inhibitor of Caspase-Activated DNase
LA ……..	Late Apoptosis

LB ……..	Luria-Bertani
LDH ……..	Lactate Dehydrogenase
MIC ……	Minimum Inhibitory Concentration
MKC ……..	Minimum Killing Concentration
MTS ……..	3-(4, 5-dimethylthiazol-2yl)-5-(3-carboxymethoxyphenyl)-2-(4-sulfophenyl)-2H-Tetrazolium Compound
NPs …….	Nanoparticles
OD ……..	Optical Density
PBS …….	Phosphate Buffered Saline
PCR ……	Polymerase Chain Reaction
RT-PCR ……..	Reverse Transcriptase-Polymerase Chain Reaction
SAD ……	Selected Area Diffraction
SDS-PAGE	Sodium Dodecyl Sulphate-Polyacrylamide Gel Electrophoresis
SEM	Scanning Electron Microscope
SPIP	Scanning Probe Image Processor
TEM	Transmission Electron Microscope
UPRT	Uracil Phosphoribosyl Transferase
XRD	X-Ray Diffraction

Indian Institute of Technology Guwahati

1

INTRODUCTION

Cancer is still considered as a threat of mortality even though medical technology has progressed a lot and many new anticancer drugs have been discovered. According to the report of American Cancer Society (ACS), cancer remained one of the biggest killers in 2007, accounting for 7.6 million deaths worldwide or 20,000 deaths a day (http://www.cancer.org/docroot/stt/stt_0.asp). There is high risk of 12 million new cancer cases this year (2008) - a majority of them in developing countries.

The major limitation to conventional therapies like surgery, irradiation and chemotherapy for cancer treatment is the lack of specificity to target tumor cells. Non- specific chemotherapy drugs affect all dividing cells, including normal cells and especially those with a high proliferation rate, such as bone marrow and gastrointestinal tract cells. The efficiency of these approaches is often hindered by an inadequate therapeutic index, lack of specificity, and the emergence of acquired resistance to current chemotherapeutic treatments. New treatment approaches must be required to enhance the selectivity of tumor treatment and to prevent the emergence of

TH-0560_03610605

drug resistance. One such approach is gene therapy, which was initially applied for well-characterized genetic diseases but now become applicable for cancer treatment. Both malignant and nonmalignant cells can be suitable targets in cancer gene therapy. A large number of preclinical studies are ongoing *in vitro* as well as *in vivo* and about 60% of the clinical trial protocols for gene therapies have addressed the treatment of cancer.

Recent efforts for cancer treatment using gene therapy are divided into three main areas:

1. Transfer of tumor-suppressor genes replaces missing or altered tumor suppressor genes, which in turn inactivate further growth of cancer.
2. Transfer of genes enhance immunogenicity and stimulate body's natural ability to attack cancer cells and improve patient's immune response.
3. Transfer of suicide genes in cancer cells converts the non-toxic prodrug into toxic drug, which kill the cancer cell as well as neighboring damaged cells or normal cells (Figure 1.1). So, the bystander effect is not only limited to tumor cells

Suicide gene therapy often referred to as Gene-Directed Enzyme Prodrug Therapy (GDEPT) gains much importance over the other two owing to its selective approach to eliminate tumor cells by the local production of toxic agents, which exhibits strong bystander effects and reduces systemic toxicity (Springer and Duvaz 2000). Suicide gene therapy is a promising approach for cancer treatment but limited by the inefficient gene delivery systems (Yazawa et al., 2002). This limitation can be

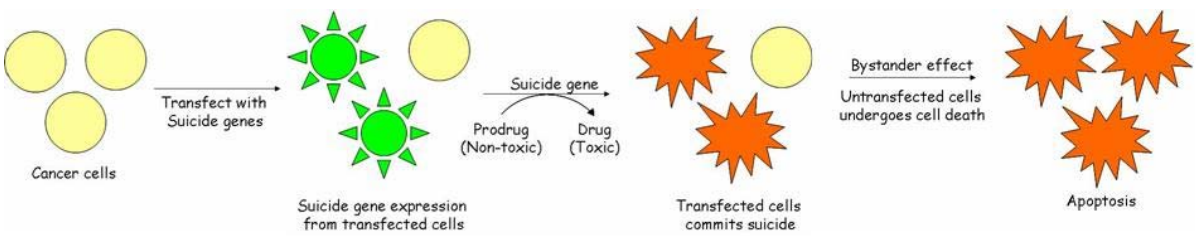

Figure 1.1: Schematic representation of Prodrug gene therapy / Suicide gene therapy

TH-0560_03610605

overcome if strong bystander effect of suicide gene therapy does exist, because 100% transduction efficiency is not necessary for total killing of cancer cells. Hence, the successful eradication of cancer cells through suicide gene therapy depends on the degree of bystander effect.

The most intensely studied suicide genes are the Herpes Simplex Virus-Thymidine Kinase (HSV-TK) and the bacterial Cytosine Deaminase (CD). HSV-TK has its limitations due to the requirement of cell-to-cell contact for active transport of toxic Ganciclovir (GCV) metabolites to neighboring cells to exert bystander-killing effect. As a consequence, such system remains ineffective for wide-range use in different cell types (Moolten 1986; Holder et al., 1993; Hotz-Wagenblatt and Shalloway 1993). On contrary, CD converts the prodrug antifungal agent 5-fluorocytosine (5-FC) into antitumor agent 5-fluorouracil (5-FU), which diffuses across the cell membrane and kills adjacent neighboring cells (Rowley et al., 1996). Therefore, the 5-FC/CD system has become more effective suicide gene therapy system. However, certain cancer cells are resistant to 5-FC treatment, where the CD enzyme exhibits poor efficiency in converting 5-FC into its toxic metabolites. This problem can be addressed by using a bifunctional cytosine deaminase-uracil phosphoribosyl transferase (CD-UPRT) gene, where UPRT, a pyrimidine salvage enzyme converts 5-FU into more cytotoxic metabolites as shown in schematic Figure 1.2.

Another challenging task of gene therapy is the delivery vehicle. Viral vectors are commonly used (Ghosh et al., 2006) for such purpose (Figure 1.3). Recently much attention is paid to non-viral based gene delivery due to the safety risks with the viral vectors**.** Among the non-viral vectors electroporation based gene transfer methodology attracts the researchers by its simple, rapid, efficient, inexpensive,

TH-0560_03610605

reproducible and relatively nontoxic nature to target cells. It has advantages, like ability to transfect populations, such as, non-replicating cells and solid tumors, which are resistant to other gene-transfer methods. Moreover, instruments are readily available for this method and are easy to operate. The application of electroporation

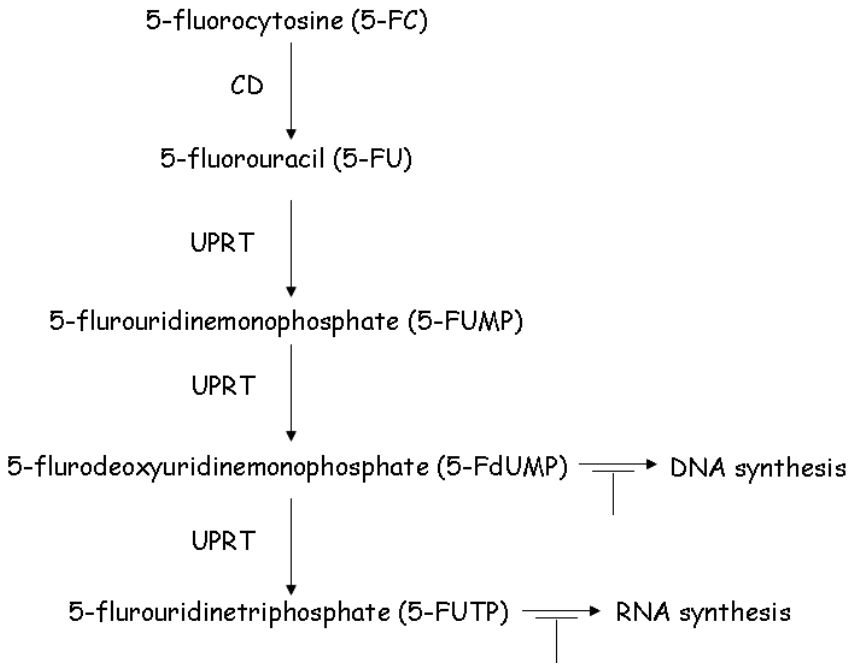

Figure 1.2: Schematic representation of metabolite pathway of CD and UPRT enzymes.

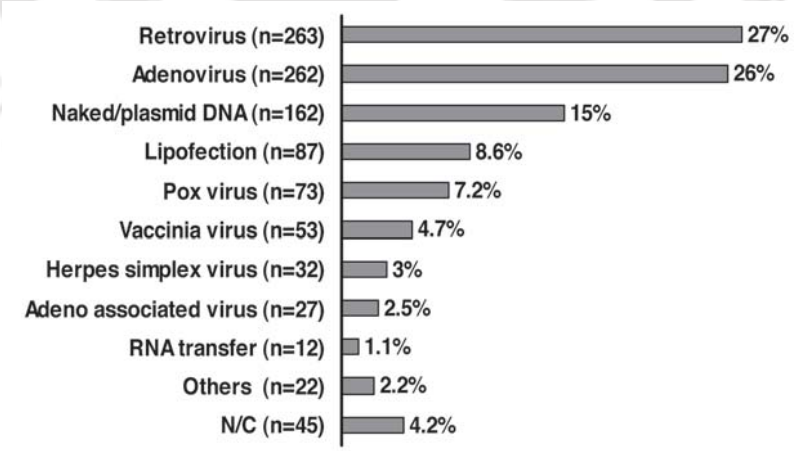

Figure 1.3: Gene therapy vectors currently used in clinical trials. *n* is the number of individuals in gene therapy clinical trials. N/C, numerical control. (www.wiley.co.uk/genmed/clinical).

TH-0560_03610605

for gene therapy (Vanbever et al., 1996) is named as electro-gene therapy (EGT). EGT was extensively used for treating various organs affected by hereditary disease (Mir 2001) or acquired disease such as malignant tumors (Orlowski et al., 1988).

Over the past several years, there has been increasing interest in combining gene therapy with the conventional therapy to attain high therapeutic index. Combination therapy in many cancer treatments were reported to be effective, where both drugs can be used below their IC_{50} to synergize the therapeutic effects as well as to reduce the chance of development of resistance against particular drug. Most of the cancer therapy drugs induced apoptotic cell death. Thus it is very essential to completely understand the molecular mechanism of cell death mediated by any suicide gene for its long term therapeutic application. The molecular mechanism of HSV-TK was already elucidated, but the molecular mechanism of CD, UPRT and CD-UPRT suicide gene therapy remains to be investigated.

1.1 Objectives

The main objective of the present work is as follows:

- To investigate the therapeutic efficacy of suicide genes CD, UPRT and CD-UPRT.
- To study the combinatorial effect of curcumin and silver nanoparticles (Ag NPs) on suicide genes and evaluate synergistic therapeutic effect *in vitro*.
- To investigate the molecular mechanism of cell death.

TH-0560_03610605

1.2 Experimental Approaches

In order to achieve the above objectives the following investigations were carried out:

- Construction of recombinant plasmid vectors carrying suicide genes CD, UPRT and CD-UPRT.
- Electroporation of recombinant plasmids into cancer and non-cancer cells.
- Gene transfer and expression studies by confocal microscope, Polymerase Chain Reaction (PCR), Reverse Transcriptase (RT)-PCR and High Performance Liquid Chromatography (HPLC) analysis.
- Examination of therapeutic efficacy by measuring cell viability and cell membrane damage using mitochondrial activity and lactate dehydrogenase (LDH) assays, respectively.
- Observation of apoptotic cell morphology by Scanning Electron Microscope (SEM) and Atomic Force Microscope (AFM).
- Confocal microscopic observation of uptake of nuclear stains- Acridine Orange (AO) and Ethidium Bromide (EB) by cells to study their apoptosis.
- Demonstration of apoptotic cell death by DNA laddering in agarose gel.
- Involvement of various apoptotic signaling genes by semi-quantitative RT-PCR.
- Synthesis and characterization of Ag NPs in cell culture medium.
- Assessing the effects of Ag NPs on Green Fluorescent Protein (GFP) expressing bacteria and mammalian cell lines.
- Quantification of apoptotic cell death by synergistic effect of curcumin and Ag NPs with suicide genes, using 5'-bromo-2'-deoxyuridine (BrdU) labeled cellular DNA fragmentation through Enzyme-Linked ImmunoSorbent Assay (ELISA).

TH-0560_03610605

- Generation of stable cell lines expressing CD-UPRT gene to explore the bystander effects and involvement of apoptotic signaling genes in 5-FC/CD-UPRT mediated cell death.

1.3 Significance and Salient Features of the Present Study

The significance and salient features of the present study are summarized below:

- The literature on suicide gene therapy, apoptotic mechanisms, anticancer compound and cytotoxicity of Ag NPs has been reviewed.
- Recombinant suicide gene therapy vectors were constructed and the chemotherapeutic effect was established using plasmid based system, where GFP fluorescence was used to probe the functional detection of suicide genes.
- In the present study, induction of apoptosis by suicide genes; CD, UPRT, CD-UPRT and Ag NPs were demonstrated using combination of experimental methods.
- Bystander effect of CD-UPRT was evaluated.
- Antibacterial effects of Ag NPs were established.
- Induction of apoptosis by Ag NPs represents a new chemosensitization strategy for future application in gene therapy.
- Involvement of apoptotic signaling pathway was delineated.
- The combination treatment of prodrug with curcumin or Ag NPs where the individual component, either curcumin or Ag NPs used at low concentration showed synergistic apoptosis.

TH-0560_03610605

1.4 Organization of Thesis

This thesis is organized into nine chapters. The literature review on suicide gene therapy and combination therapies are referred in Chapter 2. The methodologies followed in the present study are elaborated in chapter 3. The use of GFP as a non-invasive probe to monitor the therapeutic efficacy of *E. coli* CD mediated gene therapy in presence of prodrug 5-FC is presented in chapter 4. Chapter 5 elaborates the antibacterial and anticancer properties of Ag NPs, where Ag NPs synergized the UPRT gene therapy in presence of 5-FU. The synergistic effect of curcumin to enhance the therapeutic potential of CD-UPRT is reported in chapter 6. A comparative analysis between CD and CD-UPRT systems are presented in chapter 7. Chapter 8 reveals the bystander effect of 5-FC/CD-UPRT and involvement of different signaling genes in apoptosis of CD-UPRT and GFP expressing stable cell lines. Finally, conclusions are drawn from these studies along with the scope for future work in Chapter 9.

TH-0560_03610605

2

LITERATURE REVIEW

New approaches to improve the therapeutic effectiveness and enhanced selectivity of cancer chemotherapy for solid tumors rely on the application of gene therapy. The possibility of exposing cancer cells more sensitive to drugs by introducing "suicide genes", where the transgene encode enzymes that activate specific prodrugs to create toxic metabolites is known as suicide gene therapy or gene-directed enzyme prodrug therapy (GDEPT) (Marais et al., 1996; Bridgewater et al., 1995). Such strategy is useful in either individual or in combination with other strategies, to make a significant impact on cancer treatment. In the context of this thesis, suicide genes, electrogene therapy, anticancer compound curcumin, bystander effect, apoptosis and interaction of metal nanoparticles on cells have been reviewed.

2.1 Suicide Genes

2.1.1 Thymidine Kinase

The HSV-TK/GCV suicide gene therapy system is the most comprehensively studied and widely used till date. In the salvage pathway of nucleosides, TK play an

TH-0560_03610605

important role in phosphorylating deoxythymidine (dT) to its monophosphate form (dTMP). HSV-TK has a broad substrate specificity and hence very successful in gene therapy. Unlike human TK, HSV-TK is able to phosphorylate the purine nucleoside analog GCV to its monophosphate form, which is further phosphorylated to di- and triphosphate forms by endogenous cellular kinases. Triphosphate form of GCV is incorporated into DNA and acts as a chain terminator to prevent further DNA synthesis, thereby inducing cell death (Elion 1980). TK/GCV exerts a bystander effect through gap junctions to kill the non-transfected cells in tumor microenvironment. The phosphorylated GCV product is unable to diffuse from the cell and requires cell-to-cell contact for transfer of the antimetabolites, which limits its wide range use because many tumor cells either lack or express low levels of gap junction proteins (Holder et al., 1993; Hotz-Wagenblatt and Shalloway 1993). In spite of these issues, Freeman et al., (1993) reported that, a mixed population cells with only 10% of TK expressing cells was sufficient to kill all the cells at a concentration of GCV that was not cytotoxic to non-TK expressing cells.

2.1.2 Cytosine Deaminase

Cytosine deaminase is another most extensively studied suicide gene, found in fungi and bacteria, but not in higher eukaryotes. CD catalyzes the deamination of cytosine to uracil, and finally utilized for DNA synthesis. The catalytic property of CD was used for converting the antifungal agent, 5-FC into its active metabolite 5-fluorouracil (5-FU) an anticancer agent. 5-FU is one of the most extensively used chemotherapeutic agents. 5-FU has been clinically used for decades against many different tumor types, such as, colon, breast, stomach and pancreatic cancers (Longley et al., 2003).

TH-0560_03610605

Hoganson et al., (1996) compared the effects of three different toxin genes in lung adenocarcinoma cell lines and demonstrated that cytosine deaminase was superior to TK and deoxycytidine kinase by its high therapeutic effect and bystander effect. However, the low gene transfer efficiency of viral and nonviral vectors is a major drawback in tumor gene therapy. Wybranietz et al., (2001) utilized the intercellular transport property of HSV-1 tegument protein VP22 to compensate inadequate gene transfer efficiencies. Wild-type VP22 and CD-VP22 fusion proteins could efficiently spread from the original expressing cell to surrounding neighboring cells to potentiate the gene transfer efficiency and thereby increased the therapeutic effect.

Freytag et al., (2002) developed a replication-competent adenovirus (Ad5-CD/TK*rep*) to deliver a cytosine deaminase/herpes simplex virus-1 TK fusion gene to tumors sensitized with 5-FC, GCV and radiation. This was the first reported gene therapy trial (Phase I study) for delivering a therapeutic gene to humans using replication-competent virus. To overcome the lack of suitable vectors for effective therapy of malignant brain tumor, Guffey et al., (2007) developed a conditionally replication-competent, oncolytic herpes simplex virus type 1 (HSV-1) expressing CD that showed high therapeutic effect.

Another important task is targeting CD gene to tumor cells. Kanai et al., (1997) cloned the CD under α-fetoprotein (AFP) promoter to target the AFP expressing human hepatocellular carcinoma (HCC) cells using adenovirus (AdAFPCD). Similarly, Liu et al., (2002) utilized the catalytic subunit of the human telomerase reverse transcriptase (hTERT) which is transcriptionally upregulated in more than 90% of tumor cells. They achieved tumor specific expression of CD by

TH-0560_03610605

cloned CD under hTERT promoter and also studied the bystander effects of CD by mixing the CD positive and CD negative cell populations.

2.1.3 Uracil Phosphoribosyl Transferase

Kanai et al., (1998) developed adenoviral vector carrying UPRT gene to overcome resistance of certain cancers to 5-FU treatment, *E.coli* UPRT, a pyrimidine salvage enzyme that converts 5-FU into more cytotoxic 5-flurouridine monophosphate (5-FUMP), which is further converted to 5-flurodeoxyuridine monophosphate (5-FdUMP) and 5-flurouridine triphosphate (5-FUTP). The 5-FdUMP irreversibly inhibits thymidine deaminases and prevents DNA synthesis, whereas 5-FUTP is directly incorporated into RNA instead of uridine 5-triphosphate and inhibits the processing of rRNA and mRNA leads to enhanced therapeutic effect. *In vitro* bystander effect was also reported, when only 10% of the hepatoma Hep3B cells were infected with UPRT expressing adenovirus. Koyama et al., (2000a) demonstrated that, UPRT expression improved the sensitivity of human colon cancer cells to 5-FU both *in vitro* and *in vivo*.

Oonuma et al., (2002) first demonstrated that, injection of E1-deficient adenoviral vector (Adv) expressing UPRT (AxE1AdB-UPRT) followed by 5-FU treatment resulted significant reduction in the volume of xenotransplanted human tumors. Therefore, AxE1AdB-UPRT system potentiated the effects of anticancer drug 5-FU. Seo et al., (2005) constructed a conditionally replicating adenoviral vector (CRAd) containing UPRT gene, which further enhanced the effect of 5-FU.

TH-0560_03610605

2.1.4 Cytosine Deaminase-Uracil Phosphoribosyl Transferase

Koyama et al., (2000b) used two separate adenovirus vectors expressing the *E. coli* CD and *E. coli* UPRT genes followed by systemic 5-FC administration and showed improved antitumoral effect of the CD/5-FC system. The co-operative therapeutic effect of CD and UPRT in human colon cancer cells was also investigated. Their group demonstrated that, the combined suicide gene transduction has increased incorporation of 5-FUTP into RNA and 5-FdUMP to DNA, and inhibited the thymidylate synthase compared to the CD/5-FC system.

Chung-Faye et al., (2001) utilized a replication-deficient adenovirus containing a bifunctional fusion gene, CD-UPRT (AdCD-UPRT) to enhance the efficacy of 5-FC/CD system. They observed a strong bystander effect *in vitro*, about 70% of tumour cells were killed by 5-FC when only 10% of cells expressed CD-UPRT. Moreover, studies on athymic mice with colon cancer xenografts with intratumoral AdCD-UPRT and intraperitoneal 5-FC treatment, showed significant reduction in tumor growth rates compared to untreated controls, whereas AdCD/5-FC treated mice did not show any changes. AdCD-UPRT was more effective than AdCD and the bifunctional CD-UPRT gene could use either 5-FC or 5-FU as prodrugs.

Porosnicu et al., (2003) demonstrated the oncolytic capabilities of vesicular stomatitis virus (VSV) against a wide range of tumor models *in vitro* and *in vivo.* They generated a novel recombinant VSV (rVSV) that expressed fusion suicide gene *E. coli* CD-UPRT to potentiate the oncolytic effect. Their *in vivo* studies revealed that, intratumoral injection of VSV CD-UPRT followed by systemic administration of 5-FC produced significant decrease in the growth of syngeneic lymphoma or mammary carcinoma in BALB/c mice compared with rVSV treatments or with control 5-FU alone. They demonstrated activation of IFN-gamma-secreting cytotoxic

TH-0560_03610605

T-cells had played a major role in facilitating tumor killing. Thus, the insertion of fusion CD/UPRT suicide gene potentiated the oncolytic efficiency of VSV by generating a strong bystander effect and by contributing to the activation of the immune system against the tumor without altering the kinetics of virus-mediated oncolysis.

2.2 Electrogene Therapy

Successful gene therapy relies on the development of efficient gene delivery systems with low toxicity, low immunogenicity, and ease in handling. To date non-viral methods of gene transfer are being focused for gene therapy strategies, due to the risk factors of viral vectors that included the possibility of mutagenesis and immune responses (Verma and Somia 1997; El-Aneed 2004). Recently, electrogene therapy the electroporation-based gene transfer is gaining overwhelming importance for its safer and high efficiency in gene transfer (Hojman et al., 2007). Electrogene therapy is a non-viral approach for gene therapy, which means the electrical stimulus that creates membrane destabilization and facilitates the formation of nanometer-sized pores, which allows the passage of macromolecules into the cell (Rols MP et al., 1998). Thus, Electroporation become a relatively standard laboratory technique to transfect cells both *in vitro* as well as *in vivo* for delivering a large variety of impermeable molecules, such as drugs, antibodies, oligonucleotides, RNA and DNA plasmids.

Prechtel et al., (2006) used electroporation as an appropriate and efficient method for the delivery of siRNA into monocyte-derived dendritic cells (moDCs) due to the unwanted side effects caused by chemical transfection reagents. Recently, individual cells are reported to be electroporated both *in vitro*

TH-0560_03610605

(Rathenberg et al., 2003) and *in vivo* (Haas et al., 2001; Dezawa et al., 2002) protocols. Scheerlinck et al., (2004) demonstrated enhanced humoral responses and induction of vaccine-specific immune memory in DNA vaccine electroporated sheep. Uno-Furuta et al., (2001) explored the use of epitope peptides by *in vivo* electroporation to introduce directly into the cytoplasm for the vaccine elicitation of virus-specific CTLs in a mouse system. Recently, Kim et al., (2007) developed a multi-channel electroporation microchip made of polydimethylsiloxane (PDMS) and glass for gene transfer in mammalian cells. The advantage of the chip was that five different transfection rates and survival rates at different electric fields were produced in a single microchip.

2.3 Non-invasive Quantification of Transgene Expression

Currently, the methods available for analysis of transgene expression *in vivo* utilize destructive and invasive molecular assays of tissue specimens. Hence the need for noninvasive methodology to assess the location, magnitude, and duration of transgene expression *in vivo* would definitely facilitate correlation of therapeutic outcomes with transgene expression and would be useful in vector development. Stegman et al., (1999) demonstrated the noninvasive quantitation of CD transgene expression using magnetic resonance spectroscopy in human tumor xenografts by directly observed the CD catalyzed conversion of the 5-FC to 5-FU.

Recent advancements achieved the possibilities of visualizing the transgene expression in intact animals by noninvasive techniques, but the instruments are expensive and the protocols are complicate. Yang et al., (2000) described a simple, rapid, and eminently affordable system for visualizing transgene expression in intact live mice. Mice were labeled by directly injecting adenoviral GFP into the brain, liver,

TH-0560_03610605

pancreas, prostate, or bone marrow. The GFP expressed in brain and liver became visible within 5-8 h after adenoviral GFP injection, which was determined by recording whole-body optical images. The GFP fluorescence continued to increase for at least 12 h and remained measurable in liver for up to 4 months. The major advantage of this method is that, it does not require exogenous contrast agents, radioactive substrates and long processing times. Thus, it has gained much importance for studying the therapeutic and diagnostic potential of suitably tagged genes in moderately opaque organisms.

The fusion gene of HSV-TK and green fluorescent protein (TK-GFP) was reported to be a versatile tool for examining TK/GCV gene therapy *in vitro*. Pasanen et al., (2003) used viral vectors carrying this fusion gene to establish gene therapy form in rodent tumor models. Growth of subcutaneous rat tumors transduced *ex vivo* with TK-GFP gene was prevented by GCV treatment immediately after tumor inoculation. Induction of apoptosis/necrosis *in vitro* using TK-GFP lentivirus vector was demonstrated by propidium iodide staining. *In vivo* studies with adenovirus TK-GFP injections resulted in about 25% gene transfer efficiency to the tumors and showed significant reduction in the growth rate even when the tumor volumes were already >120 mm^3. The utility of TK-GFP fusion gene-carrying viral vectors in animal models has been reported to be useful for *in vivo* cancer gene therapy.

2.4 Combination Therapy

Recently, combinatorial approaches have gained much importance due to their high therapeutic effectiveness over monotherapeutic regiments. The major advantage of combination therapy is the concurrent use of drugs with different or same mechanisms of action or pharmacokinetics is considered more effective than each of

TH-0560_03610605

the monotherapeutic regiment alone. Such combination therapy has opened up new avenues in the cancer therapy. Kambara et al., (2002) demonstrated that, the combination of radiation therapy and 5-FC/CD plus UPRT gene therapy possessed superior antitumor effect in comparison to single therapy in malignant gliomas. Another advantage of this combination therapy is that radiosensitizing properties of 5-FU can be utilized for treatment (Kievit et al., 2000; Lawrence et al., 1994). Their *in vivo* results showed a significant bystander effect at clinically applicable 5-FC doses and radiation regimens (Hamstra et al., 1999; Stackhouse et al., 2000).

Freytag et al., (2003) utilized a replication-competent oncolytic adenovirus-mediated double-suicide gene therapy (CD/HSV-1 TK fusion gene) followed by treated with respective prodrugs 5-FC and valganciclovir with increased durations as well as combined treatment with conventional-dose three-dimensional conformal radiation therapy (3D-CRT) in patients with intermediate- to high-risk prostate cancer for enhanced therapeutic effect. Similarly, Xia et al., (2004) demonstrated the combination of suicide gene therapy (yeast CD/UPRT) and radiation have a synergic effect on nasopharyngeal carcinoma (NPC) therapy.

Kaliberov et al., (2006) utilized adenoviral vectors encoding the CD gene (Ad-CD) and CD-UPRT fusion gene (Ad-CD:UPRT) for combination therapy studies with TRA-8 monoclonal antibody. The role of TRA-8 is, it specifically bound to death receptor 5, one of two death receptors bound by tumor necrosis factor-related apoptosis-inducing ligand (TRAIL). The *in vitro* cytotoxicity was evaluated for the combination of Ad-CD:UPRT and TRA-8 against human pancreatic cancer and glioma cell lines. The results indicated that Ad-CD:UPRT infection had more 5-FC mediated cell killing efficacy as compared to Ad-CD. Animal studies with the combination of Ad-CD:UPRT/5-FC and TRA-8 showed significant inhibition of

TH-0560_03610605

tumor growth of pancreatic and glioma xenografts, when compared to either agent alone or no treatment. The combination of Ad-CD:UPRT/5-FC with TRA-8 produced an synergistic cytotoxic effect in cancer cells, which indicated that combined treatment using adenoviral-directed enzyme/prodrug therapy and immunotherapy has potential to become an alternative method of cancer therapy.

2.5 Anticancer Compound - Curcumin

Curcumin (diferuloylmethane), a phenolic compound from the rhizome of the plant *Curcuma longa* is a widely used as coloring agent in food, which has anti-inflammatory, antioxidant and anticancer properties. Jiang et al., (1996) demonstrated the concentration and time dependent of curcumin induced cell shrinkage, chromatin condensation, and DNA fragmentation, characteristics of apoptosis, in mouse embryo fibroblast NIH 3T3, mouse sarcoma S180, human colon cancer cell HT29, human kidney cancer cell 293, and human hepatocellular carcinoma HepG2 cells.

Pillai et al., (2004) investigated curcumin induced apoptosis in human lung cancer cell lines A549 (p53 proficient) and H1299 (p53 null mutant). They observed that the expression of p53, bcl-2, and bcl X_L was decreased after 12 h exposure of 40 μM curcumin. They demonstrated the p53 independent induction of apoptosis in lung cancer cells.

Belakavadi and Salimath (2005) investigated the effect of curcumin on the activation of apoptotic and anti-angiogenic pathways in Ehrlich Ascites Tumor (EAT) cells. Treatment with curcumin *in vivo* resulted in inhibition of proliferation of EAT cells and ascites formation, induction of apoptosis, nuclear condensation, DNA fragmentation and translocation of caspase-activated DNase (CAD) to nucleus.

TH-0560_03610605

Curcumin-induced apoptosis was mediated through caspase-3 activation. In curcumin-treated mice, CD31 immunohistological staining of peritoneum sections suggested its efficacy in acting as anti-angiogenic compound in EAT cells by inhibiting proliferation of endothelial cells in mouse peritoneum. Further their immunoflurescence studies of NF-kB (Nuclear Factor kB) in curcumin-treated cells revealed that the inhibition of nuclear translocation of NF-kB p65, a transcription factor required for VEGF gene expression. Taken together, the results suggested a potential clinical application of curcumin, as both proapoptotic and antiangiogenic compound in combination with conventional chemotherapeutic agents.

2.6 Bactericidal and Cytotoxicity of Silver Nanoparticles

At present, nanomaterials such as nanotubes, nanowires, fullerene derivatives and quantum dots are very important in the creation of new types of analytical tools for biotechnology and the life sciences. In spite of the wide application of nanomaterials, the information pertaining to their impact on human health and the environment is still lacking. Thus, there is an immediate need to study the toxicity of NPs for risk assessment of nanomaterials.

Sondi and Salopek-Sondi (2004) demonstrated the antimicrobial activity of Ag NPs against *E. coli* by treated with different concentrations of nanosized silver particles. Their SEM and TEM observations showed that bactericidal activity of Ag NPs was due to the damage of cell wall that led to increase in permeability and cell death. They suggested that nontoxic nanomaterials prepared in a simple and cost-effective manner, would be suitable for the formulation of new types of bactericidal agents.

TH-0560_03610605

Braydich-Stolle et al., (2005) assessed a concentration-dependent toxicity of different types of NPs in mouse spermatogonial stem cell line by light microscopy, and by cell proliferation and cytotoxicity assays. Their *in vitro* studies showed that Ag NPs were the most toxic and the molybdenum trioxide (MoO_3) NPs were the least toxic.

Hussain et al., (2005) evaluated the toxic effects of metal and metal oxide NPs using the rat liver derived cell line (BRL 3A). They studied the toxicity, using different sizes of NPs such as silver (Ag; 15, 100 nm), molybdenum (MoO_3; 30, 150 nm), aluminum (Al; 30, 103 nm), iron oxide (Fe_3O_4; 30, 47 nm), and titanium dioxide (TiO_2; 40 nm). They also evaluated the toxicity of relatively larger particles of cadmium oxide (CdO; 1 μm), manganese oxide (MnO_2; 1-2 μm), tungsten (W; 27 μm), and compared their toxicity with respect to the different sizes as well as different chemical compositions of NPs. The toxicity of NPs was evaluated by, microscopic observation of cellular morphology, mitochondrial function (MTT assay), membrane leakage of lactate dehydrogenase (LDH assay), reduced glutathione (GSH) levels, reactive oxygen species (ROS), and mitochondrial membrane potential (MMP) were assessed under control and exposed conditions. Their experimental results showed that mitochondrial function was significantly reduced in cells exposed to Ag NPs at 5-50 μg/mL. However, Fe_3O_4, Al, MoO_3 and TiO_2 had no considerable effect at lower doses (10-50 μg/mL), while there was a significantly increase of toxic effect at higher levels (100-250 μg/mL). LDH leakage increased significantly in cells exposed to Ag NPs (10-50 μg/mL), while the other NPs exhibited LDH leakage only at higher doses (100-250 μg/mL). They found Ag NPs were highly toxic whereas, MoO_3 moderately toxic and Fe_3O_4, Al, MnO_2 and W were less toxic. The microscopic studies showed that NPs exposed cells at higher

TH-0560_03610605

doses displayed cellular shrinkage, and changed to an irregular shape. Their experimental results on oxidative stress exhibited significant depletion of GSH level, reduced mitochondrial membrane potential and increase in ROS levels, which suggested high cytotoxicity of Ag (15, 100 nm) in liver cells.

2.7 Bystander Effects

A major constraint in cancer gene therapy, specifically for GDEPT, is ineffective gene delivery and expression, which can be overcome by using suicide genes with strong bystander effect. Moolten (1986) first described the bystander effect as, the extension of cell killing effects of the active drug to non-transfected adjacent tumor cells. This effect is due to the transfer of the toxic antimetabolites from transfected cells to adjacent non-transfected cells through gap junctions; (Dilber et al., 1997; Mesnil et al., 1996; Touraine et al., 1998), apoptotic vesicles (Colombo et al., 1995) or by passive diffusion (Greco et al., 2000; Stribbling et al., 2000). The bystander effect of CD/5-FC is not dependent upon gap junctions (Lawrence et al., 1998) and it produced very high bystander effects (Nishihara et al., 1998; Trinh et al., 1995) as compared to the TK/GCV combination. The strong bystander effect of CD/5-FC could be due to the small size uncharged 5-FU molecule is capable to undergo non-facilitated diffusion diffuse through cellular membranes.

Denning and Pitts (1997) studied the therapeutic effect of two suicide genes herpes simplex virus TK/GCV and thymidine phophorylase/5'-deoxy-5-fluorouridine (tp/DFUR) and also demonstrated the bystander effect in human and rodent cell lines by mixed cultures of cells with and without the suicide gene, death occurred in both cell types. They also observed that TK/GCV required gap junctional intercellular communication (GJIC) to exert bystander effect whereas tp/DFUR system exerted a

TH-0560_03610605

medium-mediated bystander effect, independent of GJIC. Their results showed that combining TK/GCV and tp/DFUR suicide gene systems was more effective than either therapy alone *in vitro*. Matono et al., (2003) suggested that GJIC could be chemically enhanced with retinoic acid treatment to potentiate the HSV-TK/GCV suicide gene therapy.

Lee et al., (2006) explored the CD/5-FC system, which exert a gap junction independent bystander effect by diffusion of the cytotoxic metabolite 5-fluorouracil (5-FU) to kill the untransfected neighboring cells. They fused the *Saccharomyces cerevisiae* CD to the HSV-1 tegument protein vp22 and demonstrated that fusion of vp22 to CD resulted in CD translocation, which led to augment conversion of 5-FC to 5-FU and improved the therapeutic effect *in vivo*.

2.8 Apoptosis

Apoptosis is a programmed cell death mechanism to replenish aged or injured cells (Figure 2.1). Identifying the genes involved in apoptosis, their mechanisms of action and structures of apoptotic regulatory and effector proteins, has laid a base for the discovery of drugs, some of which are now being evaluated in human clinical trials (Reed 2002). Advancement in understanding the molecular mechanisms of drug induced DNA damage leading to apoptotic death has helped in designing new drugs with potentially more selective approaches for cancer treatment. Several of these strategies use proapoptotic factors that sensitized tumor cells to the cytotoxic actions of traditional cancer chemotherapeutic drugs (Waxman and Schwartz 2003).

Tomicic et al., (2002) explored the molecular mechanism of GCV-induced cell death. They investigated the mechanism of apoptosis triggered by GCV using a stably transfected CHO cells with HSV-1 TK. GCV- induced DNA instability correlated

TH-0560_03610605

with the declined Bcl-2 level and caspase-9/-3 activation. Further the reason for declined level of Bcl-2 was due to cleavage of the protein by caspase-9, which was confirmed by using caspase inhibitors and transfection with trans-dominant negative caspase expression vectors. The cleavage of Bcl-2 resulted in the appearance of a pro-apoptotic 23 kDa Bcl-2 fragment and in excessive cytochrome c release, dephosphorylation of BAD, PARP cleavage and finally led to degradation of DNA. GCV-induced apoptosis was mainly by activating the mitochondrial damage pathway and independent of p53. GCV induced apoptosis was reported to be accelerated by caspase-9 mediated cleavage of Bcl-2. Kurozumi et al., (2004) elucidated 5-FC/CD gene therapy-induced cell death.

In summary, the literature review elaborated therapeutic effect of different suicide genes, their limitations and advantages. Till now, there is a very little focus on non-viral based suicide gene delivery as well as non-invasive quantitation of gene expression. Hence, there is a necessity for non-viral based gene delivery methods to

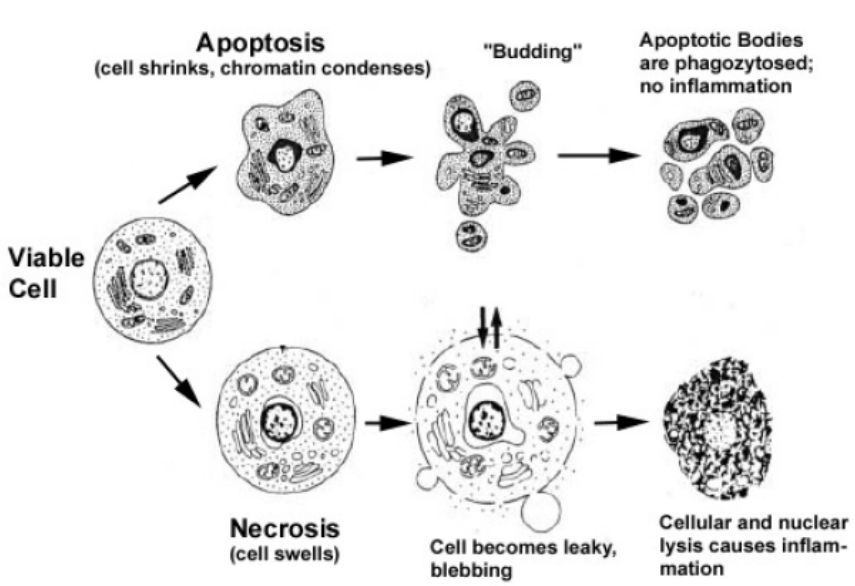

Figure 2.1: Features of the apoptotic and necrotic cell death process. *(Source: Andreas Gewies (2003), ApoReview - Introduction to Apoptosis, 1-26.)*

TH-0560_03610605

attain high therapeutic effect with no safety risks and also non-invasive based approach to study the transgene expression. The combination therapies, which enhance the therapeutic effect of suicide gene, focus mainly on combining radiation therapy with suicide genes. The combination therapy with conventional and non-conventional drug is also worth evaluating, due to the limitations and drawbacks of radiation therapy. The complete success of suicide gene therapy depends on its bystander effect, but very little details are available on CD-UPRT bystander effect, which needs to be further explored for better understanding the magnitude of therapeutic effect. The details about the molecular mechanism of TK gene mediated cell death are currently available, but the complete molecular mechanism of CD, UPRT and CD-UPRT remains to be investigated thoroughly. With these observations and understanding from the literature, the scope for further research along the stream was identified, as listed in section 1.1. The experimental investigations, analysis and the inferences drawn to achieve the targeted goal are mentioned in detail in the following chapters.

TH-0560_03610605

3

MATERIALS AND METHODS

3.1 Cell Culture

HT29 (Human colon adenocarcinoma), BHK21 (Baby Hamster Kidney), HEK293 (Human Embryonic Kidney) and Hep3B (Human hepatoma) were obtained from the cell repository of National Centre for Cell Science, India. The cell lines were routinely propagated in DMEM medium supplemented with 10% FBS, 50 U/mL penicillin and 50 mg/mL streptomycin. Cells were maintained at 37 ºC in a humidified atmosphere with 5% CO_2.

3.2 Recombinant Plasmids and Stable Cell Lines

3.2.1 Construction of Recombinant Plasmid Vector

The suicide genes namely CD or UPRT or CD-UPRT gene was PCR amplified from pORF-codA::upp (*InvivoGen*) plasmid. The codA and upp stands for bacterial cytosine deaminase (CD) gene and uracil phosphoribosyl transferase (UPRT) gene, respectively. The linker primers mentioned in the Table 3.1 were used for PCR amplification at the following cycle conditions: denaturation at 94 ºC for 30s,

TH-0560_03610605

annealing at 55 ºC for 1 min and extension at 72 ºC for 1 min. The amplified gene was restriction digested with *Nco*I and *Nhe*I enzymes and cloned into the *Nco*I and *Nhe*I restriction sites of the pVITRO2-GFP/LacZ (*InvivoGen*) replacing LacZ gene and also cloned into the pORF-codA::upp plasmid replacing codA::upp fusion gene. The gene and vector was ligated using T4 DNA ligase at 12 ºC for overnight. Then, the ligated mixture was transformed into competent *E. coli* DH5α cells (Chung et al., 1989) and the recombinant clones were selected in LB hygromycin and LB ampicillin agar plates, according to their antibiotic resistance marker in the plasmid (Figure 3.1). The recombinant clones were confirmed by restriction enzyme digestions and sequencing. The CD and CD-UPRT genes were cloned under the control of ferritin promoter (Figure 3.1 A). These recombinant clones named as pCD-GFP and pVITRO2 GFP/CD-UPRT were used in Chapters 4 & 6, respectively. Similarly, CD, UPRT and CD-UPRT genes were cloned under the control of elongation factor (EF-1α) promoter (Figure 3.1 B). The corresponding recombinant clones were named as pCD, pORF UPRT and pCD-UPRT was used in Chapters 4, 5 & 7, respectively.

Table 3.1: Linker primers for CD, UPRT and CD-UPRT

Gene	Primers
CD (1.2kb)	CD1: (5'-CCACCATGGTGTCGAATAACGC-3', with *Nco*I linker) CD2: (5'-CGGCTAGCGCCATTAGCTCCGCTG-3', with *Nhe*I linker)
UPRT (651bp)	UPRT1:(5'-GCCCATGGATGGCTAAGATCGTGGAAG-3',with *Nco*I linker) UPRT2: (5'-GAGCTAGCGAATTTCGACAAGC-3', with *Nhe*I linker)
CD-UPRT (1.9kb)	CD1: (5'-CCACCATGGTGTCGAATAACGC-3', with *Nco*I linker) UPRT2: (5'-GAGCTAGCGAATTTCGACAAGC-3', with *Nhe*I linker)

TH-0560_03610605

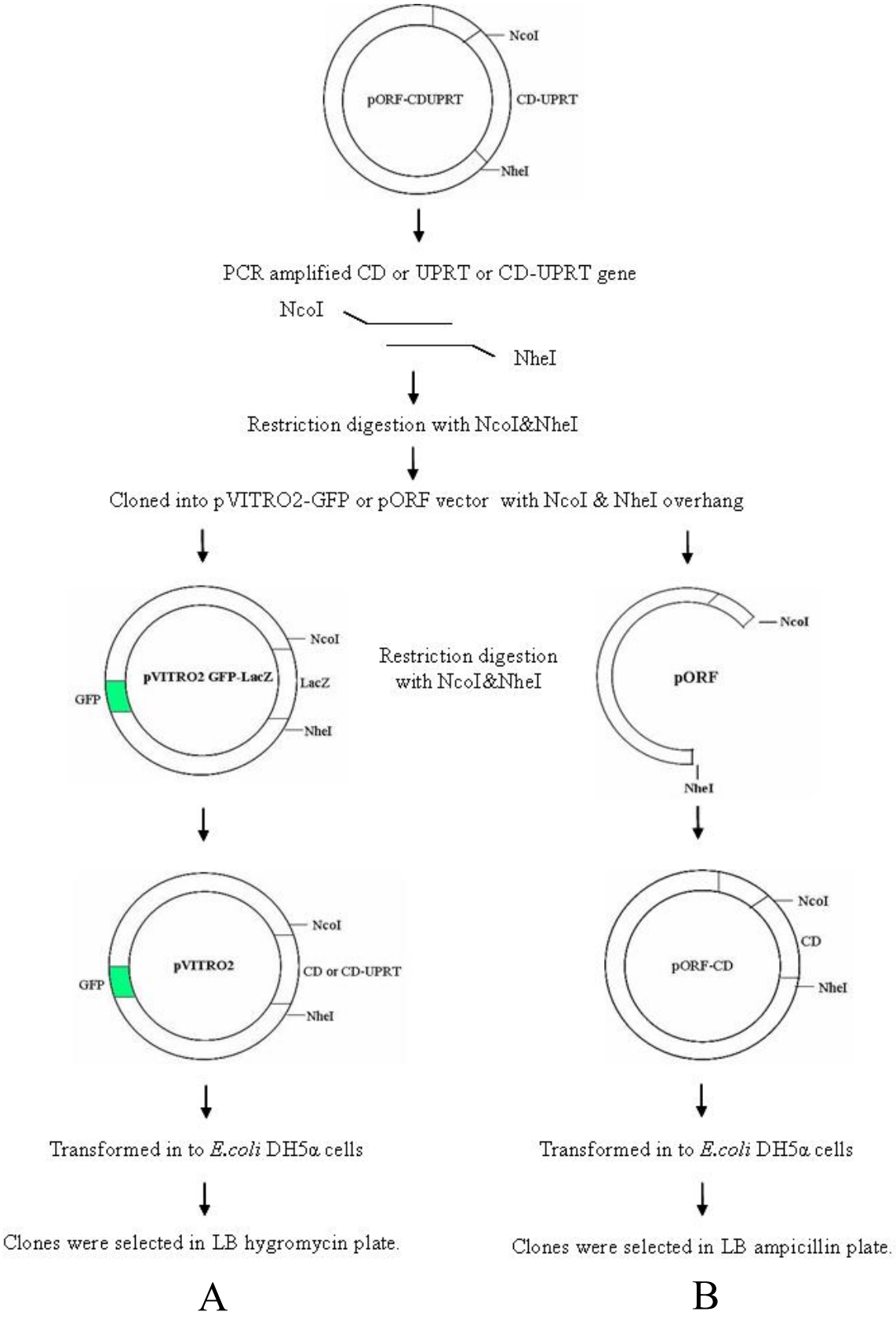

Figure 3.1: Schematic representation of plasmid vector construction. **(A)** Plasmid with ferritin promoter. **(B)** Plasmid with elongation factor (EF-1α) promoter.

TH-0560_03610605

3.2.2 Electroporation

Cells grown up to 70% confluent was trypsinized and resuspended in serum free medium. A 100 µL of resuspended cells were electroporated with plasmid (2 µg DNA / 35 mm plate) in a 0.2 cm electroporation cuvette using BIO-RAD Gene Pulser Xcell. For BHK21 and HEK293 cells, a square wave of 25 ms at 140 V was used. For HT29 and Hep3B cells, an exponential wave of 500 µF at 160 V was used. After electroporation, cells were resuspended in DMEM medium and added to 6 well or 96 well plates according to the experimental requirement.

3.2.3 Generation of CD-UPRT::GFP Expressing Cell Lines

pVITRO2-GFP/CD-UPRT construct (Gopinath and Ghosh, 2007b) was electroporated into BHK21 cells to generate stable transfectants. Stable clones were selected by the GFP as well as Hygromycin resistant gene expression and maintained under Hygromycin B selection (200-400 µg/mL).

3.3 Bactericidal Activity of Silver Nanoparticles

3.3.1 *E. coli* GFP Construct

The recombinant GFP expressing *E. coli* (DH5α) was generated by cloning the GFP gene into an ampicillin-resistant pUC-derived plasmid vector (GeNei ™ GFP cloning kit).

3.3.2 Determination of Minimum Inhibitory Concentration and Minimum Killing Concentration of Ag NPs

GFP-expressing *E. coli* DH5α cells (10^8 CFU) were grown in the presence of 5.66, 11.32, 16.98, 22.64, and 28.3 µg/mL of preformed Ag NPs in the LB medium.

TH-0560_03610605

MIC and MKC values were determined in the following ways. MIC is the minimal inhibitory concentration of an antimicrobial substance. Concentrations of the antimicrobial test compound below the MIC failed to inhibit microbial growth. Recombinant GFP expressing bacterial cells were grown overnight in the presence various concentrations of Ag NPs. Cell growth was observed by the turbidity of the culture. The lowest concentration of Ag NPs, at which no visual turbidity could be observed, represented the MIC of Ag NPs. The cultures that lacked turbidity were reinoculated into fresh LB media to test their ability to grow. MKC is the minimal killing concentration of the test compound that prevented growth of the bacterial cells following reinoculation, as observed by the lack of visual turbidity.

3.3.3 Optical Density Measurement and Bacterial Cell Viability Count

GFP recombinant *E. coli* (DH5α) cells were grown overnight in 300 mL of LB (100 μg/mL) ampicillin medium. The cells were separated by centrifugation, resuspended in 3 mL of LB medium, inoculated to 100 mL of fresh LB medium (control), and the LB medium with preformed Ag NPs at two different concentrations (56.5 and 84.83 μg/mL). Cells were grown at 37 °C and 180 rpm shaking condition. Samples, prepared at several concentrations of Ag NPs, were withdrawn periodically to measure the Optical Density (OD) at 595 nm using a UV-Vis spectrophotometer (SPEKOL 1200, Analytikjena, Germany). The cell viability count was performed by serial dilution of the pregrown culture followed by plating on a solid media (LB agar ampicillin plate). The viable cell number was recorded by counting the number of bacterial colonies grown on the plate multiplied by the dilution factor and expressed as CFU/mL.

TH-0560_03610605

3.3.4 Plasmid DNA and Protein Gel Electrophoresis

Plasmid DNA carrying GFP gene was isolated from control and Ag NPs treated *E. coli* cells by an alkaline lysis method and analyzed by agarose gel electrophoresis (Sambrook and Russell 2001) For the whole cell protein analysis, cells from the control and treated samples (1 mL each) were separated by centrifugation, washed with phosphate-buffered saline and resuspended in 200 µL of Laemlli's buffer [60 mM Tris-HCl (pH 6.8), 25% glycerol, 2% SDS, 14.4 mM 2-mercaptoethanol, 0.1% bromophenol blue]. Whole cell lysate was prepared by incubating the samples in boiling water for 5 min. A 10 µL aliquot of each sample was subjected to SDS-PAGE. Protein profiles obtained from the control and treated samples were visualized by staining the gel in Coomasie Brilliant Blue R-250 solution.

3.4 Microscopic Analysis

3.4.1 Fluorescence Microscopic Analysis

The bactericidal activity of Ag NPs on GFP expressing *E. coli* cells was determined by observing the treated and untreated samples under an epifluorescence microscope (Axioskop2MAT, Karl Zeiss) at different time intervals. Individual aliquots of 50 µL were withdrawn from the appropriate medium and then placed over microscope slides, which were air-dried for further observation. The excitation wavelength was 445-495 nm, and the observation filter had a long-pass filter wavelength above 515 nm. Similarly, GFP expression of the transfected cells was observed under inverted fluorescent microscope (Nikon Eclipse TS100).

3.4.2 Phase-Contrast Microscopic Analysis

Ag NPs presynthesized in cell culture DMEM medium was added to BHK21 and HT29 cells at the following concentrations: 2.75, 5.5, 11.0, 27.5, 44.0 and

TH-0560_03610605

55.0 µg/mL of Ag NPs. After incubation for 12 h, the cytotoxicity was observed by the changes of cell morphology under inverted phase-contrast microscopy (Nikon Eclipse TS-100).

3.4.3 Confocal Microscopic Analysis

Apoptotic cell and nuclear morphology was studied by staining of nuclei with Acridine orange (AO) / Ethidium bromide (EB) (100 µg/mL in PBS) and observed the treated and untreated cells under confocal microscope (LSM 510 Meta, Carl Zeiss, Germany). AO staining showed green fluorescence at 488 nm excitation with a band pass filter ranging between 505-530 nm, where as the EB staining showed red fluorescence at 585 nm long pass filter. Final images were generated by superimposition of both green and red fluorescence. Three represented pictures of each sample were chosen for counting, in order to quantify the percentage of live, apoptotic and necrotic cells. GFP fluorescence of the transfected cells and clone cells was also observed at 488 nm excitation with the 505-530 nm band pass filter.

3.4.4 Scanning Electron Microscopic Analysis

The transfected cells grown in 6 well tissue culture plates were treated with test compound. The treated cells and untreated cells were washed gently with PBS. The wells (containing cells) were cut out from the plate with a heated metal cutter, immediately dried and coated with gold film in the sputter coater. Finally, the cell morphology changes were recorded in LEO 1430VP SEM instrument at 15 – 20 kV.

3.4.5 Atomic Force Microscopic Analysis

BHK21 CD-UPRT::GFP cells were seeded on poly-L-lysine-coated cover

TH-0560_03610605

slips which were placed in six-well plates. After treatment with 5-FC for 48 h, the cells attached to the cover slips were gently rinsed with PBS to remove loosely attached cells and air-dried. AFM imaging was performed on an AFM (PicoScan™ 2500, Molecular imaging corporation-USA) operated in a non-contact mode. Measurements were carried out using silicon cantilevers with a spring constant of 21 N/m and a resonance frequency of 160 kHz. The images were acquired at a scan field of 10 μm × 10 μm. The three-dimensional images were obtained using the software's; Picoscan 5.3.3 and SPIP 4.6.3.

3.4.6 Transmission Electron Microscopy Analysis

The effect of presynthesized Ag NPs on the bacteria was monitored by depositing 10 μL of Ag NPs treated bacterial sample on carbon-coated copper TEM grids followed by air-drying. Ag NPs treated *E. coli* cells were analyzed by a Hitachi H-600 TEM instrument operating at an accelerating voltage of 200 keV.

Similarly, HT29 cells were treated with Ag NPs for 0 h and 16 h, washed gently with PBS and removed from culture dish by rubber policeman. Cells were then resuspended in sterile water and immediately 20 μL of the suspension was deposited on carbon-coated copper TEM grids followed by air-drying. TEM images of Ag NPs in DMEM media and on Ag NPs treated cells were analyzed by Jeol 2100 HR- TEM. Selected area diffraction (SAD) was observed by the TEM instrument operating at an accelerating voltage of 200 keV.

3.5 X-Ray Diffraction Measurement

X-Ray Diffraction (XRD) was performed to confirm the presence of Ag NPs in the cell membrane. Cells treated with Ag NPs for 12 h was centrifuged at 20 000 *g*

TH-0560_03610605

for 20 min. The cell pellet was washed twice with PBS and spread on a glass slide. The X-ray diffractogram of the presynthesized Ag NPs in DMEM, Ag NPs treated BHK21 cells and HT29 cells was recorded using a Bruker Advance D8 XRD machine (Cu α source with 1.5406 Å wavelength)

3.6 Spectrophotometric and Chromatographic Analysis

3.6.1 Fluorescence Spectrophotometric Analysis

Cells transfected with pCD-GFP plasmid were grown up to 24 h, scraped off and resuspended in PBS. The GFP fluorescence was quantified using a fluorescence spectrophotometer (Fluromax 3, Jobin yvon) at 488 nm excitation wavelength. The untransfected cells, which did not express GFP was used as control.

3.6.2 High-Performance Liquid Chromatographic Analysis

A reverse phase HPLC based assay was conducted to assess the functionality of CD and CD-UPRT by measuring the catabolism of the prodrug 5-FC to 5-FU and its derivatives. BHK21 and HT29 cells transfected with pCD and pCD-UPRT were lysed by brief sonication in ice cold PBS. Cell debris was removed by centrifugation (15 000 *g*, 5 min) and the total protein content of the supernatants was determined by UV spectrometer [protein concentration (mg/mL) =1.55 × A_{280}-0.76 × A_{260}]. Then, 100 µL (0.3 mg) of the supernatant were incubated with 900 µL of 0.5 mM 5-FC at 37 ºC for 24 h and stored at −20 ^{o}C, after heat inactivated for 10 min at 85 ºC. HPLC (PerkinElmer series 200) was performed using a C18 column (250mm × 4.6mm × 5 µm) under isocratic conditions (0.05% trifluoroacetic acid in H_2O) at a flow rate of 0.7 mL/min to analyze 20 µL of samples. Absorbance was recorded at 275 nm.

TH-0560_03610605

3.7 Cell Viability and Cytotoxicity Assay

3.7.1 Cell Proliferation Assay

Cell proliferation was studied by measuring the mitochondrial activity using MTS assay (CellTiter 96 AQueous One Solution Assay kit, Promega, Madison, WI). MTS is 3-(4, 5-dimethylthiazol-2yl)-5-(3-carboxymethoxyphenyl)-2-(4-sulfophenyl)-2H-tetrazolium compound. Transfected cells were seeded in 96-well microplates at a density of 1 x 10^4 cells, and treated with various concentrations of test compounds according to the respective experimental requirement. Finally, 10 µL of AQueous One solution was directly added to the well and incubated for 2 h and the absorbance was measured at 490 nm in a microplate reader BIO-RAD, USA (Model 680). The absorbance of formazan product formed is directly proportional to the number of living cells in culture. The relative cell viability (%) related to control wells containing cell culture medium without test compounds was calculated by $(A)_{test}/(A)_{control}$ x 100, where $(A)_{test}$ is the absorbance of the test sample and $(A)_{control}$ is the absorbance of the control untreated sample.

3.7.2 Cytotoxicity Assay

Cytotoxicity due to test compounds was assayed by measuring the activity of lactate dehydrogenase (LDH) enzyme released in culture media using CytoTox 96 Non-Radioactive Cytotoxicity Assay Kit (Roche Applied Science). Aliquots (50.0 µL) of culture media was collected at different time points, diluted with 1: 1 fresh medium and incubated with 50.0 µL of tetrazolium salt (INT) solution (substrate) for 30 min at room temperature. LDH converted INT to the red formazan product, which was detected at 490 nm with a microplate reader BIO-RAD, USA (Model 680). LDH leakage (%) related to control wells containing cell culture medium without test

TH-0560_03610605

compounds was calculated by $[A]_{test}/[A]_{control}$ x 100, where $[A]_{test}$ is the absorbance of the test sample and $[A]_{control}$ is the absorbance of the untreated control sample.

3.8 Molecular Analysis

3.8.1 RNA and DNA Extraction

BHK21 and HT29 cells were grown confluent in six well plates were treated with respective test compounds according to the experimental requirement. Treated cells were lysed with 1 mL tri reagent / single well of a six well plate. Cell lysate were passed through a pipette several times and incubated at 15 ºC for 5 min. After incubation, 0.2 mL of chloroform was added and shaked vigorously for 15 s and incubated at 15 ºC for 3 min. Then the samples were centrifuged at 12 000 *g* for 15 min at 4 ºC and the colorless aqueous phase was transferred to a fresh tube for RNA isolation and the interphase was stored for subsequent isolation of DNA. RNA was precipitated from the aqueous phase by adding 0.5 mL isopropanol and incubated at 15 ºC for 10 min. After incubation, centrifuge it at 12 000 *g* for 10 min at 4 ºC and the RNA pellet was washed with 1 mL of 75% ethanol. RNA pellet was air dried and dissolved in 20 µL of RNase free water by passing the solution a few times through pipette tip and incubated for 10 min at 55 ºC.

To precipitate the DNA from the interphase, 0.3 mL of absolute ethanol was added, mixed by inversion and allowed to stand for 2-3 min at room temperature, centrifuged at 2 000 *g* for 5 min at 4 ºC. DNA pellet was washed twice with 1 mL of 0.1 M Sodium citrate in 10%ethanol solution. During each wash, the DNA was allowed to stand for at least 30 min, then centrifuged at 2 000 *g* for 5 min at 4 ºC. DNA pellet was resuspended in 1 mL of 75% ethanol and allowed to stand for 20 min at room temperature and centrifuged at 2 000 *g* for 5 min at 4 ºC. The DNA pellet was

TH-0560_03610605

air dried and dissolved in 100 µL of TE (20 mM Tris-Cl, 1 mM EDTA pH 8.0) buffer by passing the solution a few times through pipette tip and incubated for 10 min at 55 ºC. Then, finally centrifuged at 12 000 *g* for 10 min to remove any insoluble material and the supernatant was transferred to a new tube. The isolated DNA and RNA were stored at -20 ºC.

3.8.2 PCR and RT-PCR analysis

Total DNA and RNA extracted with Tri reagent from the treated as well as untreated control cells were used for PCR and RT-PCR analysis with the primers mentioned in Table 3.1. PCR cycle conditions were as follows: denaturation at 94 ºC for 30 s, annealing at 55 ºC for 1 min and extension at 72 ºC for 1 min. RT-PCR was performed with the same primers (Table 3.1) according to the manufacturer's instructions using Enhanced Avian HS RT-PCR kit (Sigma, USA) in Gene Amp PCR system 9700, Applied Biosystems. RT- PCR cycle conditions are as follows: First strand synthesis at 42 ºC for 50 min, denaturation/ RT inactivation at 94 ºC for 2 min, For cycles 1-35: Denaturation at 94 ºC for 15 s, Annealing at 55 ºC for 30 s, Extension at 68 ºC for 1 min and final extension at 68 ºC for 5 min

3.8.3 Semi-quantitative RT-PCR

Apoptotic signaling genes was studied using semi-quantitative RT-PCR. The housekeeping β actin gene was used as internal control. Total RNA was isolated using Tri reagent and cDNA was generated by reverse transcription of 3 µg of total denatured RNA. Reverse Transcription was performed at 37 ºC for 50 min using M-MLV Reverse Transcriptase (Sigma, USA) in a total mixture of 20 µL. Two microlitres from the above RT product was used for PCR reaction. PCR was carried

TH-0560_03610605

out using the gene specific upstream and downstream primers in Gene Amp PCR system 9700, Applied Biosystems. Initial denaturation at 94 ºC for 2 min was followed by a PCR cycle of denaturation at 94 ºC for 15 s, annealing at 55 ºC for 30 s, extension at 68 ºC for 1 minute and final extension at 68 ºC for 5min . The PCR products were separated on a 1.2% agarose gel and stained with ethidium bromide. The primer sequences used were mentioned in Table 3.2.

Table 3.2: Primers for apoptotic signaling genes.

Genes	Primers
β–actin	Forward: 5'-CTGTCTGGCGGCACCACCAT-3' Reverse: 5'-GCAACTAAGTCATAGTCCGC-3'
Bcl-2	Forward: 5'AGATGTCCAGCCAGCTGCACCTGAC-3' Reverse: 5'-AGATAGGCACCCAGGGTGATGCAAGCT-3'
Caspase-3	Forward: 5'-TTTGTTTGTGTGCTTCTGAGCC-3' Reverse: 5'-ATT CTGTTGCCACCTTTCGG-3'
Bak	Forward: 5'-TCCAGATGCCGGGAATGCACTGACG-3' Reverse: 5'-TGGTGGGAATGGGCTCTCACAAGG-3'
Bcl X_L	Forward: 5'-ATGGCAGCAGTAAAGCAAGCGC-3' Reverse: 5'- TTCTCCTGGTGGCAATGGCG-3'
C-myc	Forward: 5'-CCAGGACTGTATGTGGAGCG-3' Reverse: 5'-CTTGAGGACCAGTGGGCTGT-3'
p53	Forward: 5'-TGGCCCCTCCTCAGCATCTTAT-3' Reverse: 5'-GTTGGGCAGTGCTCGCTTAGTG-3'
Bad	Forward: 5'-CCTTTAAGAAGGGACTTCCTCGCC-3' Reverse: 5'-ACTTCCGATGGGACCAAGCCTTCC-3'
Bax	Forward: 5'-AAGCTGAGCGAGTGTCTCAAGCGC-3' Reverse: 5'-TCCCGCCACAAAGATGGTCACG-3'

3.8.4 BrdU Cellular DNA Fragmentation ELISA

A cellular DNA fragmentation ELISA kit (Roche Diagnostics GmbH, Mannheim, Germany) was used to determine the amount of 5'-bromo-2'-deoxyuridine

TH-0560_03610605

(BrdU) labeled fragmented DNA (Figure 3.1). The assay was performed according to the manufacturer's instructions. The cell number adjusted to 2 x 10^5 cells. cells were incubated with 10 µM BrdU labeling solution for 20 h in a humidified atmosphere in 5% CO_2 at 37 ºC. After 20 h, BrdU incorporation was terminated by aspirating the medium. Cells were washed with PBS, trypsinized and centrifuged with 10 mL of DMEM at 250 *g* for 6 min. Cell pellet was resuspended in serum free medium for transfection with respective plasmid according to the experimental requirement. The transfected and untransfected cells were allowed to grow in 96 well plates for 12-24 h. Followed by treatment with test compounds, cells were collected, lysed and centrifuged at 250 *g* for 10 min. Aliquots of the cell lysate were stored at -20 ºC for further analysis. Another microtitre plate was coated with 100 µL of anti-DNA antibody coating solution for 1 h at 37 ºC. After 1 h, the coating solution was removed and washed thrice with 200 µL of washing solution (containing EDTA, Tween 20). Then the 100 µL sample which was stored at -20 ºC was thawed and added to the anti-DNA antibody coated well and incubated at 25 ºC for 90 min. After incubation, wells were washed thrice with 200 µL of washing solution and leave the washing solution in the well after the last wash. The uncovered microtitre plate were placed in a microwave oven along with a 500 mL beaker containing 300 mL water in the microwave oven and irradiated for 5 min on medium power 500 W. After irradiation the plate were kept at -20 ºC for 10 min. Then the fluid was removed from the wells and 100 µL of anti-BrdU-peroxidase conjugate solution was added to each well and incubated at 25 ºC for 90 min. Plates were washed thrice with washing solution to remove the unbound antibody. Then 100 µL of substrate was added and incubated in the dark until color development was sufficient. A 25 µL of stop solution (containing

TH-0560_03610605

H_2SO_4 solution) was added and further incubated for 1 min, and the absorbance was measured at 450 nm using microplate reader BIO-RAD, USA (Model 680).

3.8.5 DNA Laddering

DNA fragmentation visualized by agarose gel electrophoresis is considered as a biochemical hallmark for apoptosis (Figure 3.3).

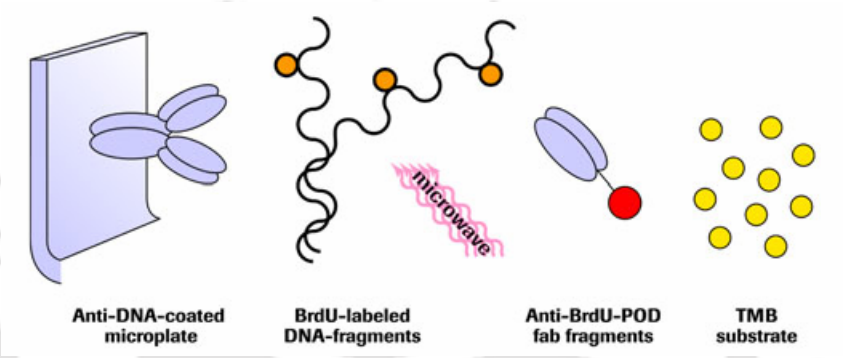

Figure 3.2: Schematic representation of BrdU labeled DNA fragmentation ELISA *(Source: Roche Applied science catalogue).*

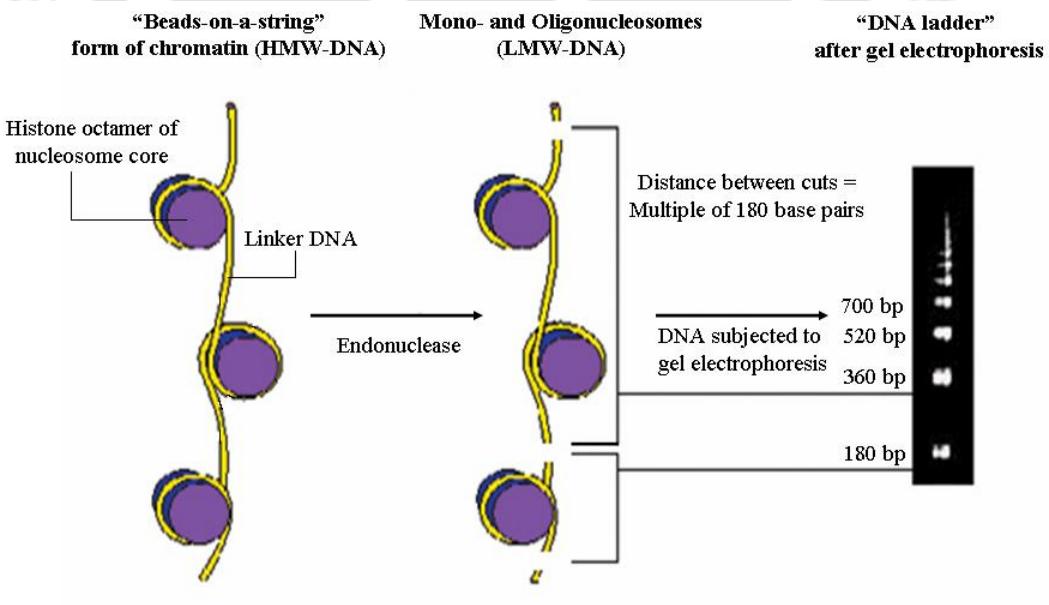

Figure 3.3: Schematic representation of DNA laddering due to internucleosomal DNA cleavage *(Source: Roche Applied science catalogue).*

TH-0560_03610605

BHK21 and HT29 cells grown in 35 mm dishes were treated with respective test compounds and the cells were harvested and centrifuged at 1000 *g* for 6 min at 4 °C. The cells were lysed with buffer containing 5 mM Tris-HCl, pH 8.0, 20 mM EDTA, and 0.5% Triton X-100, and kept on ice for 20 min. After centrifugation at 12 000 *g* for 30 min at 4 °C, the fragmented DNA in the supernatant was extracted with phenol/chloroform/isopropyl alcohol (25:24:1, v/v) and precipitated with absolute ethanol and 2.5 M ammonium acetate for 1 h to overnight at -80°C. Then the DNA was pelleted by centrifuged at 12 000 *g* for 10 min at 4 °C and washed once with 70% ethanol and resuspended in TE buffer containing RNaseA (100 µg/mL) and incubated at 37 °C for 1 h to remove RNA. The DNA fragments were separated by 1.2% agarose gel electrophoresis and stained with ethidium bromide.

3.9 Statistical Analysis

Data represented were the mean and standard deviation of three independent experiments. Statistical analysis was done using one way analysis of variance (ANOVA) followed by Dunnett's method for multiple comparisons were calculated for the appropriate experiments using GRAPHPAD PRISM software (Version 4). The $p<0.05$ were considered as significant.

TH-0560_03610605

4

5-FC/CD GENE THERAPY

Overview

Recently, much attention has been given for development of nonviral gene transfer vectors as well as noninvasive probes for assessing the location, magnitude, and duration of transgene expression. Herein, a recombinant plasmid vector with cytosine deaminase (CD) suicide gene and green fluorescent protein (GFP) as reporter gene was constructed in a plasmid vector. CD is known to convert nontoxic prodrug 5-flurocytosine (5-FC) to toxic chemotherapeutic agent 5-flurouracil (5-FU), and its strong therapeutic effect depends on its high expression in different cell types. GFP expression has been used as a noninvasive probe for monitoring CD gene transfer and to investigate the mechanism of cell death. In the plasmid construct, the CD gene was cloned under two different promoters: human ferritin and elongation factor promoter. Ferritin promoter CD construct showed strong therapeutic effect was used for subsequent experiments.

CD gene transfer and its expression were confirmed by PCR and RT-PCR, respectively, whereas concentration dependent cell death was monitored by confocal

TH-0560_03610605

microscopic observation of GFP and cell viability assay (MTS). 5-FC/CD mediated apoptotic cell death was observed by microscopic experiments, DNA fragmentation ELISA, DNA laddering and expression of apoptotic genes. Experimental evidence revealed that the synergistic effect of curcumin on CD suicide gene enhanced its therapeutic efficacy.

Results and Discussions

4.1 CD-GFP Gene Transfer and its Expression

The application of viral vectors for gene transfer is limited due to the safety risks and high toxicity (Ghosh et al., 2006). However, nonviral vectors as an alternative approach of gene transfer reduce toxic effects. High efficiency of nonviral vectors could be achieved by electroporation technique (Somiari et al., 2000; Goto et al., 2000). Analysis of transgene expression is another major challenge, which can be overcome using GFP reporter gene systems that can be easily monitored non-invasively (Vooijs et al., 2002).

In the present study, a recombinant plasmid containing CD gene and GFP as reporter gene has been constructed. GFP has advantage over the other conventional non invasive methods, by its minimal photobleaching effect and simple molecular expression assays. The recombinant plasmid (pCD-GFP) was transferred to both cancer HT29 and non-cancer BHK21 cells by electroporation. After 48 h, high GFP expression was observed under confocal microscopy for both the cell types (Figure 4.1). The GFP expression from the plasmid was monitored by confocal microscopy, as a direct evidence of functional CD gene transfer by the same plasmid. In addition, CD gene transfer was quantitated by measuring the GFP fluorescence intensity (Richards et al., 2003) of the transfected cells using fluorescence

TH-0560_03610605

spectrophotometer, as shown in Figure 4.2. At 24 and 48 h post transfection the fluorescence intensity was almost same. GFP expression was an index to study the therapeutic potential of 5-FC/CD.

PCR analysis confirmed the CD gene transfer, where a 1.2 kb amplicon was obtained for BHK21 (lane 4) and HT29 cells (lane 5) in Figure 4.3, and the corresponding CD gene expression was confirmed by RT-PCR analysis (Xia et al., 2004) on total RNA of the transfected cells, as represented in lane 7 & 8 of Figure 4.3.

BHK21 and HT29 cells were transfected with pCD-GFP and treated with different concentrations of 5-FC (0, 5, 10, 20 and 50 mM) to study the therapeutic effect of CD gene. GFP fluorescence was used as a direct probe to monitor the therapeutic effect of 5-FC/CD using confocal microscope, as represented in Figure 4.4 (panel A-E for BHK21 and F-J for HT29 cells).Concentration dependent cell death was observed with a gradual decrease of fluorescence with more number of cells got detached and rounded off, due to the enhanced cytotoxic effect of 5-FC/CD (Ueda et al., 2001). This therapeutic effect of 5-FC/CD was further authenticated with the biochemical experiments.

4.2 Comparative Study of Promoter Strength on Cell Viability

To select a strong expression vector, a comparative study was performed between human ferritin promoter and EF-1α promoters on CD gene expression. The cell proliferation assay, which measures the activity of live mitochondria (Bernt et al., 2002), was used to evaluate cell viability at various concentrations of 5-FC for BHK21 and HT29 cell types, as shown in Figure 4.5 A & B. CD gene under human ferritin promoter showed more anti-cell proliferation activity as compared to the EF-1α promoter. Thus, the pCD-GFP construct, where CD gene under the control of

TH-0560_03610605

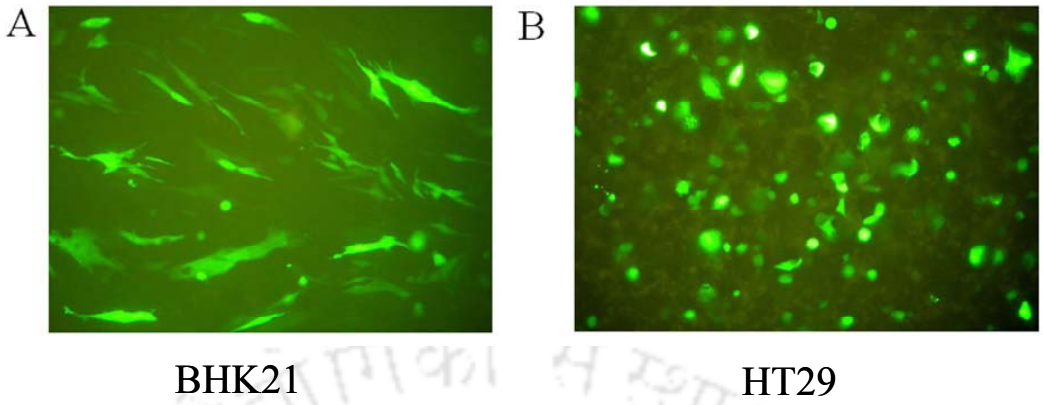

Figure 4.1: GFP expression of BHK21 and HT29 cells observed under confocal microscope at 48 h post transfection.

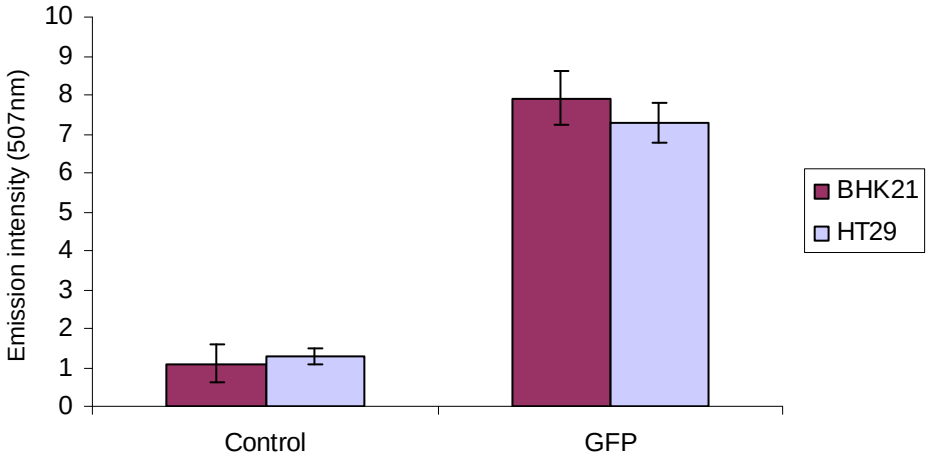

Figure 4.2: Fluorescence intensity measurement of GFP of the transfected cells at 24 h.

TH-0560_03610605

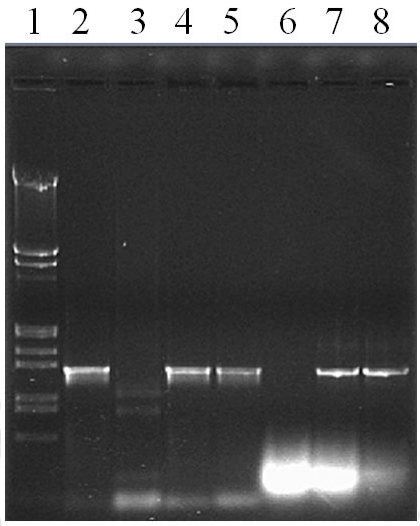

Figure 4.3: Agarose gel picture of PCR and RT-PCR analysis of the transfected cells. Cellular DNA & RNA extracted from the transfected cells were subjected to PCR (lane 2- 5) & RT-PCR (lane 6- 8) analysis. Lane 1: λ DNA/ *Eco*R I +*Hind* III marker; lane 2: 1.2 kb PCR amplicon of CD as positive control; lane 3 & 6: untransfected control BHK21 cells; lane 4 & 7: CD transfected BHK21cells; lane 5 & 8: CD transfected HT29 cells.

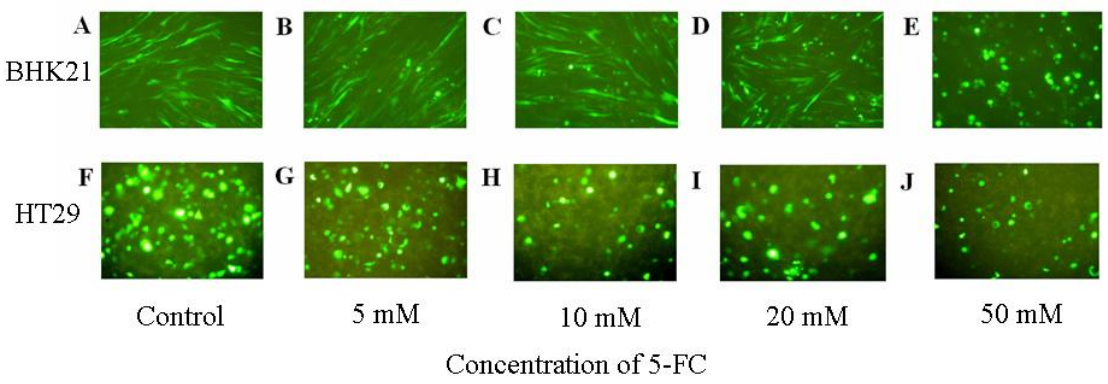

Figure 4.4: Fluorescent images of transfected BHK21 **(A-E)** and HT29 cells **(F-J)** at varying concentrations (0, 5, 10, 20 and 50 mM) of 5-FC.

TH-0560_03610605

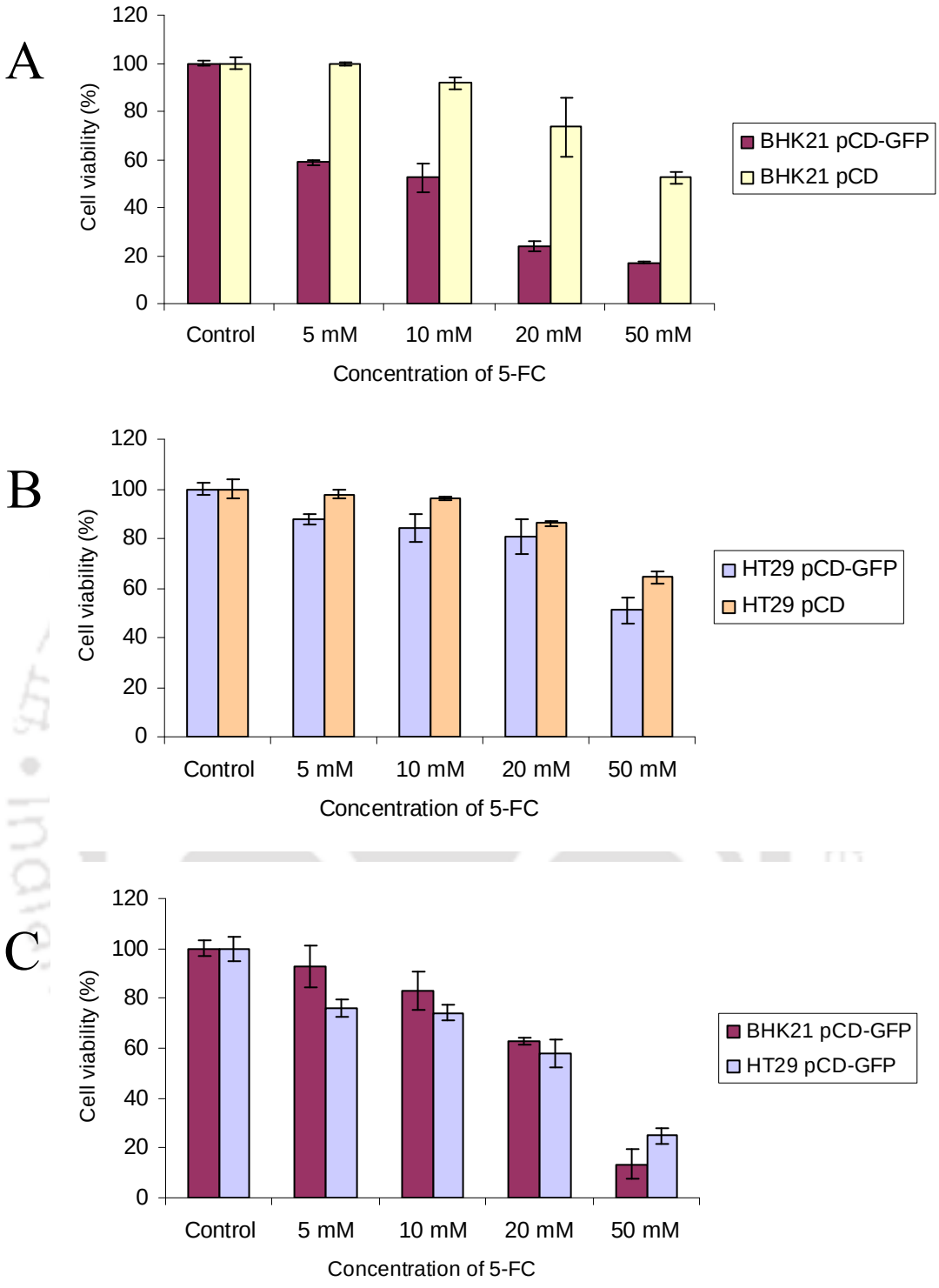

Figure 4.5: Cell viability by MTS assay. **(A)** and **(B)** represented BHK21 and HT29 cells transfected with pCD-GFP and pCD constructs. **(C)** represented cell viability measurement of both the cells transfected with pCD-GFP and treated with different 5-FC concentrations. The IC_{50} of 5-FC for both the cell types were calculated.

TH-0560_03610605

ferritin promoter was used for the subsequent experiments. Cell viability assay was used to assess the IC_{50} (the concentration of 5-FC required to inhibit cell growth by 50% as compared to the control) was found to be ~20 mM (Figure 4.5C). But, it was found that 10 mM 5-FC, which is below IC_{50} value was sufficient to induce cell death, and thus was considered as the working 5-FC concentration for further investigations (Rowley et al., 1996).

4.3 Molecular Mechanism of 5-FC/CD Mediated Cell Death

The mechanism of 5-FC/CD mediated cell death was revealed by microscopic and molecular experimental analysis to correlate the information obtained by tracking GFP fluorescence.

4.3.1 Microscopic Observations

The 5-FC/CD induced apoptosis was studied by Acridine Orange (AO) and Ethidium Bromide (EB) double staining method (Ribble et al., 2005). Confocal microscopy images of the AO/EB dual stained nuclei of treated cells depicted apoptosis at 48 h post transfection after 5-FC treatment, as represented in Figure 4.6. The live cells nuclei would stain green due to the uptake of AO. Thus, live cells would have a normal green nucleus and the cells which are in the early stage of apoptosis would have bright green nucleus with condensed or fragmented chromatin. Cells which lost the cytoplasmic membrane integrity would take up the EB and stained nucleus red. Thus, cells which were in late apoptotic stage displayed condensed and fragmented orange chromatin. The changes in cell morphology due to 5-FC/CD induced apoptosis were examined by SEM analysis (Figure 4.7). Cells

TH-0560_03610605

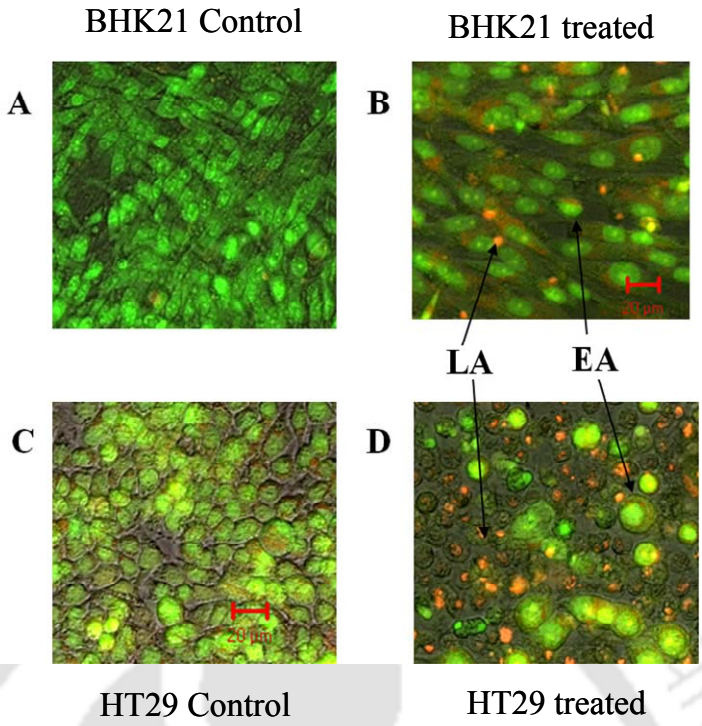

Figure 4.6: Confocal micrographs of AO/EB stained cells. The representative images for BHK21 and HT29 cells are shown in panels **(A & B)** and **(C & D)**, respectively. The arrows indicated green stained nuclei for early apoptosis (EA) and orange stained nuclei for late apoptotic (LA).

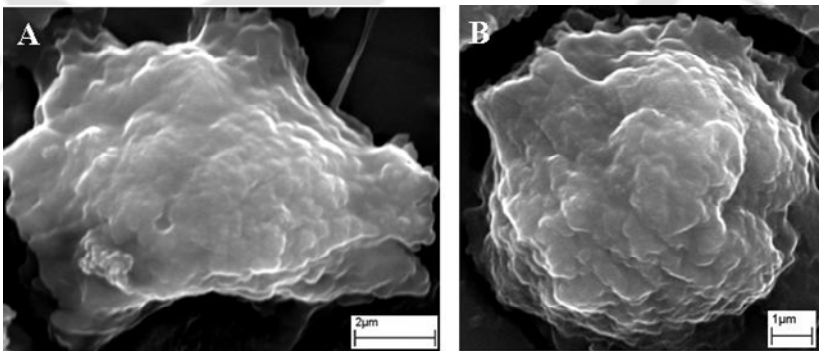

Figure 4.7: Scanning electron micrographs of apoptotic cell morphology. The panels **(A & B)** are the representative images of BHK21 and HT29 cells.

TH-0560_03610605

treated with 5-FC/CD became rounded off with progressive membrane shrinkage and membrane blebbing, which are the characteristic features of apoptosis (Cohen et al., 1999 and Dini 2005).

4.3.2 Effect of Curcumin on Cytotoxicity and Cell Viability

Various concentration of curcumin was used to evaluate the cell cytotoxicity and cell viability by LDH and MTS assay, respectively, in Figure 4.8 A & B. (Pillai et al., 2004) IC_{50} value of curcumin was detected by treating BHK21 and HT29 cells with different concentrations of curcumin followed by MTS assay, which showed initially a gradual decline of cell viability at 10, 20, 40 μM of curcumin, and then a sharp decline at higher concentrations (80 & 100 μM). The IC_{50} was ~ 80 μM, which was more than reported value for other cell types (Bielak-Zmijewska et al., 2000 and Fang et al., 2005). Therefore, the 40 μM curcumin which was below IC_{50} was used to evaluate the synergistic effect on CD gene therapy system.

4.3.3 Synergistic Apoptosis with 5-FC/CD and Curcumin Treatment

Apoptosis induced by 5-FC/CD and the synergistic effect of curcumin was evaluated by confocal microscopic observation of GFP and cellular DNA fragmentation ELISA. GFP expression was used to monitor the therapeutic effect of 5-FC/CD treated cells, in presence and in absence of curcumin. It was observed that, in combination treatment, GFP expression markedly reduced with more rounded off cells (panel C & F) compared to the untreated control samples (panel A & D) and 5-FC/CD treatments alone (panel B & E) for BHK21 and HT29 cells, respectively, as depicted in Figure 4.9. Hence, GFP expression was used as an index to study the 5- FC/CD mediated cell death and its synergistic effect in presence of

TH-0560_03610605

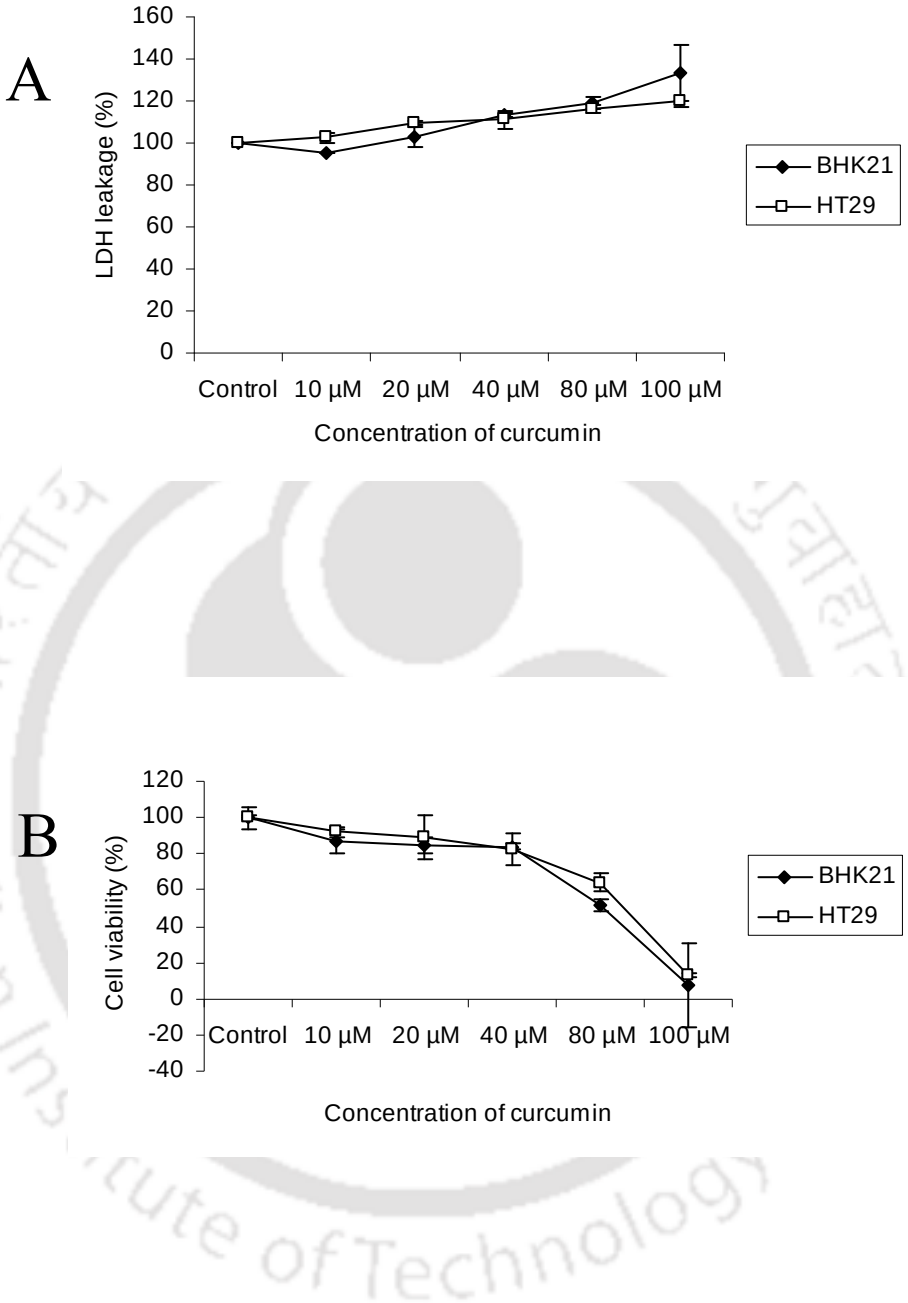

Figure 4.8: Effect of curcumin on membrane leakage and cell viability. Cells were treated with 10, 20, 40, 80 & 100 µM concentrations of curcumin for 72 h. At the end of the incubation period LDH **(A)** & MTS **(B)** assays were performed to assess LDH release and cell viability.

TH-0560_03610605

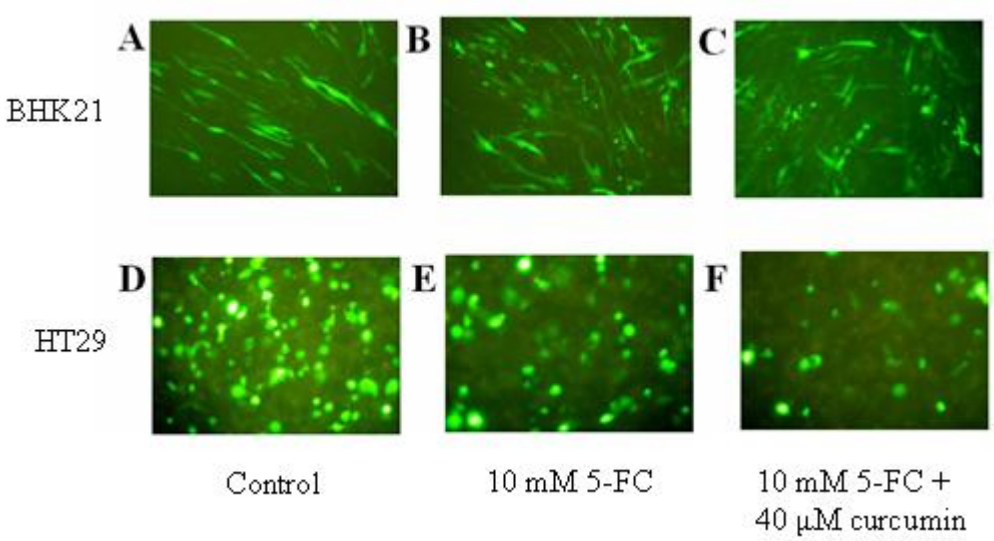

Figure 4.9: Confocal micrograph of the transfected cells in presence of 10 mM 5-FC and 40 µM curcumin for 72 h.

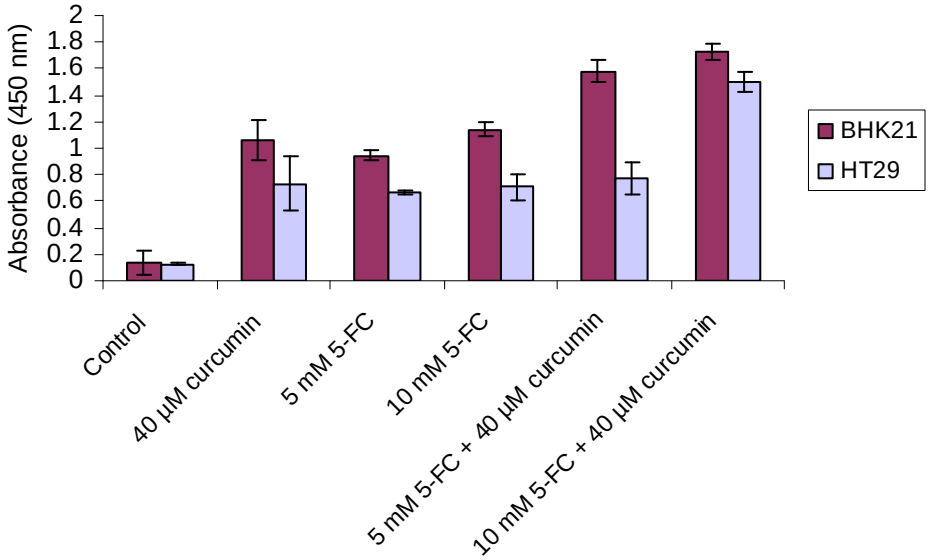

Figure 4.10: Cellular DNA fragmentation ELISA. BrdU labeled cells were transfected with pCD-GFP and treated with 5-FC alone or 5-FC in combination with curcumin (40 µM) for 72 h. The amount of DNA fragments released from nuclei to cytoplasm due to apoptosis was measured by recording absorbance at 450 nm.

TH-0560_03610605

curcumin. The synergistic effect of curcumin with 5-FC/CD was quantitated using 5'-bromo-2'-deoxyuridine (BrdU) labeled cellular DNA fragmentation ELISA (Pan et al., 2001).BrdU labeled DNA fragments released to cytoplasm of the cells treated with 5-FC/CD, in presence and in absence of curcumin was quantitated by ELISA (Figure 4.10). This result confirmed the synergistic effect of curcumin on apoptotic cell death, as the DNA fragments was released more in the combined treatment, when compared to the control and 5-FC/CD alone.

4.3.4 Apoptotic DNA Laddering and Gene Expression

The oligonucleosomal fragments formed due to the catalytic action of caspase activated DNase (CAD) generate a laddering pattern in agarose gel. DNA laddering was observed in 5-FC/CD treated samples obtained at 48 h (Figure 4.11), which is widely considered as biochemical hallmark of apoptosis (Cao et al., 2001). No laddering pattern was observed in untreated controls (lane 2 & 4, Figure 4.11), whereas DNA ladders were obtained for treated samples (lane 3 & 5, Figure 4.11), which confirmed apoptosis.

The expression of apoptotic gene caspase-3 and suppression of anti apoptotic gene bcl-2 was studied by semi-quantitative RT-PCR of total RNA isolated from 5-FC/CD and 5-FC/CD with curcumin treated HT29 cells at 12 h (Huang et al., 2002). β-actin was used as an internal control. The PCR products were analyzed in 1.2% agarose gel. It was observed that there was a slight increase in caspase gene expression for both 5-FC and combine treatment (lane 2 & 3, Figure 4.12) as compared to the untreated control (lane 1, Figure 4.12), but the corresponding signals of bcl-2, an anti-apoptotic regulatory gene was considerably reduced in both treatments (Figure 4.12). Such results revealed the involvement of caspase signaling

TH-0560_03610605

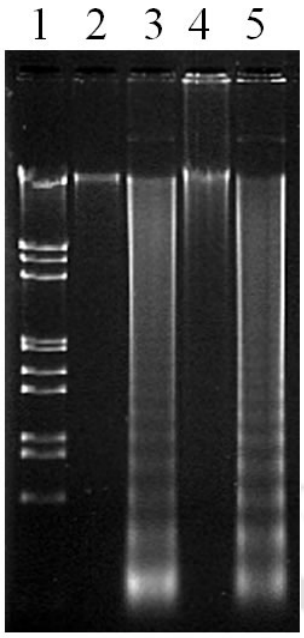

Figure 4.11: DNA laddering of 5-FC/CD treated cells. BHK21 and HT29 cells were transfected with CD gene and subsequently treated with 10 mM of 5-FC for 48 h. Cellular DNA was extracted and subjected to agarose gel electrophoresis. Lane 1: λ DNA/*Eco*R I + *Hind* III marker; lane 2: untreated control BHK21 cells; lane 3: CD transfected BHK21 cells treated with 10 mM 5-FC; lane 4: untreated control HT29 cells; lane 5: CD transfected HT29 cells treated with 10 mM 5-FC.

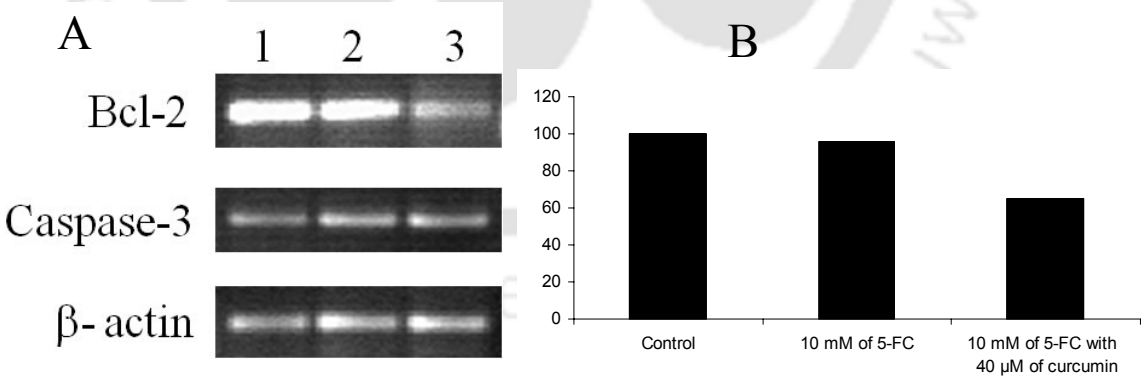

Figure 4.12: (A) Expression of pro-apoptotic caspase and anti-apoptotic bcl-2 gene. Lane numbers: 1, 2, 3 are for untreated control cells; 10 mM of 5-FC and 10 mM of 5-FC with 40 µM of curcumin treated cells. **(B)** The bcl-2 gene expression was quantified using ImageJ software.

TH-0560_03610605

pathway in 5-FC/CD induced apoptosis (Todorova et al., 2004). The above results correlated DNA laddering (Figure 4.11) and an increase in release of DNA fragments in combined treatment (Figure 4.10).

In summary, a plasmid based 5-FC/CD-GFP system was used to induce cell death via apoptosis in BHK21 and HT29 cells. GFP expression was used as noninvasive probe to estimate the CD gene transfer and to measure therapeutic effect *in vitro*. Ferritin promoter construct showed increased therapeutic effect of CD gene. A 5-FC concentration dependent induction of apoptotic cell death and synergistic effect of curcumin were demonstrated. The major advantage in combination treatment of 5-FC/CD with curcumin is, the individual component either 5-FC or curcumin can be used at much lower concentration than their IC_{50} values. Hence, the noninvasive fluorescent based method could be used as a simple tool to monitor combinatorial therapy with high therapeutic efficacy *in vitro*.

TH-0560_03610605

5

5-FU/UPRT GENE THERAPY

Overview

Combination therapies have gained much importance in the area of medical sciences, where conventional drugs or new compounds are therapeutically used along with established tools, such as, surgery, chemotherapy, radiation therapy or gene therapy in cancer treatment. Recently, metal nanoparticles have been also reported with strong therapeutic potential. The impact of nanomaterials on human health and environment is a major concern for commercial use of nanotechnology based products. Herein, therapeutic effect of suicide vector has been tested in combination with metal nanoparticles (NPs). Among the metal NPs, Silver nanoparticles (Ag NPs) are known to be bactericidal and also cytotoxic to mammalian cells. Understanding the interaction of silver nanoparticles with prokaryotic and eukaryotic cells as well as the molecular mechanism of its cytotoxicity is crucial. The antimicrobial activity of Ag NPs was examined using recombinant *Escherichia coli* (*E. coli*) bacteria

TH-0560_03610605

expressing green fluorescent protein (GFP) as a model system. Moreover, the molecular mechanism behind the cytotoxicity of Ag NPs was also explored with combination of experiments *in vitro.* The optimum NPs concentration required to induce apoptosis were established in both cancer and non-cancer cells. Synergistic induction of apoptosis with uracil phosphoribosyltransferase (UPRT) expression system in presence of Ag NPs has sensitized the cells more towards drug 5-fluorouracil (5-FU) treatment. Such synergistic effect of Ag NPs on conventional gene therapy attributes Ag NPs as a representative of new chemosensitization strategy for future application in gene therapy.

Results and Discussions

5.1 GFP Expressing *E. coli* as a Model System to Study Ag NPs Induced Bactericidal Effect

5.1.1 MIC and MKC of Ag NPs on GFP Expressing *E. coli*

The effect of Ag NPs on prokaryotic system (GFP expressing *E. coli*) has been demonstrated. Ag NPs were synthesized in the LB medium (Bacterial growth medium) by reduction of $AgNO_3$ using $NaBH_4$ as the reducing agent in LB medium with a slight modification of the standard method (He et al., 2001; Li et al., 2003). The sizes typically ranged from 2 to 5 nm and the NPs retained their sizes even after 10 h of synthesis, and there was no significant aggregation of particles. The Ag NPs produced in the LB medium was used for studying their effect on recombinant GFP *E. coli*. The effect of Ag NPs on the growth of recombinant GFP *E. coli* were monitored by measuring optical density (OD) at 595 nm for different time intervals, as represented in Figure 5.1. From the Figure 5.1, it was clear that Ag NPs concentrations 22.64 and 28.3 μg/mL completely abolished bacterial growth, whereas

TH-0560_03610605

it was marginal at a concentration of 5.66 µg/mL. The control sample (grown in the absence of Ag NPs and $NaBH_4$) and the sample treated with 6.66×10^{-4} M $NaBH_4$ used to synthesize Ag NPs showed no growth inhibition. Thus the present method involving the use of $NaBH_4$ for the synthesis of Ag NPs did not affect the bacterial growth in any way and provided a convenient tool for the study of the antibacterial effect of preformed NPs. The minimum inhibiting concentration (MIC) and minimum killing concentration (MKC) values obtained were 22.64 and 28.3 µg/mL and are less than those reported previously (Li et al., 2005).

5.1.2 Microscopic Observations

The time-dependent fluorescence microscopic studies of the control (untreated) and Ag NPs treated bacteria (Figure 5.2). From the Figure 5.2 (A1, B1, and C1) it was clear that, there was almost same population of bacteria at 0 h in all three samples. In the control sample, the bacterial number increased with time, as represented in Figure 5.2 (A1, A2, A3, and A4) and for the samples treated with 56.5 and 84.83 µg/mL of Ag NPs showed continuous decrease in fluorescence intensity with a concomitant reduction in bacterial population (Figure 5.2, panels in the B and C series). Furthermore, the morphology of Ag NPs treated recombinant bacteria was deformed, slender and truncated (Figure 5.3) as compared to the control. TEM studies (Sondi and Salopek-Sondi, 2004) on Ag NPs treated bacterial cell showed perforation on the cell wall (Figure 5.4).Accumulation of NPs in the vicinity of the bacterial cell wall and perforation of the cell wall was very clear, which was not reported previously. The high affinity of Ag NPs for attachment to the bacterial cell wall could be due to the presence of thiol groups in the cell wall proteins. There was no significant agglomeration of NPs once they were attached to the cell wall.

TH-0560_03610605

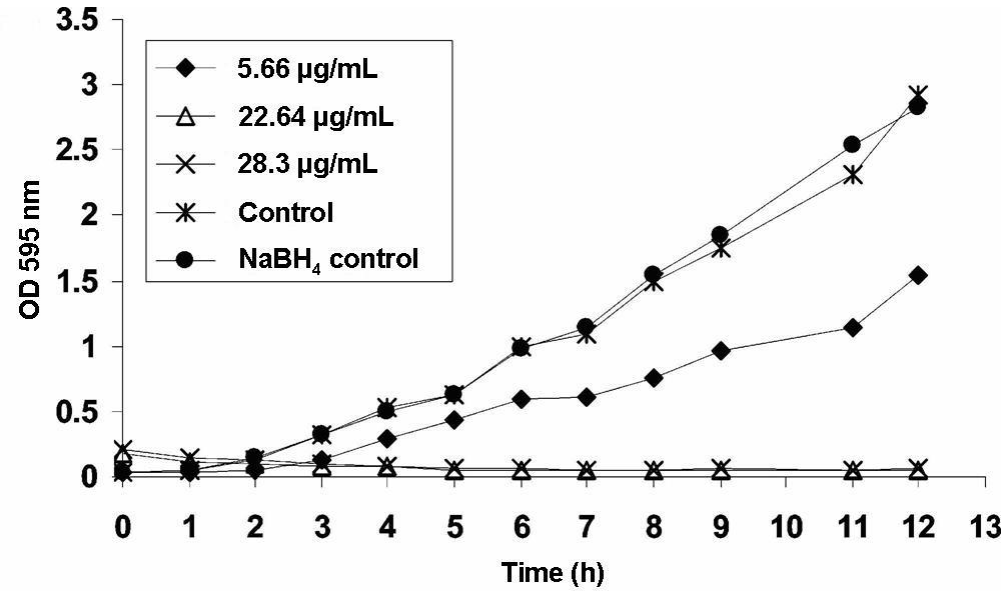

Figure 5.1: Effect of various concentrations of Ag NPs on the growth of recombinant GFP *E. coli*.

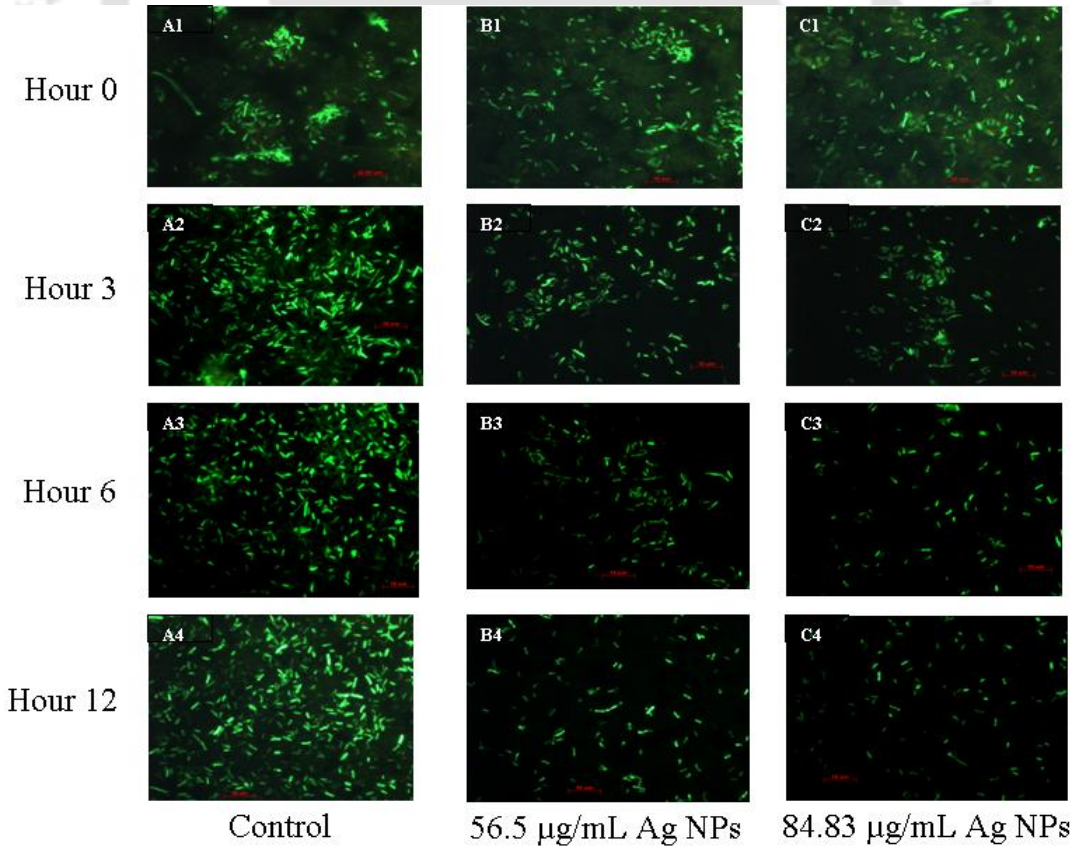

Figure 5.2: Time-dependent fluorescence micrograph of recombinant GFP *E. coli*.

TH-0560_03610605

5.1.3 Bacterial Count

The viable cell count method was used to determine the loss of viability of bacterial cells due to Ag NPs (56.5 and 84.8 μg/mL) treatment (Figure 5.5). After 6 h of treatment, bacterial growth was totally eliminated as compared to the control, confirmed the lethal effect of Ag NPs treatment.

5.1.4 SDS-PAGE Analysis

The SDS-PAGE analysis showed a quantitative difference in the protein profiles of the untreated control and treated samples (Figure 5.6). In control sample, the protein yield and band intensities were high due to more cell growth. However, in the treated samples, the protein profiles remain unchanged, although the band intensities were comparatively less as a result of fewer bacteria due to cell death. The results indicated that the Ag NP treatment had no qualitative effect on protein migration profile.

5.1.5 Plasmid DNA Analysis

Recombinant GFP plasmids isolated from the control and treated samples at different time points were analyzed by agarose gel electrophoresis (Figure 5.7). The results indicated a decrease in the relative amount of plasmid DNA in the treated samples, but the migration patterns of DNA remained same.

The electrophoretic mobility of DNA and protein isolated from AgNP-treated bacteria did not reveal any gross anomaly in structure or migration pattern, which indicated that Ag NPs possibly had no direct effect on either cellular DNA or protein.

TH-0560_03610605

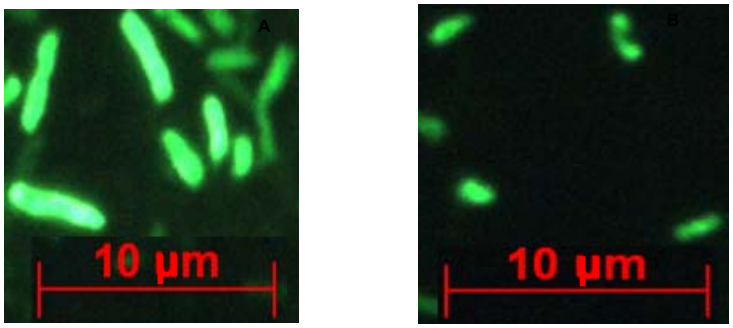

Figure 5.3: Fluorescence micrographs of GFP *E. coli* at 12 h

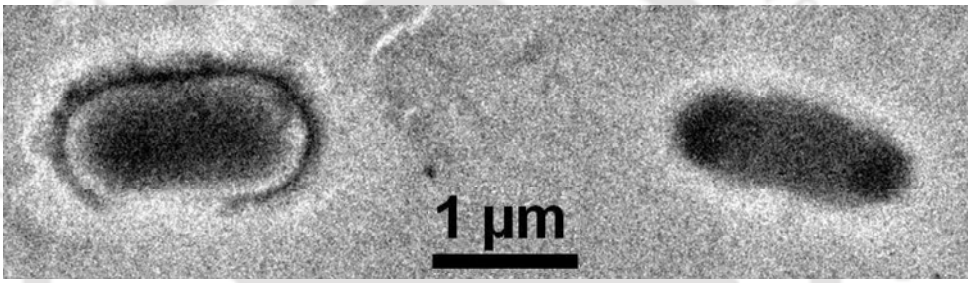

Figure 5.4: TEM micrograph showed perforation on the cell wall of bacteria.

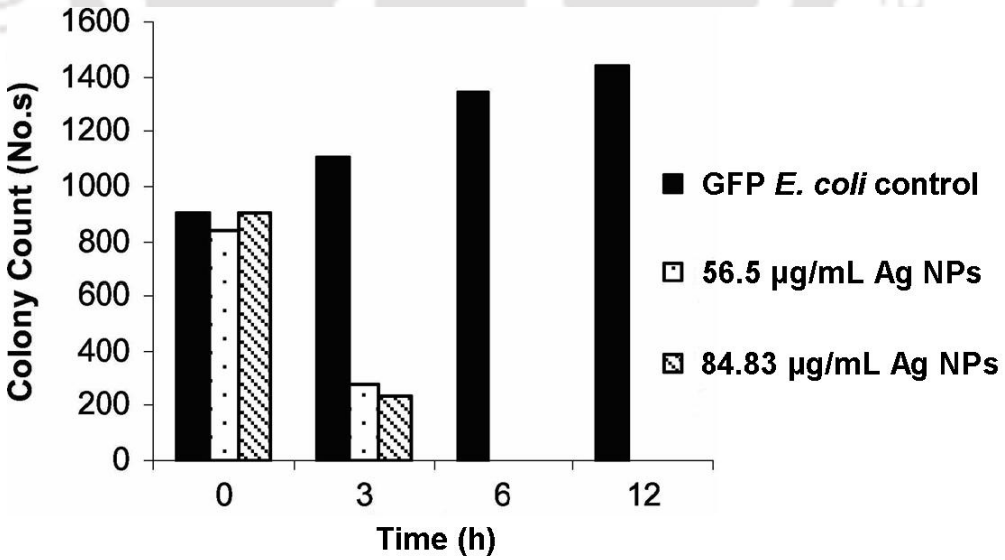

Figure 5.5: Effect of Ag NPs on the viability of GFP expressing *E. coli* at 0, 3, 6 and 12 h.

TH-0560_03610605

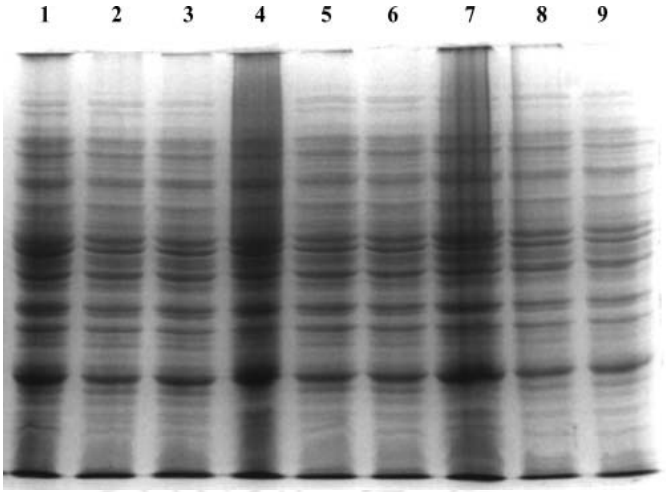

Figure 5.6: SDS-PAGE of Ag NPs treated *E. coli* whole cell lysate (a) Lanes 1, 4 and 7 show proteins isolated from the untreated control. (b) Lanes 2, 5 and 8 showed proteins isolated after Ag NPs (56.5 µg/mL) treatment. (c) Lanes 3, 6 and 9 showed protein isolated after Ag NPs (84.83 µg/mL) treatment of *E. coli* cells at 3, 6 and 12 h, respectively.

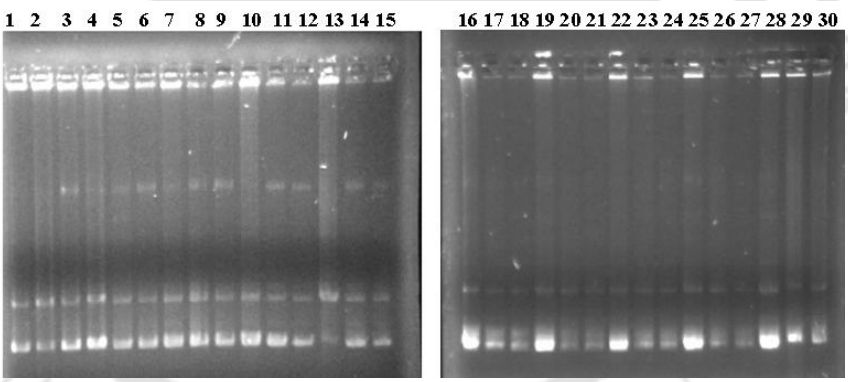

Figure 5.7: Effect of Ag NPs on the recombinant GFP plasmid DNA migration pattern. (a) Lanes 1, 4, 7, 10, 13, 16, 19, 22, 25 and 28 showed plasmid DNA isolated from the control. (b) Lanes 2, 5, 8, 11, 14, 17, 20, 23, 26 and 29 showed plasmid DNA isolated from Ag NPs (56.5 µg/mL) treated cells. (c) Lanes 3, 6, 9, 12, 15, 18, 21, 24, 27 and 30 showed plasmid DNA isolated from Ag NPs (83.83 µg/mL) treated *E. coli* cells at time intervals of 0 min, 30 min, 1 h, 2 h, 3 h, 4 h, 6 h, 8 h, 10 h, 12 h and 24 h, respectively.

TH-0560_03610605

5.2 Synthesis of Ag NPs in Cell Culture Medium

Ag NPs were synthesized in the DMEM medium (cell culture medium) by reduction of $AgNO_3$ using $NaBH_4$ as the reducing agent using with a slight modification of the standard method (Rhodes et al., 2006; Kanduc et al., 2002) The major advantage of NPs synthesized in the cell growth medium circumvented additional stringent conditions for chemical methods of NP synthesis.

5.2.1 TEM and XRD Measurements

TEM micrographs of Ag NPs before treatment with the cells (at 0 h) and at 16 h after treatment, confirmed the formation of well dispersed and stable NPs with sizes ranging between 10-15 nm (Figure 5.8), which was further supported by XRD analysis, which confirmed the formation of Ag NPs and its stability in the medium at least up to the 16^{th} hour of measurements (Figure 5.9). Both the TEM and XRD measurements evidenced the production of small sized Ag NPs (10-15 nm) as well as their stability for at least up to 16 h of study. Hence, Ag NPs produced in the cell culture medium was used for further studies.

5.3 Effect of Ag NPs on Mammalian Cells

5.3.1 Cytotoxic Effects

The cytotoxic effects of Ag NPs were investigated on BHK21 and HT29 cells *in vitro*. Different concentrations of Ag NPs were used to study the effect on cells. Morphological changes, LDH release to the media and mitochondrial activity measurement by cell proliferation assay were studied, as shown in the Figure 5.10, 5.11, & 5.12, respectively**.** The concentration of Ag^+ ions at 10^{-4} M (in absence of $NaBH_4$) was highly cytotoxic, whereas Ag^+ concentrations at 10^{-6} M and 10^{-8} M were

TH-0560_03610605

non-toxic to the cells, as obtained by microscopic observation in Figure 5.13 and MTS assay (Figure 5.14). Furthermore, 10^{-4} M $NaBH_4$ alone used for reduction was found to be nontoxic to the cells (Figure 5.13 & 5.14). Higher concentrations of Ag NPs (> 44.0 µg/mL) became necrotic to cells, led to rapid cell membrane rupture (Figure 5.10).

From cell proliferation assay, IC_{50} (the concentration of Ag NPs required to inhibit cell growth by 50% as compared to the control) was found to be 27.0 µg/mL, but coagulation of Ag NPs in the culture medium was observed at this concentration. On the other hand, Ag NPs concentration of 11.0 µg/mL (< IC_{50}) was sufficient to induce cell death and NPs were stable in the medium, and thus was taken as the standard NPs concentration for further investigations.

5.3.2 Microscopic Observations

Time dependent SEM analysis of Ag NPs treated BHK21 and HT29 cells became rounded off with progressive membrane shrinkage and widening of cell to cell gaps (Figure 5.15).This was followed by eventual detachment of the cells from culture dish and sprouted multiple small white buds around the surface of the cells suggested apoptosis of the cells begins at 4-6 h after Ag NPs treatment (Dini 2005; Okada and Mak 2004). The appearance of apoptotic bodies and characteristic cell membrane blebbing due to apoptosis (Cohen et al., 1999) of cells at 6 h after treatment was observed (Figure 5.15). Ag NPs mediated apoptosis was further studied by AO/EB double staining method (Ribble et al., 2005). At different time intervals, Ag NPs treated cells were stained with AO/EB and observed under confocal microscope (Figure 5.16). From the Figure 5.16, it was clearly evidenced that live cells nuclei stained green due to AO uptake and their numbers gradually decreased

TH-0560_03610605

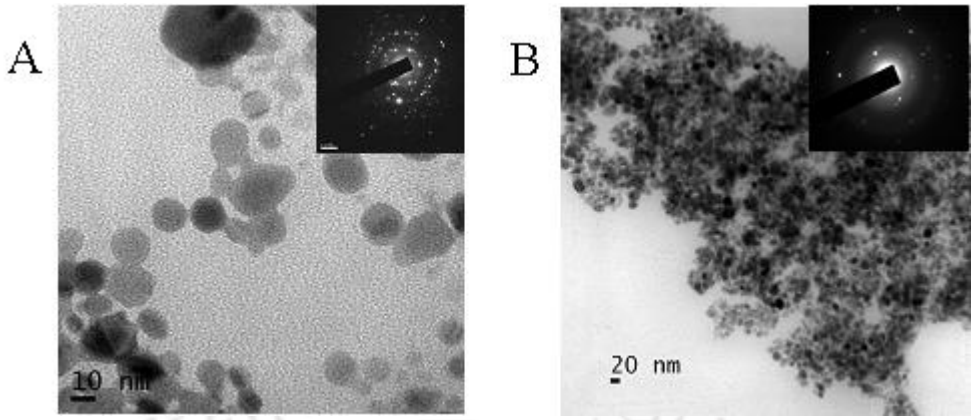

Figure 5.8: Transmission electron microscopy for characterization of Ag NPs. **(A)** Ag NPs synthesized in DMEM medium; **(B)** Ag NPs at 16 h with the cells. The average particle size was around 10-15 nm. Selected area diffraction pattern (SAD) in inset showed the hexagonal pattern of Ag NPs.

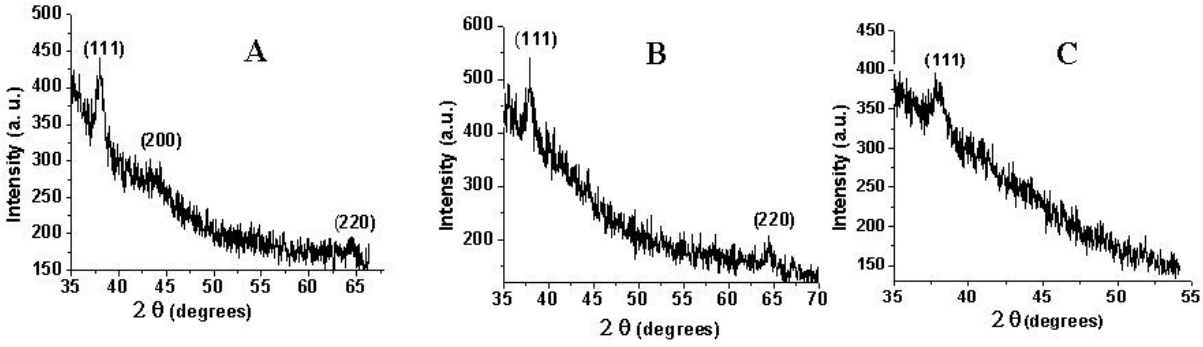

Figure 5.9: XRD Analysis of Ag NPs. The characteristic peaks of Ag NPs were recorded in **(A)** DMEM media; **(B)** BHK21 cells and **(C)** HT29 cells

TH-0560_03610605

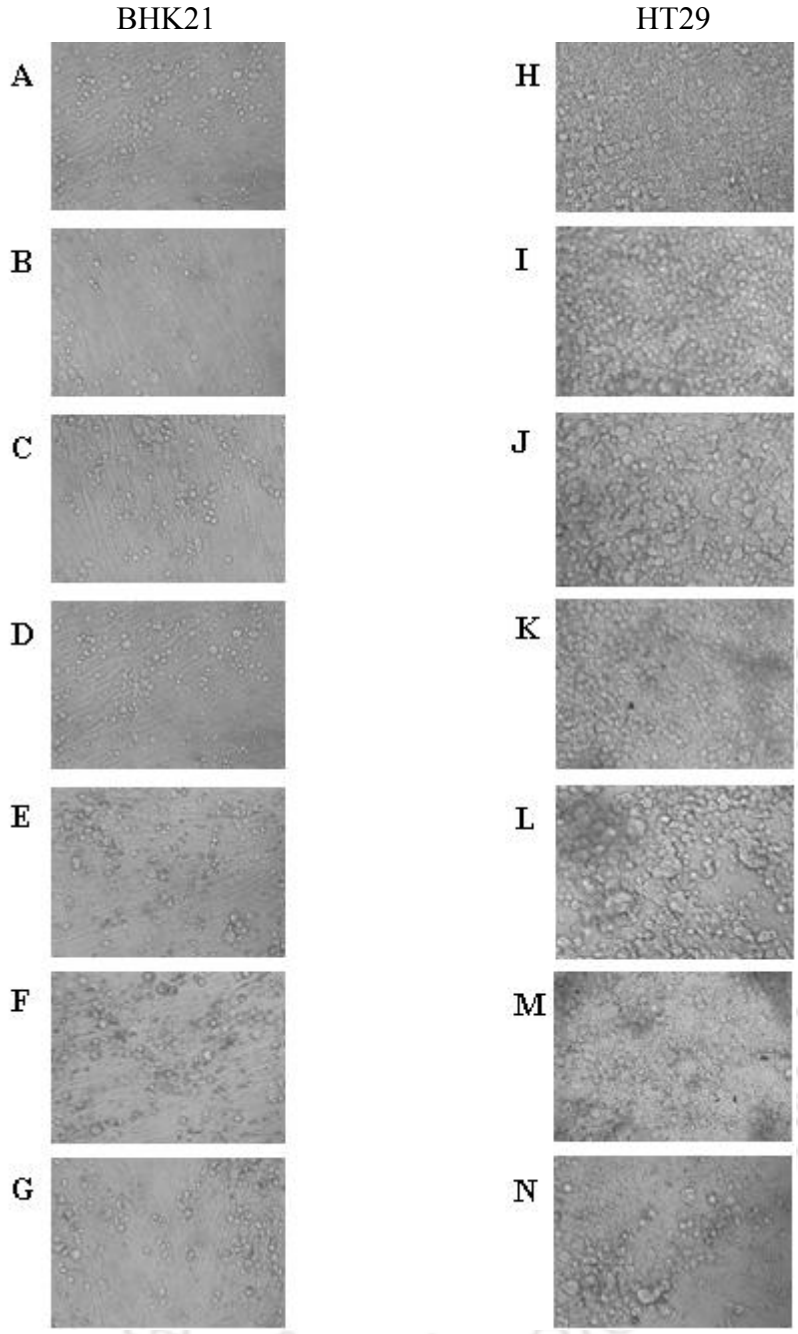

Figure 5.10: Microscopic observations of Ag NPs treated cells. BHK21 **(A-G)** and HT29 **(H-N)** cells were treated with different concentrations of Ag NPs in DMEM Medium for 12 h. At the end of 12 h, the cells were visualized under inverted microscope (at 20X magnification). **(A, H)** untreated control; **(B, I)** 2.75 µg/mL; **(C, J)** 5.5 µg/mL; **(D, K)** 11.0 µg/mL; **(E, L)** 27.5 µg/mL; **(F, M)** 44.0 µg/mL; **(G, N)** 55.0 µg/mL of Ag NPs.

TH-0560_03610605

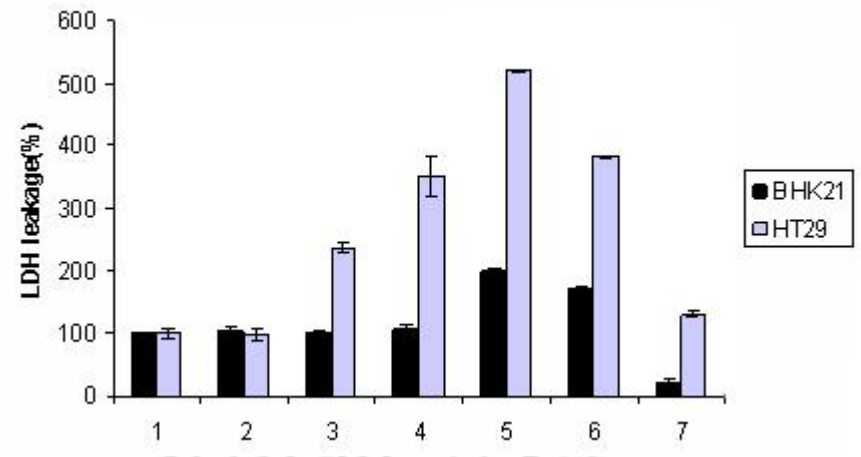

Figure 5.11: LDH assay of Ag NPs treated cells. Cells were treated with different concentrations of Ag NPs for 12 h. At the end of the incubation period, the LDH assay was performed to assess the LDH leakage. Column1: untreated control; column 2: 2.75 µg/mL; column 3: 5.5 µg/mL; column 4: 11.0 µg/mL; column 5: 27.5 µg/mL; column 6: 44.0 µg/mL, column 7: 55.0 µg/mL of Ag NPs.

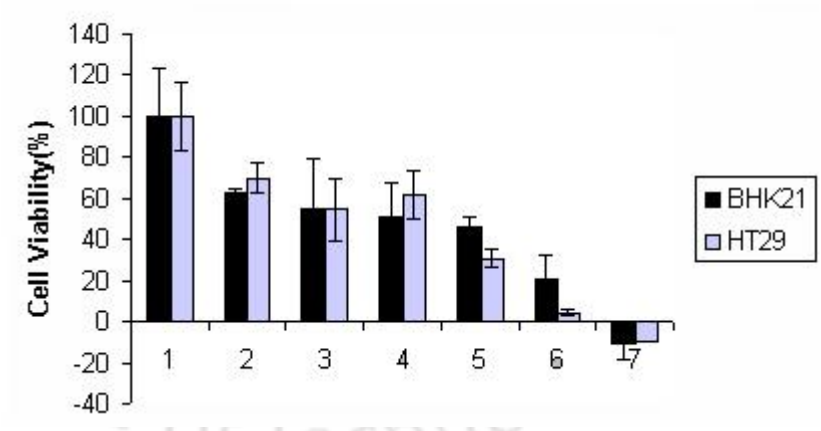

Figure 5.12: MTS assay of Ag NPs treated cells. BHK21and HT29 cells were treated with different concentrations of nanoparticles for 12 h. At the end of the incubation period, cell viability was determined by the MTS assay and IC_{50} was calculated. Column 1: untreated control; column 2: 2.75 µg/mL; column 3: 5.5 µg/mL; column 4: 11.0 µg/mL; column 5: 27.5 µg/mL; column 6: 44.0 µg/mL; column 7: 55.0 µg/mL of Ag NPs.

TH-0560_03610605

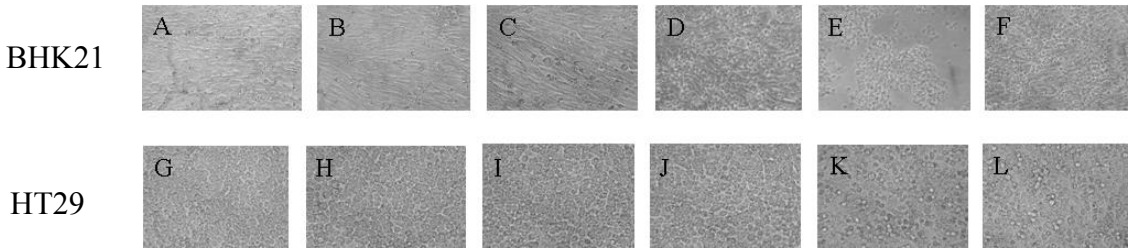

Figure 5.13: Microscopic observations of Ag^+ ions treated cells.BHK21 **(A-F)** and HT29 **(G-L)** cells were treated with different concentrations of Ag NPs for 4 h. At the end of 4 h exposure, the cells were visualized under inverted microscope (at 20X magnification). **(A, G)** untreated control; **(B, H)** 10^{-4} M $NaBH_4$; **(C, I)** 10^{-8} M Ag^+ ions; **(D, J)** 10^{-6} M Ag^+ ions; **(E, K)** 10^{-4} M Ag^+ ions; **(F, L)**, 11.0 µg/mL of Ag NPs.

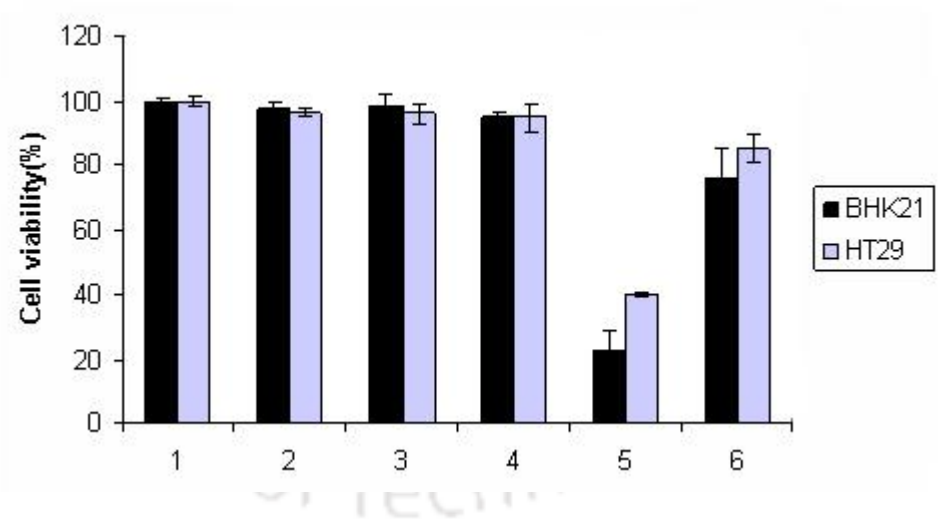

Figure 5.14: MTS assay of Ag^+ ions treated cells. Cells were treated with different Ag^+ concentrations for 4 h. At the end of the incubation period, mitochondrial function was determined by the MTS assay. Column 1: untreated control; column 2: 10^{-4} M $NaBH_4$; column 3: 10^{-8} M Ag^+; column 4: 10^{-6} M Ag^+; column 5: 10^{-4} M Ag^+; column: 11.0 µg/mL of Ag NPs.

TH-0560_03610605

with time owing to more cell death, which correlated with the SEM data (Figure 5.15). The nuclear uptake of EB due to cell membrane perforation during apoptosis, which stained nuclei red and such effect, was prominent from 4 h onwards. High magnified images of treated as well as untreated cells at 6 h (Figure 5.16 M, N, O & P), indicated that live untreated cells had well organized chromatin structures exhibited normal green nucleus, whereas the treated cells had fragmented or condensed chromatin consisting of apoptotic nuclei exhibited bright green nucleus. Cells which are in the late stage of apoptosis exhibited condensed and fragmented orange chromatin due to the progressive nuclear uptake of EB. Nuclear staining experiment demonstrated that apoptosis started between 4-6 h after Ag NPs addition to the culture medium (Tsangaris and Tzortzatou-Stathopoulou 1996).

5.3.3 Molecular Analysis

Ag NPs induced apoptosis was studied by BrdU labeled cellular DNA fragmentation ELISA. Ag NPs treated cells released BrdU labeled DNA to cytoplasm was monitored up to 6 h. The BrdU labeled DNA increased significantly at 4 and 6 h in the cytoplasm of the treated cells as compared to the untreated control cells, which confirmed the apoptosis (Figure 5.17 A).

During apoptosis, the endonucleases activated by caspase cleave the chromosomal DNA at internucleosomal linker sites to produce 180–200 bp mono and oligonucleosomal fragments that gives a characteristic laddering pattern in agarose gel electrophoresis. Cellular DNA obtained at 12 h from Ag NPs treated cells showed DNA laddering in agarose gel electrophoresis (Figure 5.17 B).

A semi-quantitative RT-PCR was used to study the apoptotic and anti-apoptotic gene expression or suppression in Ag NPs treated BHK21 and HT29 cells.

TH-0560_03610605

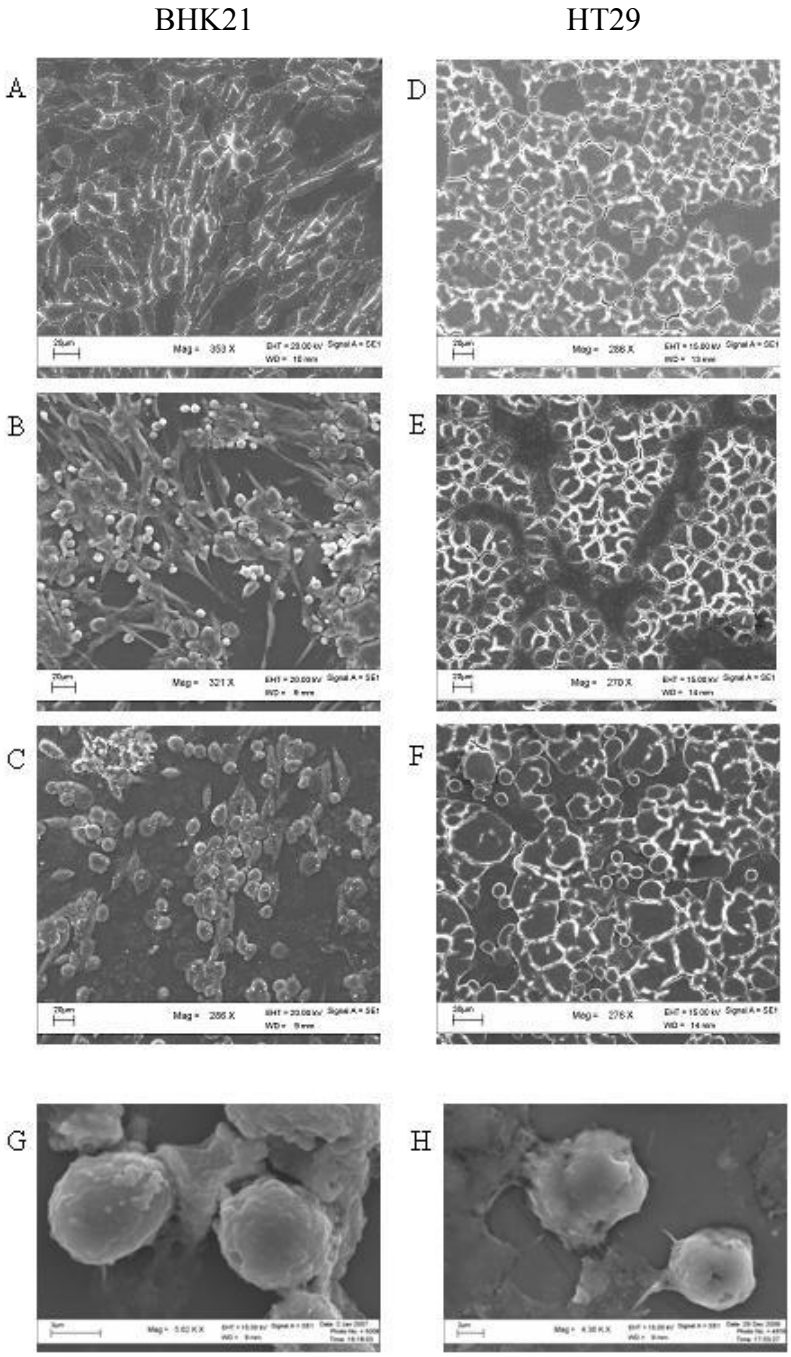

Figure 5.15: SEM analysis of Ag NPs treated cells. **A-C** and **D-F** are the representative images of BHK21 cells HT29 cells treated with Ag NPs (11.0 μg/mL) for 2, 4 and 6 h, respectively. Cells population decreased with time and cell to cell gaps increases. Cell membrane blebbing are shown in **G** and **H** for BHK21 and HT29 cells, respectively, at 6 h of treatment.

TH-0560_03610605

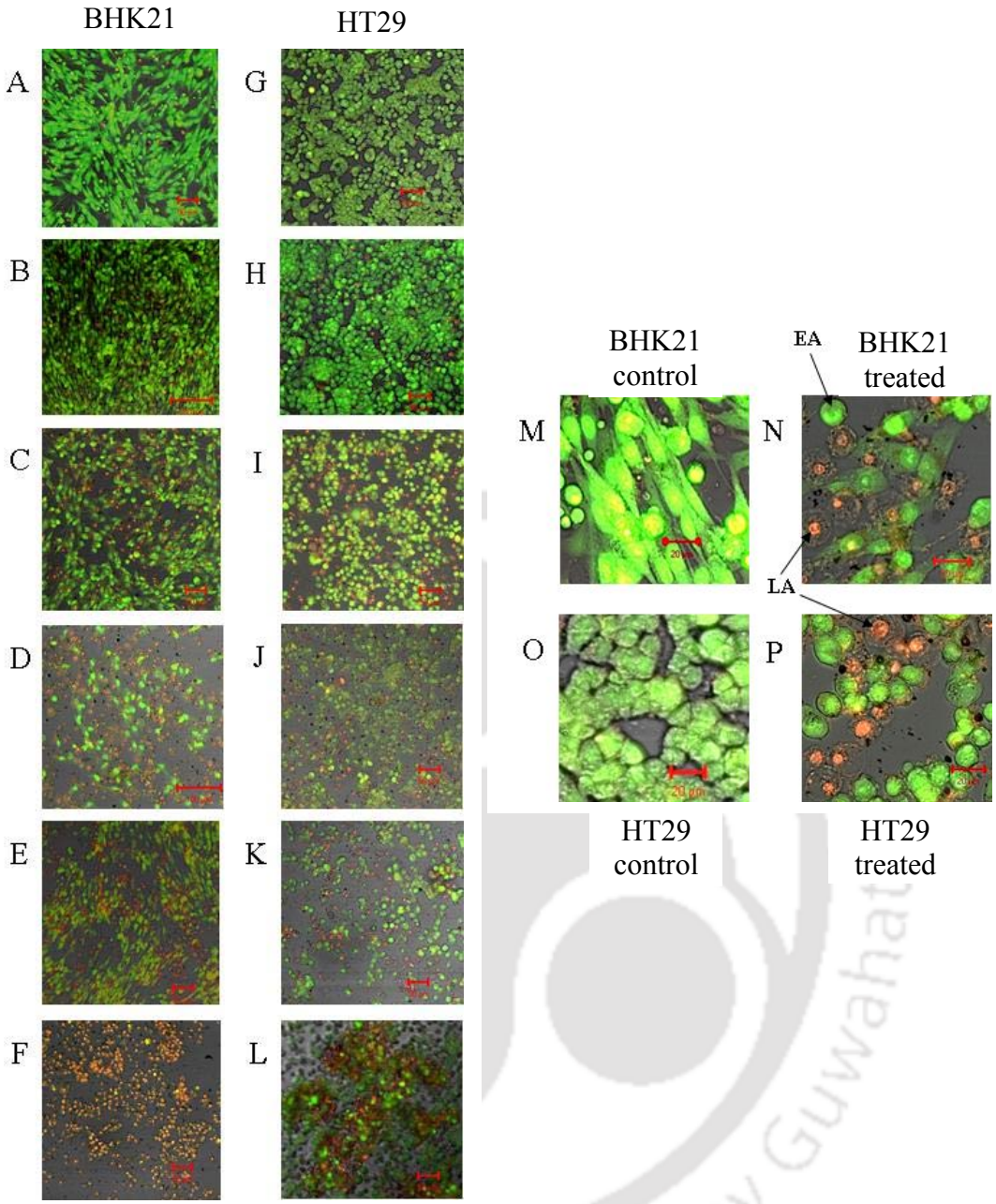

Figure 5.16: Time dependent confocal micrographs of AO/EB stained cells. **A-F** & **G-L** are the representative images of BHK21 cells and HT29 cells, respectively, at 0, 2, 4, 6, 8 and 24 h of Ag NPs (11.0 µg/mL) treatment. High magnification micrographs **M** & **N**, of BHK21 and **O** & **P**, of HT29 cells show that the untreated cell nuclei **M** & **O** stained green, whereas treated nuclei **N** & **P** consist of early apoptotic (EA) nuclei that stained green and late apoptotic (LA) fragmented nuclei that stained orange.

TH-0560_03610605

Caspase gene expression was increased in Ag NPs treated cells (lane 2 and 4) than untreated control in lane 1 and 3 of Figure 5.17 C, whereas the corresponding signals of bcl-2, an anti-apoptotic gene expression was considerably reduced in both the cell types (Figure 5.17 C). These data confirmed the caspase mediated apoptosis in Ag NPs treated cells. Here, β-actin was used as an internal control.

5.4 UPRT Expression and Cell Apoptosis

The chemotherapeutic drug 5-FU has been reported cytotoxic to a large numbers of cells, but its activity is quite low in many cancer cells. This problem can be overcome by using UPRT gene transduction in the cells to convert 5-FU to more lethal 5-FdUMP and 5-FUTP which are known to inhibit DNA and RNA synthesis. In this context, a recombinant UPRT plasmid was constructed (Figure 5.18 A). UPRT plasmid was electroporated in to BHK21 and HT29 cells. Cellular DNA & total RNA extracted from the transfected cells was subjected to PCR and RT-PCR analysis, which confirmed the UPRT gene transfer and its expression in BHK21 and HT29 cells (Figure 5.18 B). The UPRT transduced cells were more sensitized towards 5-FU treatment as compared to non-transduced 5-FU treated cells, which was observed by reduced mitochondrial activity in MTS assay (Figure 5.19) and cell membrane damage by AO/EB double staining (Figure 5.20). The 5-FU induced apoptosis was also confirmed by the characteristic DNA laddering (Figure 5.21).

5.5 Synergistic Effect in Combination Therapy

The chemosensitization effect of Ag NPs in addition to 5-FU, in the UPRT non-transduced and transduced cells was studied. The LDH enzyme released (Kolber et al., 1988; Rhodes et al., 2006) to the culture media of Ag NPs treated cells (Figure 5.22 A) showed only a slight increase in LDH leakage at 6h samples due to

TH-0560_03610605

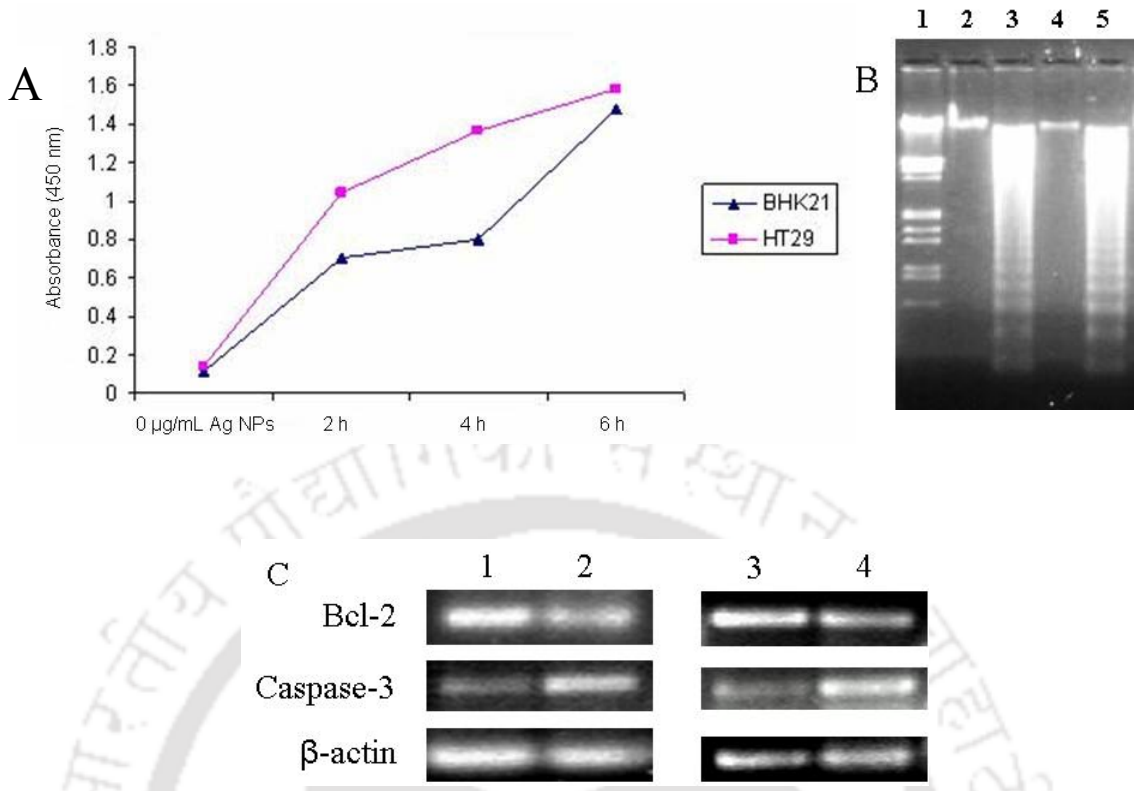

Figure 5.17: Detection of Ag NPs induced apoptosis by cellular DNA fragmentation ELISA, DNA laddering and apoptotic gene expression. For DNA fragmentation ELISA **(A)**, the BrdU-labeled 2 $\times 10^4$ cells/well were incubated with Ag NPs (11.0 µg/mL) for 2, 4 and 6 h, respectively. The amount of fragmented DNA as measured by absorbance at 450 nm increased with time of incubation. For laddering **(B)**, DNA extracted from cells at 12 h of Ag NPs treatment was resolved on 1.2% agarose gel electrophoresis. Lane 1: λ □/EcoR I + Hind III marker; lane 2: untreated control BHK21 cells; lane 3: 11.0 µg/mL of Ag NPs treated BHK21 cells; lane 4: untreated control HT29 cells; lane 5: 11.0 µg/mL of Ag NPs treated HT29 cells. **(C),** Ag NPs treated cells were harvested, RNA was isolated and RT-PCR was performed for caspase-3, bcl-2 and β-actin genes. Lane: 1 and 3 were for untreated control BHK21 & HT29 cells; 2 and 4 for Ag NPs (11.0 µg/mL) treated BHK21 & HT29 cells, respectively.

TH-0560_03610605

combination therapy as compared to 5-FU or Ag NPs alone, which indicated that cell death, was due to regulated event, like apoptosis and not due to necrosis. The apoptosis was synergized in combination therapy, which was supported by cellular DNA fragmentation ELISA (Figure 5.22 B) and DNA laddering experiments (Figure 5.22 C). When Ag NPs were used in combination with 5-FU more number of cells undergo apoptosis as compared to Ag NPs or 5-FU treatment alone (Figure 5.22 B). The results shown in Figure 5.22 B, confirmed that the BrdU DNA release due to apoptosis greatly increased in combination treatment on UPRT transduced cells. The results of 11 μg/mL Ag NPs on UPRT transduced cells without 5-FU treatment was similar that of 11 μg/mL Ag NPs on non-transduced cells.

DNA ladders of the corresponding treated samples, as represented in Figure 5.22 C, confirmed apoptosis. Ag NPs or 5-FU alone induced DNA ladders were also shown in lane 7 and 14 of Figure 5.22 C. DNA fragmentation during apoptosis was quantified by ELISA. It was observed that the Ag NP mediated-apoptosis involved caspase and bcl-2 signaling molecules (Figure 5.17 C). The combination of Ag NPs on UPRT expressing cells upon 5-FU treatment enhanced apoptosis by synergy of the two systems involving caspase signaling.

In summary, the antibacterial property of Ag NPs was investigated using GFP expressing *E. coli* bacteria as a prototype. GFP expressing *E. coli* has the advantage of easy morphological identification by fluorescence microscopy and the possibility of a noninvasive detection method, whereas the other wild-type bacterial strains relied essentially on viability tests, which are time-consuming and error prone. Furthermore, the direct effect of Ag NPs on DNA and protein migration profiles was also studied. GFP expressing *E. coli* was established as a reliable model system to study the antibacterial efficacy of NPs.

TH-0560_03610605

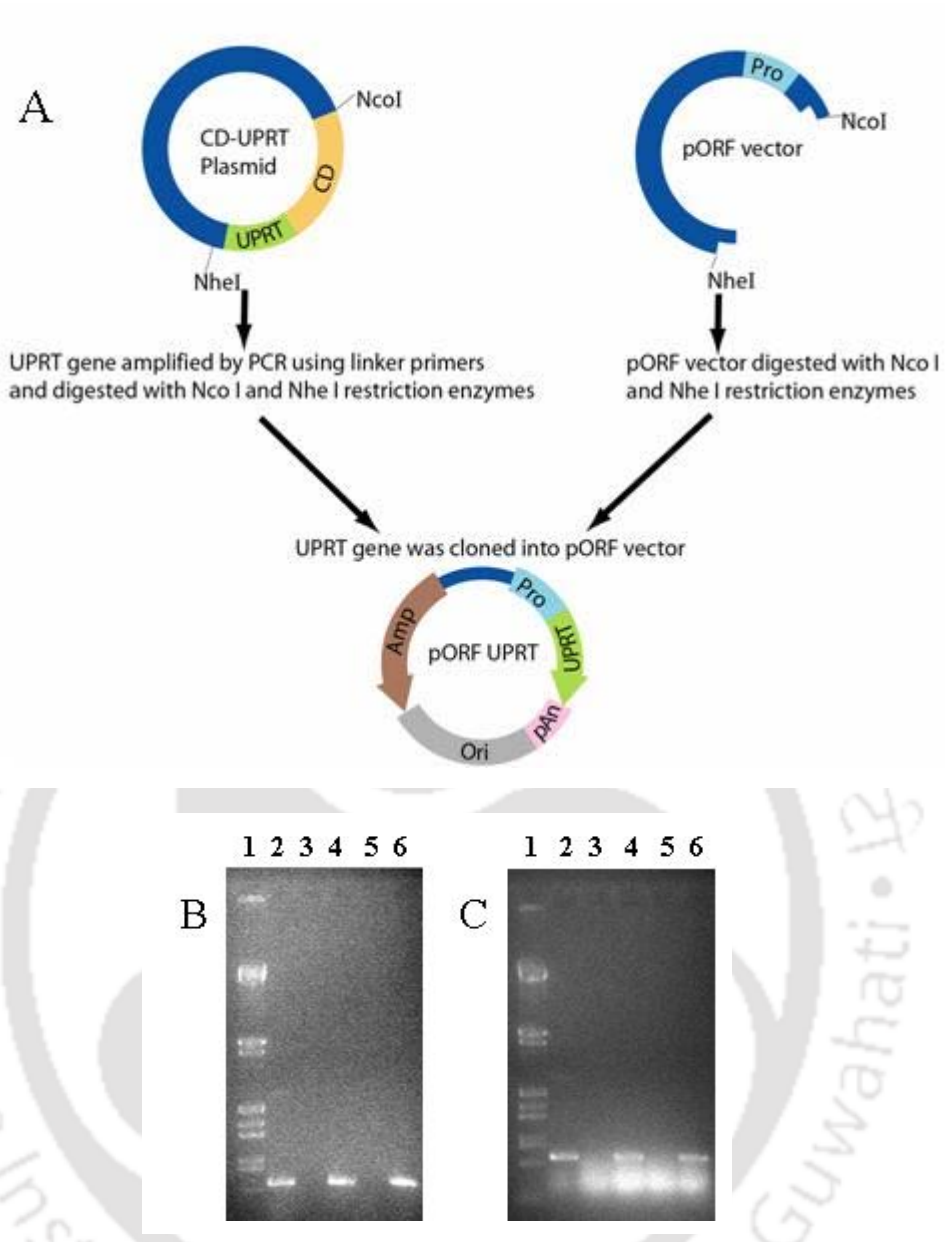

Figure 5.18: Construction of UPRT vector and confirmation of UPRT gene transfer and expression by PCR and RT-PCR analysis. **A,** schematic of UPRT vector* construction. **B**, PCR & **C**, RT-PCR analysis. Lane 1: λ DNA/*Eco*R I + *Hind* III marker; lane 2: control UPRT PCR product (651bp); lane 3: untransfected control BHK21 cells; lane 4: UPRT transfected BHK21cells; lane 5: untransfected control HT29 cells; lane 6: UPRT transfected HT29 cells.

**(Pro-promoter, Amp-Ampicillin resistance gene, ori- origin of replication, pAn-Poly adenylation)*

TH-0560_03610605

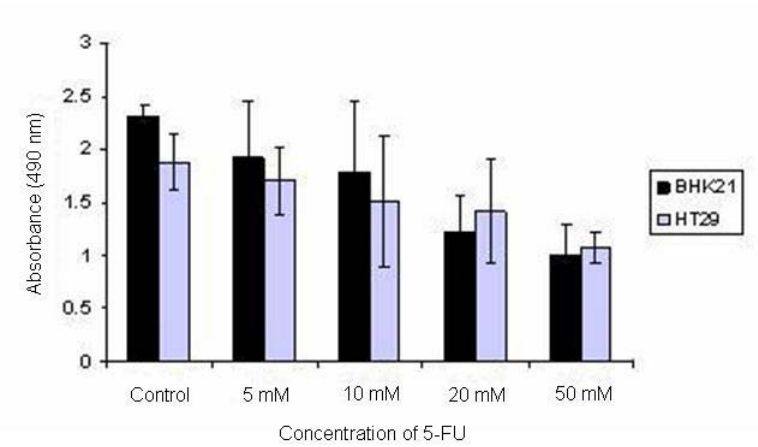

Figure 5.19: MTS assay of 5-FU treated cells. BHK21 and HT29 cells were transduced with UPRT gene and treated with different concentrations of 5-FU.

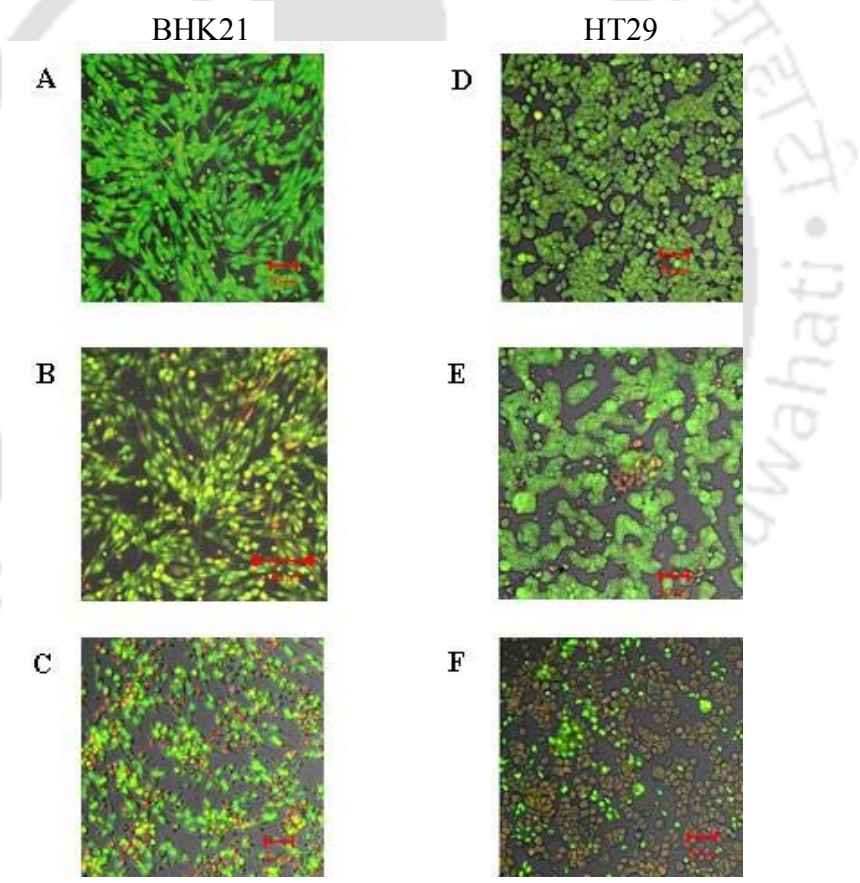

Figure 5.20: Confocal micrographs of AO/EB stained 5-FU treated cells. **(A-C)** & **(D-F)** are the representative images of BHK21 cells and HT29 cells, respectively at 0, 8 and 24 h of 20 mM 5-FU treatment.

TH-0560_03610605

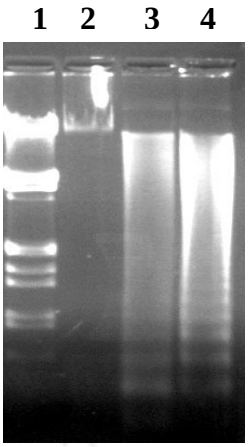

Figure 5.21: DNA laddering of 5-FU treated cells.BHK21 and HT29 cells were transfected with UPRT plasmid and subsequently treated with 20 mM of 5-FU for 12 h. Cellular DNA was extracted and subjected to agarose gel electrophoresis. Lane 1: λ DNA/EcoR I + Hind III marker; lane 2: untreated control BHK21 cells; lane 3: UPRT transfected BHK21 cells treated with 20 mM 5-FU; lane 4: UPRT transfected HT29 cells treated with 20 mM 5-FU.

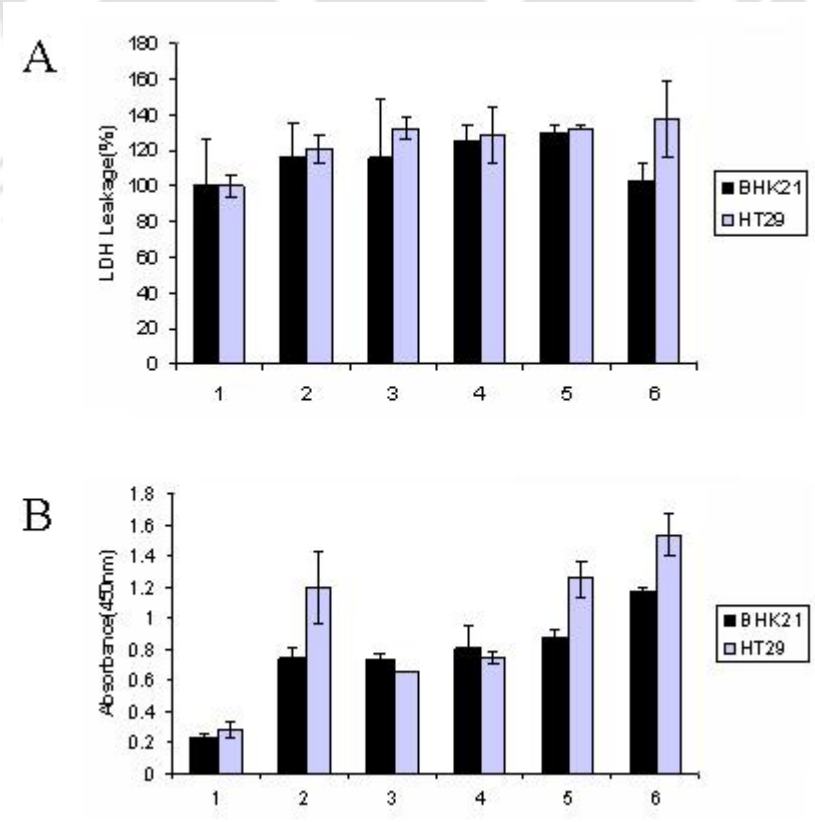

TH-0560_03610605

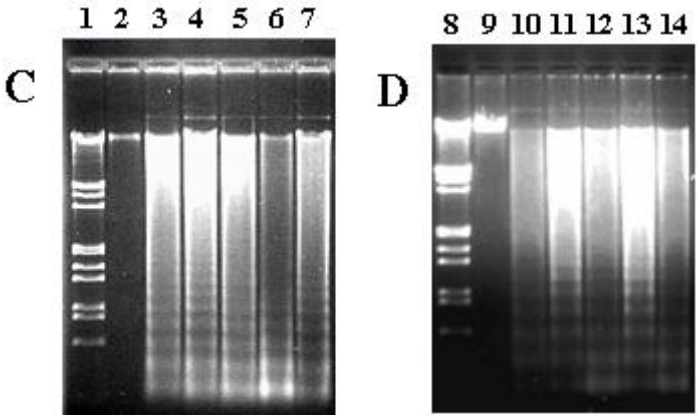

Figure 5.22: LDH release and synergistic apoptosis due to combine therapy. **A,** Cells were treated with different combinations of Ag NPs and drug 5-FU for 6 h and LDH assay was performed to assess the LDH leakage in the medium. **B,** for synergistic apoptosis by cellular DNA fragmentation ELISA, the BHK21 and HT29 cells were labeled with BrdU and a portion of the labeled cells was transfected with UPRT vector. The UPRT transfected and non transfected BrdU labeled cells were treated with combinations of Ag NPs and 5-FU for 6 h. The amount of detected DNA fragments measured by absorbance at 450 nm was higher for combination treatment on UPRT expressed cells compared to the 5-FU, Ag NPs or 5-FU treatment on UPRT expression alone. Nos. 1: untreated controls, 2: 11.0 µg/mL of Ag NPs; 3: 20 mM 5-FU, 4: 11.0 µg/mL of Ag NPs with 20 mM 5-FU; 5: 20 mM 5-FU on UPRT transduced cells; 6: combine treatment of 11.0 µg/mL Ag NPs with 20 mM 5-FU on UPRT transduced cells. For synergistic effect on DNA laddering cellular DNA fragments of **C**, BHK21 cells and **D**, HT29 cells were analyzed by 1.2% agarose gel electrophoresis. Lane 1 & 8: λ DNA/*Eco*R I + *Hind* III marker; lane 2 & 9: control untreated; lane 3 & 10: treatment with 11.0 µg/mL of Ag NPs; lane 4 &11: treatment with 20 mM 5-FU; lane 5 & 12: combine treatment of 11.0 µg/mL of Ag NPs and 20 mM 5-FU; lane 6 & 13: treatment with 20 mM 5-FU on UPRT transduced cells; lane 7 & 14: combine treatment of 11.0 µg/mL of Ag NPs with 20 mM 5-FU on UPRT transduced cells.

TH-0560_03610605

Furthermore, the concentration and time dependent induction of apoptosis in Ag NPs treated cancer HT29 as well as non-cancer BHK21 cells was established. Experimental observations suggested Ag NPs further enhanced apoptosis of 5-FU/UPRT gene therapy system. The important feature of the Ag NPs has been to sensitize cancer cells towards drug treatment even in absence of gene therapy. The switching behavior of Ag NPs could be useful in cancer treatment in conjunction with gene therapy. The major advantage in combination treatment of 5-FU/UPRT with Ag NPs is the individual component either 5-FU or Ag NPs can be used at much lower concentration than their IC_{50} values. Such treatment reduces development of resistance to any particular drug. For application in animal model, the Ag NPs and 5-FU/UPRT could be incorporated in delivery systems such as liposomes and virosomes for targeted delivery.

TH-0560_03610605

6

5-FC/CD-UPRT GENE THERAPY

Overview

Generation of new suicide gene therapy vectors with high therapeutic efficacy is a demanding task. Such vectors could be developed by fusion of two suicide genes or using suicide gene in combination with any drug to achieve high therapeutic effect at low concentrations of drug. Another important task is to understand the complete molecular mechanism of cell death, which is crucial for any potential therapeutic agent for its long term use. The bifunctional *E. coli* cytosine deaminase and uracil phosphoribosyl transferase (CD-UPRT) has been reported very effective in converting the nontoxic prodrug 5-FC to its toxic metabolites, but the exact pathway of cell death is yet to be defined. Herein, the molecular mechanism of cell death induced by 5-FC/CD-UPRT suicide gene therapy was evaluated by combination of experimental strategies. The 5-FC concentration, which induced apoptotic cell death, was optimized for BHK21 and HT29 cells *in vitro*.

The transfer of CD-UPRT gene and its expression was analyzed by the PCR and RT-PCR methods. 5-FC/CD-UPRT induced cell death was estimated by standard

TH-0560_03610605

biochemical assays, such as MTS and LDH measurements. Apoptotic cell death of 5-FC/CD-UPRT treated cells was detected by confocal and scanning electron microscopic observations, which was further supported by expression of apoptotic genes, characteristic DNA laddering and quantitative cellular DNA fragmentation ELISA. In addition, the 5-FC/CD-UPRT mediated apoptosis was synergized by combination treatment with a known anticancer compound curcumin. Similar therapeutic effect was observed in 5-FC/CD-UPRT with curcumin treated HEK293 and Hep3B cells.

Results and Discussions

6.1 CD-UPRT Gene Transfer and its Expression

The recombinant plasmid pVITRO2 GFP/CD-UPRT was electroporated into BHK21 and HT29 cells. The efficiency of electroporation was estimated by observing the GFP expression under fluorescence microscope at 24 h after electroporation (Figure 6.1 A). At 48 h post-transfection, PCR and RT-PCR analysis on total DNA and RNA of the transfected cells, using gene specific primers confirmed the presence of CD-UPRT gene and its expression (Xia et al., 2004). A 1.9 kb PCR amplicon was observed in agarose gel for both BHK21 (lane 3) and HT29 cells (lane 4), in Figure 6.1 B The RT-PCR results depicted in lane 6 & 7 of the Figure 6.1 B, confirmed the presence of full length 1.9 kb RNA transcript of bifunctional CD-UPRT gene.

6.2 Cytotoxicity and Cell Viability Measurements

The CD-UPRT electroporated BHK21 and HT29 cells were treated with different concentrations of 5-FC to determine the cytotoxicity and cell viability

TH-0560_03610605

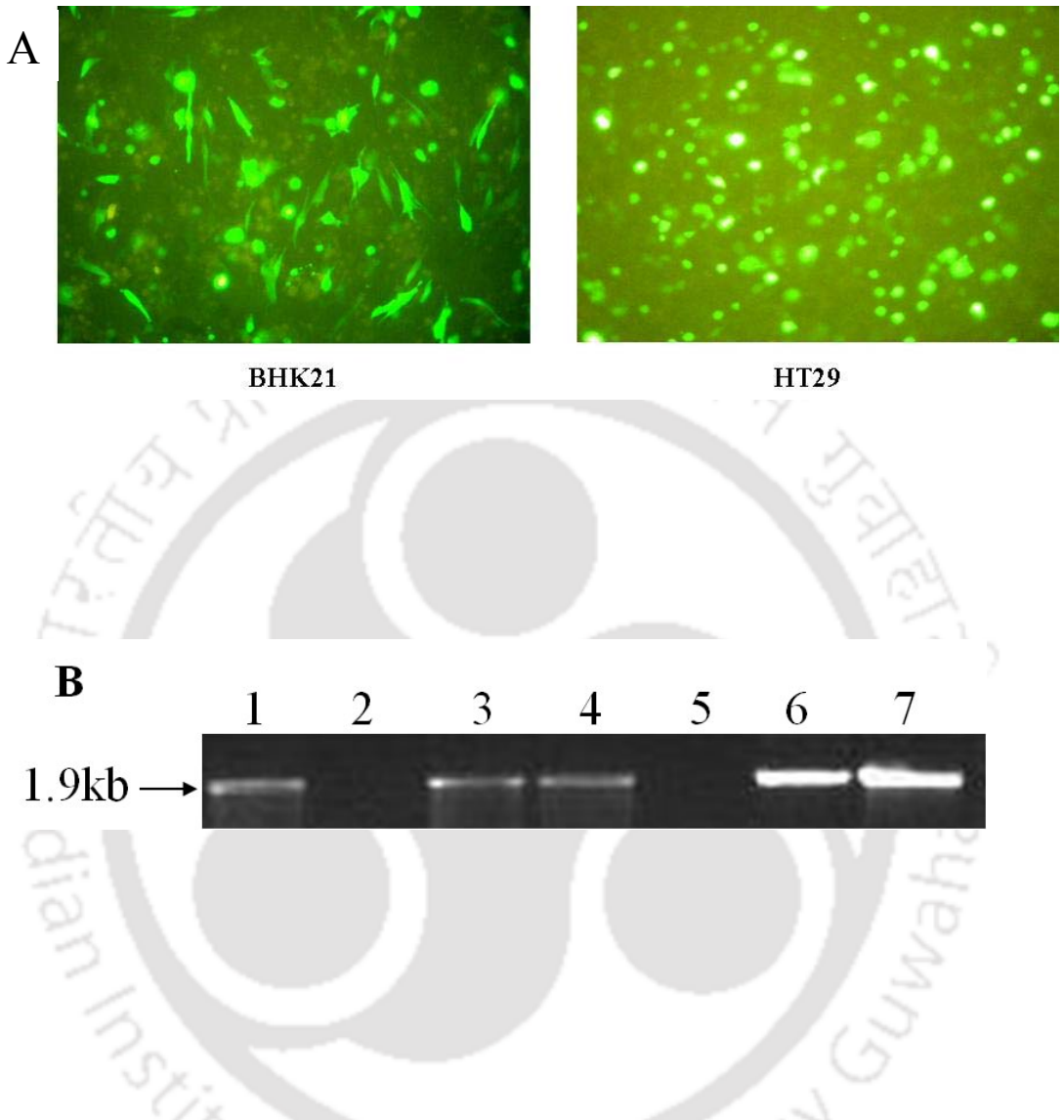

Figure 6.1: CD-UPRT gene transfer and expression. **(A)** GFP expression in BHK21 and HT29 cells at 24 h after electroporation with the pVITRO2 GFP/CD-UPRT plasmid. **(B)** PCR and RT-PCR analysis on CD-UPRT transfected cells. Lane 1: 1.9 kb PCR amplicon of CD-UPRT as positive control; lane 2 & 5: untransfected control BHK21 cells; lane 3 & 6: CD-UPRT transfected BHK21cells; lane 4 & 7: CD- UPRT transfected HT29 cells.

TH-0560_03610605

(Miyagi et al., 2003). The cytotoxicity of 5-FC/CD-UPRT was estimated measuring LDH activity in the cell culture media. LDH was released from the treated cells due to membrane leakage. Concentration dependent cytotoxicity of 5-FC/CD- UPRT treated cells were shown in Figure 6.2. LDH assay demonstrated that CD-UPRT transfected cells became more sensitive at higher concentrations (20 & 50 mM) of 5-FC as compared to untreated control cells. The lower concentrations of 5-FC (5 & 10 mM) did not show significant cytotoxicity.

Similarly, the CD-UPRT transfected cells were treated with different concentrations of 5-FC and the percentage of cell viability was estimated by MTS assay. A significant (p<0.05) concentration dependent gradual decrease in cell viability of the treated cells was observed. From, the cell proliferation assay (MTS) the IC_{50} of 5-FC was determined as ~20 mM (Figure 6.3). Furthermore, 5 & 10 mM of 5-FC concentration (below the IC_{50}) were found sufficient to induce cell death with less cytotoxic effect. Thus, both 5 mM and 10 mM 5-FC concentrations were considered as the working 5-FC concentrations for subsequent experiments. The LDH release assay and the cell viability measurement showed chemosensitization effect of 5-FC/CD-UPRT system *in vitro*.

6.3 Apoptosis Induced with 5-FC/CD-UPRT

6.3.1 Microscopic Observations

5-FC/CD-UPRT induced apoptosis was studied by stained the cells with AO/EB and observed under confocal microscope (Ribble et al., 2005). The confocal microscopic images depicted in Figure 6.4 A, represented the untreated control and 5-FC/CD-UPRT treated BHK21 and HT29 cells. AO permeated the live cells and stained the nuclei green. Untreated control cells with well organized chromatin

TH-0560_03610605

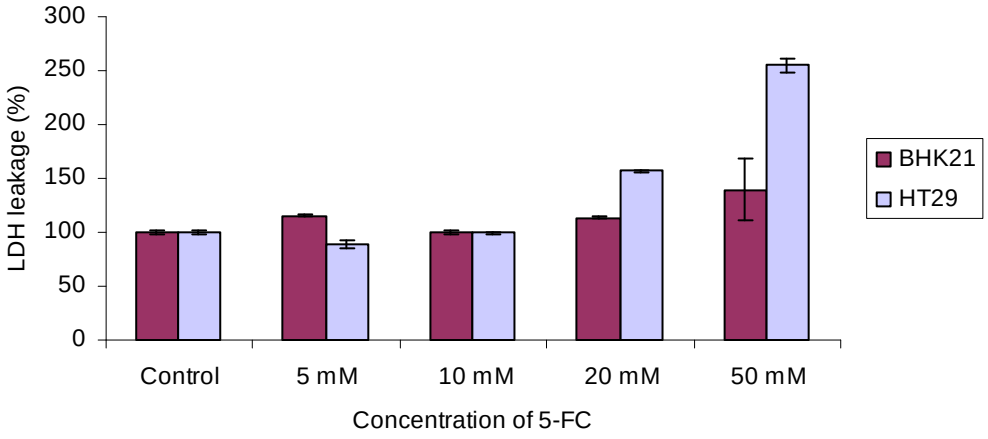

Figure 6.2: Effect of 5-FC/CD-UPRT on membrane leakage by LDH assay.

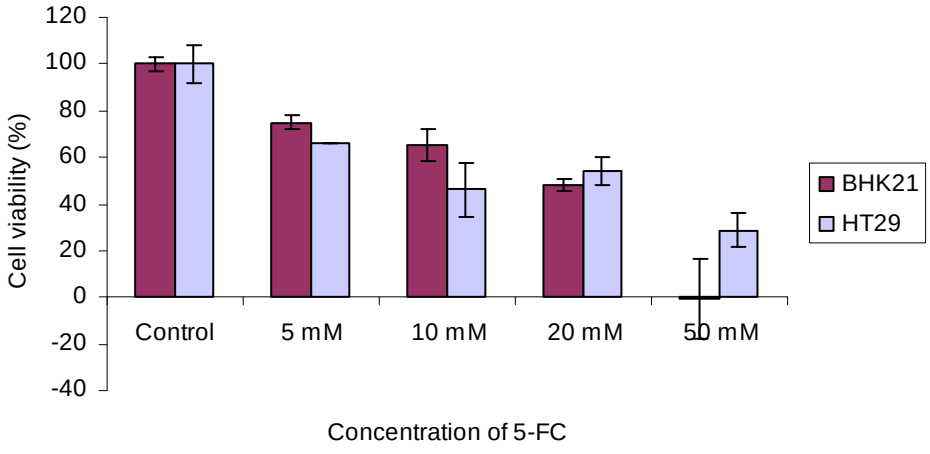

Figure 6.3: Effect of 5-FC/CD-UPRT on cell proliferation by MTS reduction assay.

TH-0560_03610605

structure exhibited normal green nucleus (Figure 6.4 A[a & c]) and the 5-FC/CD-UPRT treated cells, which were in early stage of apoptosis with fragmented or condensed chromatin exhibited bright green nucleus (Figure 6.4 A[b & d]). The number of treated cells gradually decreased with time due to more cell death.

Progressive nuclear uptake of EB that stained nuclei red due to cell membrane perforation during the late stage of apoptosis displayed condense and fragmented orange chromatin. Necrotic cells displayed structurally normal orange nucleus. The percentage of live, apoptosis and necrotic cell population were manually calculated by counting the cells (Figure 6.4 B). Thus, the nuclear staining experiments showed evidence of the 5-FC/CD-UPRT induced apoptosis.

Scanning electron microscopic observation of 5-FC/CD-UPRT treated cells exhibited the characteristic apoptotic cell surface morphology (Figure 6.5). 5-FC/CD-UPRT treated BHK21 and HT29 cells became rounded off with progressive membrane shrinkage with cell membrane blebbing due to apoptosis (Cohen et al., 1999 ; Dini 2005).

6.3.2 Synergistic Effect of 5-FC/ CD-UPRT with Curcumin

The Synergistic effect of 5-FC/CD-UPRT with curcumin was examined by quantitative apoptotic ELISA (Figure 6.6) (Nakamura and Wada 2000; Kusunoki et al., 2004). The amount of DNA fragments released into cytoplasm at 72 h after combine treatment of 5 mM or 10 mM 5-FC with 40 μM curcumin significantly increased (p<0.01) as compared to the 5-FC treatment alone and untreated control cells (Figure 6.6). The experiment revealed the synergistic effect of curcumin on 5-FC/CD-UPRT induced apoptosis. High therapeutic efficacy with low toxicity was achieved by combination of 5-FC with curcumin below their IC_{50} concentrations in

TH-0560_03610605

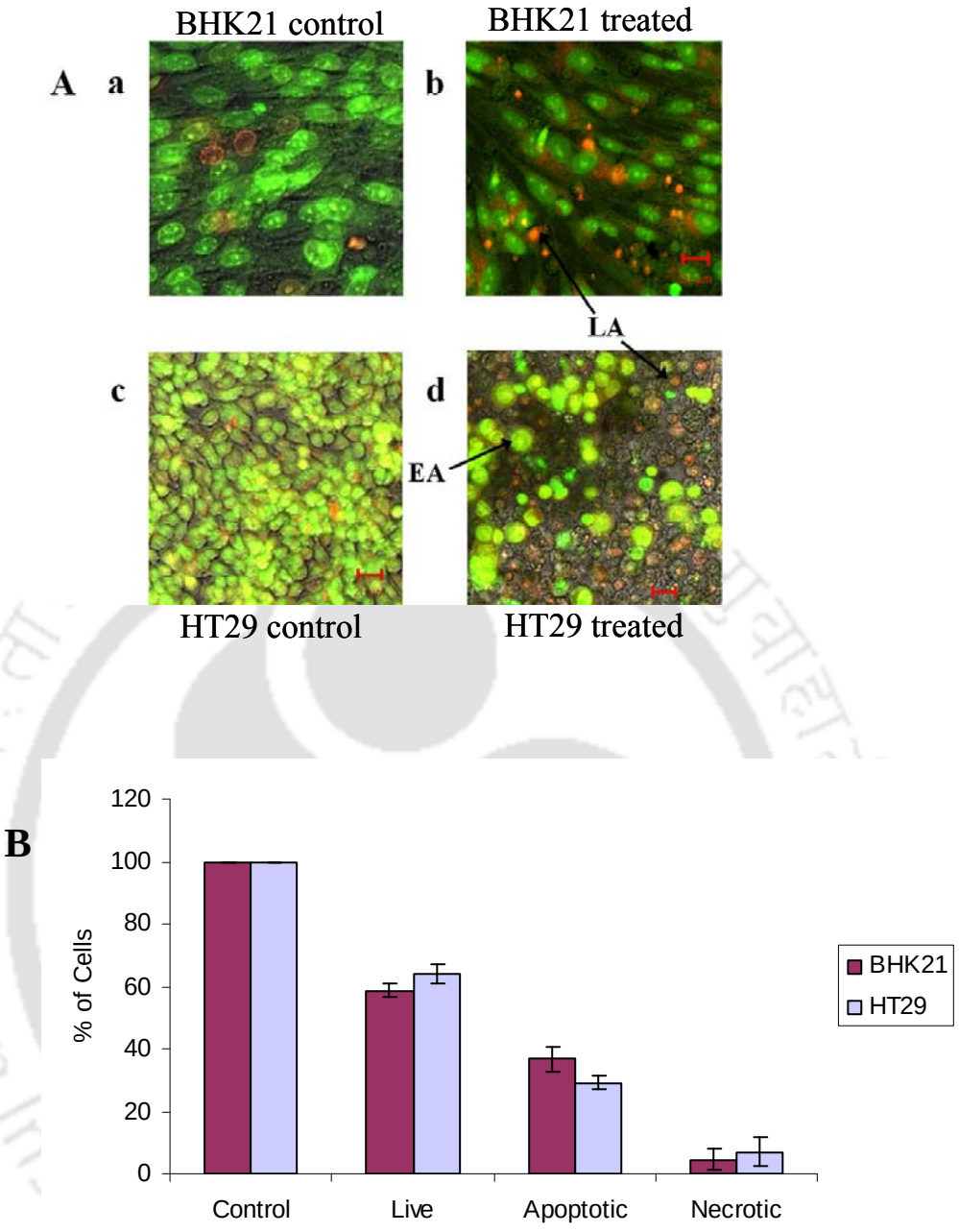

Figure 6.4: Confocal micrographs of AO/EB stained cells. **(A)** CD-UPRT transfected cells were treated with 10 mM 5-FC for 48 h. The representative images are **a** (control) & **b** (treated) for BHK21 cells and **c** (control) & **d** (treated) for HT29 cells. Green stained nuclei for early apoptosis (EA) and orange stained nuclei for late apoptotic (LA) are indicated by arrows. **(B)** represents the percentage of live, apoptotic and necrotic cells. Untreated control cells were considered as 100%.

TH-0560_03610605

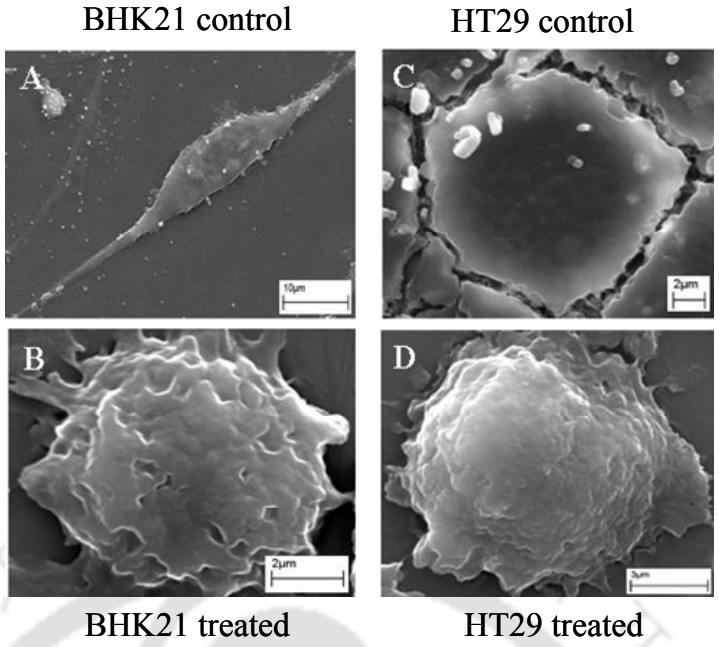

Figure 6.5: SEM analysis of 5-FC/CD-UPRT treated cells. **A** & **C** were the images of untreated control BHK21 and HT29 cells. **B** & **D** are the representative images of transfected BHK21 and HT29 cells treated with 10 mM of 5-FC for 48 h.

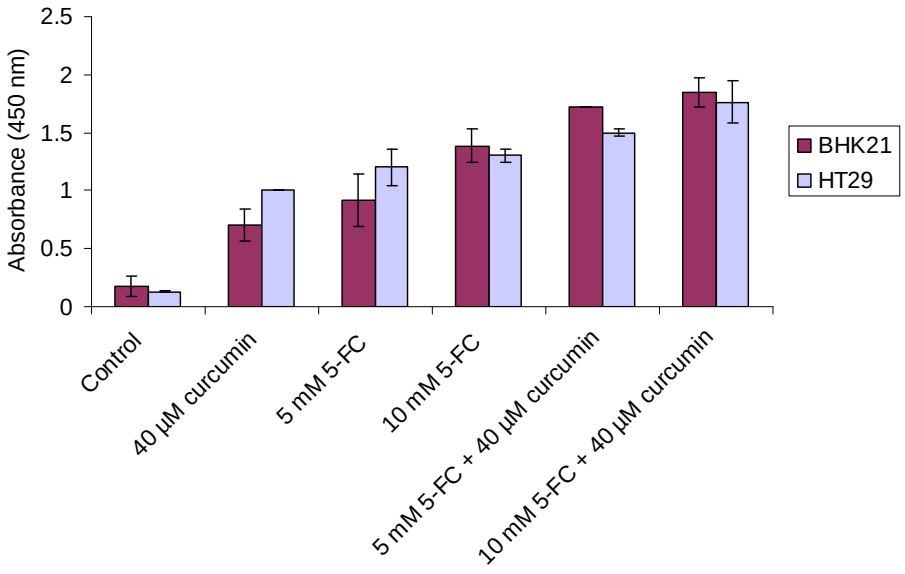

Figure 6.6: Quantification of 5-FC/CD-UPRT induced apoptosis by cellular DNA fragmentation ELISA.

TH-0560_03610605

CD-UPRT expressed cells. Thus, the possibility of utilizing such combined therapy for wide range use was investigated with two other cell lines, HEK293 and Hep3B, which also showed similar results.

Efficient transfer of CD-UPRT gene, reduction of cell viability and synergistic apoptotic induction on other cell types (HEK293 and Hep3B cells) was evidenced by fluorescence microscopy observation, MTS assay and DNA fragmentation ELISA respectively (Figure 6.7 A, B & C). Thus, combination therapy was equally effective for other cells types under similar experimental conditions.

6.3.3 Apoptotic DNA Laddering and Gene Expression

The internucleosomal cleavage of cellular DNA by CAD generates oligonucleosomal fragments. The oligonucleosomal DNA fragments displayed a characteristic laddering pattern in agarose gel, which is widely considered as biochemical hallmark of apoptosis (Wolf et al., 1999; Ishihara and Shimamoto 2006). Agarose gel electrophoresis of cellular DNA obtained from 5-FC/CD-UPRT treated BHK21 and HT29 cells showed characteristic DNA laddering in lane 3 & 5 of Figure 6.8 as compared to the untreated control (lane 2 & 4) confirmed apoptosis.

The involvement of apoptotic genes in 5-FC/CD-UPRT induced apoptosis was examined by semi-quantitative RT-PCR. Gene specific primers were used to study the expression of caspase-3, a well known signaling molecule of apoptotic pathway in cells treated with 5-FC/CD-UPRT alone or its combination with curcumin (Park et al., 2005). Here, β-actin gene expression was used for an internal control. RT-PCR products of caspase-3 in lane 2 & 3 for 5-FC treatment and combine therapy, was unaltered in both the conditions up to 12 h (Figure 6.9), which confirmed the active participation of caspase signaling in apoptotic pathway. The corresponding signals of

TH-0560_03610605

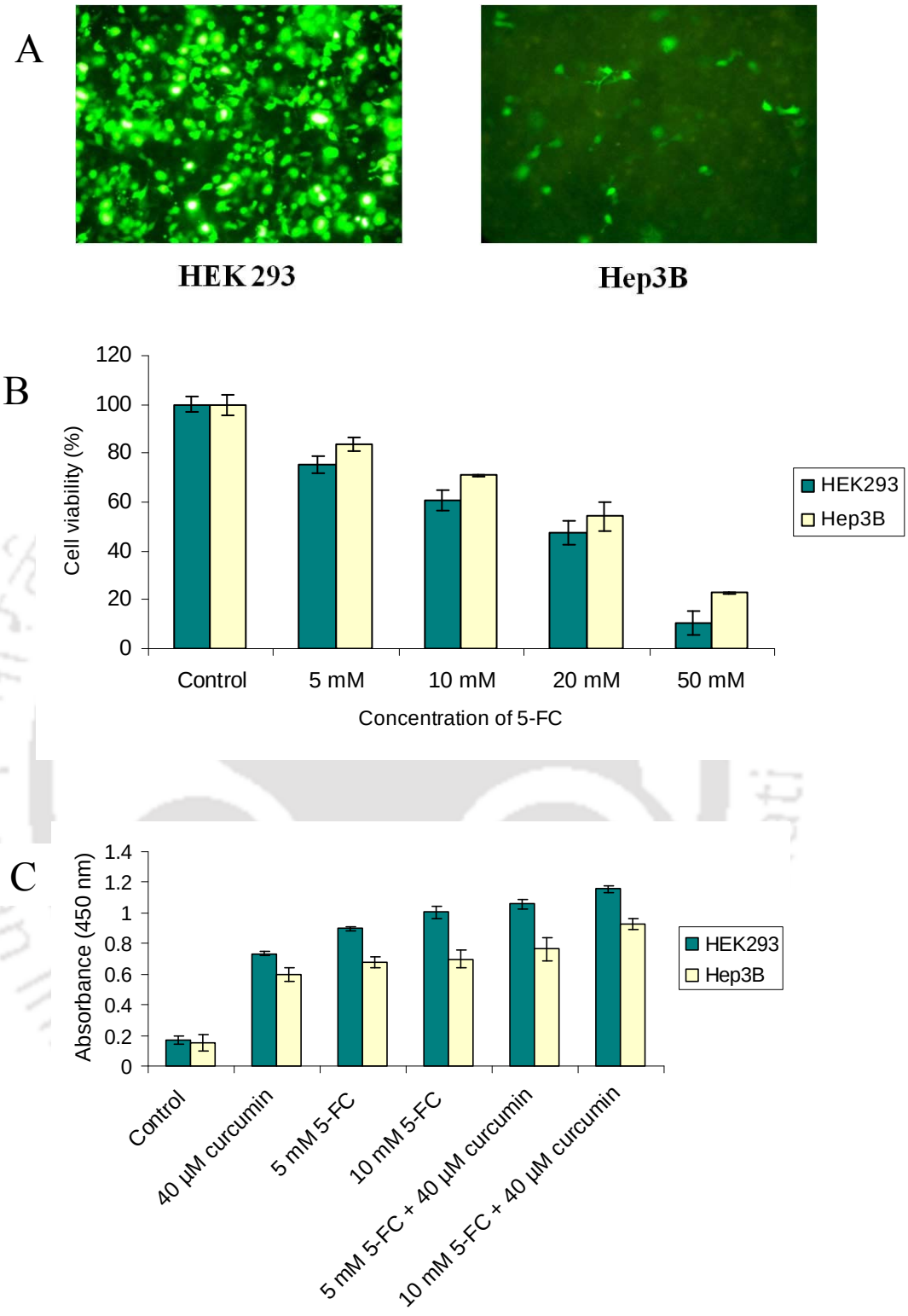

Figure 6.7: 5-FC/CD-UPRT treated HEK293 and Hep3B cells. **(A)** Fluorescence microscopic observation of GFP expression, **(B)** MTS assay and **(C)** DNA fragmentation ELISA.

TH-0560_03610605

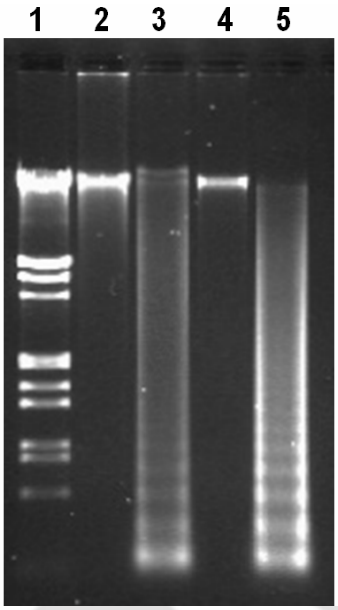

Figure 6.8: DNA laddering of 5-FC/CD-UPRT treated cells. BHK21 and HT29 cells were transfected with CD-UPRT gene and subsequently treated with 10 mM of 5-FC for 48 h. Cellular DNA was extracted and subjected to agarose gel electrophoresis. Lane 1: λ DNA/*Eco*R I + *Hind* III marker; lane 2: untreated control BHK21 cells; lane 3: CD-UPRT transfected BHK21 cells treated with 10 mM 5-FC; lane 4: untreated control HT29 cells; lane 5: CD-UPRT transfected HT29 cells treated with 10 mM 5-FC.

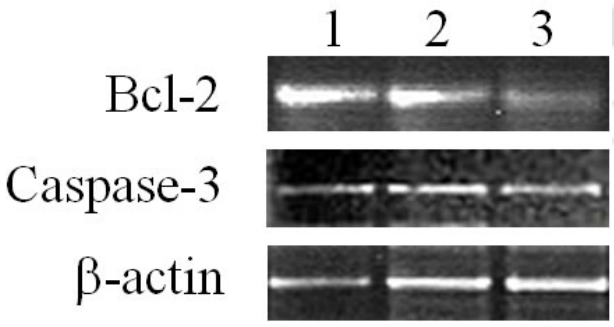

Figure 6.9: Expression profile of pro-apoptotic and anti-apoptotic genes. Lane numbers: 1, 2, 3 are for untreated control cells; 10 mM of 5-FC, and 10 mM of 5-FC with 40 μM of curcumin treatment.

TH-0560_03610605

bcl-2, an anti-apoptotic gene were significantly reduced for 5-FC treatment and combine therapy as compared to the control (Figure 6.9).These data confirmed the involvement of apoptotic genes in 5-FC/CD-UPRT induced cell death.

In summary, a recombinant plasmid pVITRO2 GFP/CD-UPRT was used and the therapeutic effect of CD-UPRT gene was studied in different cell types, which exerted strong anti-proliferation effect *in vitro*. The 5-FC/CD-UPRT induced apoptosis was evidenced by combination of experimental methods. The synergy in apoptosis is of great importance especially for cancers that are resistant to either conventional drug treatment or gene therapy become susceptible towards combined treatment. The combination of suicide gene therapy with curcumin showed high therapeutic efficacy for *in vitro* experiments.

TH-0560_03610605

7

COMPARATIVE ANALYSIS OF CD AND CD-UPRT

Overview

Success of gene therapy in cancer treatment is becoming a challenging task in the new era of medical sciences, where selection of suitable gene therapy vector is a major hurdle to achieve greater efficacy. Herein, the functional activity of two suicide genes namely, CD and CD-UPRT have been revealed by reverse phase HPLC of the various toxic metabolites that were formed during enzymatic conversion of the prodrug 5-FC. Therapeutic efficacy of these two suicide vectors was compared *in vitro*. PCR analysis established gene transfer, whereas RT-PCR confirmed expression of these genes in BHK21 and HT29 cells. A comparative therapeutic effect of these two suicide systems was done by cell viability assay (MTS), cell cytotoxicity assay (LDH) and quantitative DNA fragmentation ELISA. The synergistic effect of curcumin on 5-FC/CD and 5-FC/CD-UPRT systems was demonstrated. The

TH-0560_03610605

therapeutic efficiency of 5-FC/CD-UPRT was more than 5-FC/CD alone, which was further enhanced with curcumin treatment.

Results and Discussions

7.1 CD and CD-UPRT Gene Transfer and Expression

BHK21 and HT29 cells were electroporated with recombinant plasmids pCD and pCD-UPRT. PCR amplification of 1.9 kb and 1.2 kb confirmed the CD-UPRT and CD gene transfer respectively, for BHK21 (lane 4 for CD-UPRT, and lane 11 for CD) and for HT29 cells (lane 5 for CD-UPRT and lane 12 for CD), as represented in Figure 7.1. The corresponding RT-PCR analysis on total RNA confirmed the gene expression in BHK21 (lane 7 for CD-UPRT, and lane 14 for CD) and HT29 cells (lane 8 for CD-UPRT, lane 15 for CD), as represented in Figure 7.1.

7.2 CD and CD-UPRT Enzymatic Activity *in vitro*

The functional activity of CD and CD-UPRT enzymes *in vitro* was shown by reverse phase HPLC analysis of the products (Khatri et al. 2006). The enzymatic conversion of 5-FC to 5-FU by CD enzyme, and 5-FC to 5-FU and other metabolites (possibly, 5-FUMP, 5-FdUMP and 5-FUTP) by the enzyme CD-UPRT was determined in transfected BHK21 and HT29 cells. The HPLC profile of the reaction products showed various retention times (Figure 7.2). Untransfected cells did not show any detectable enzymatic activity.

7.3 Comparative Analysis of Cell Viability and Cytotoxicity

BHK21 and HT29 cells transfected with pCD and pCD-UPRT were treated with different concentrations of 5-FC (0, 5, 10, 20 and 50 mM) to compare the

TH-0560_03610605

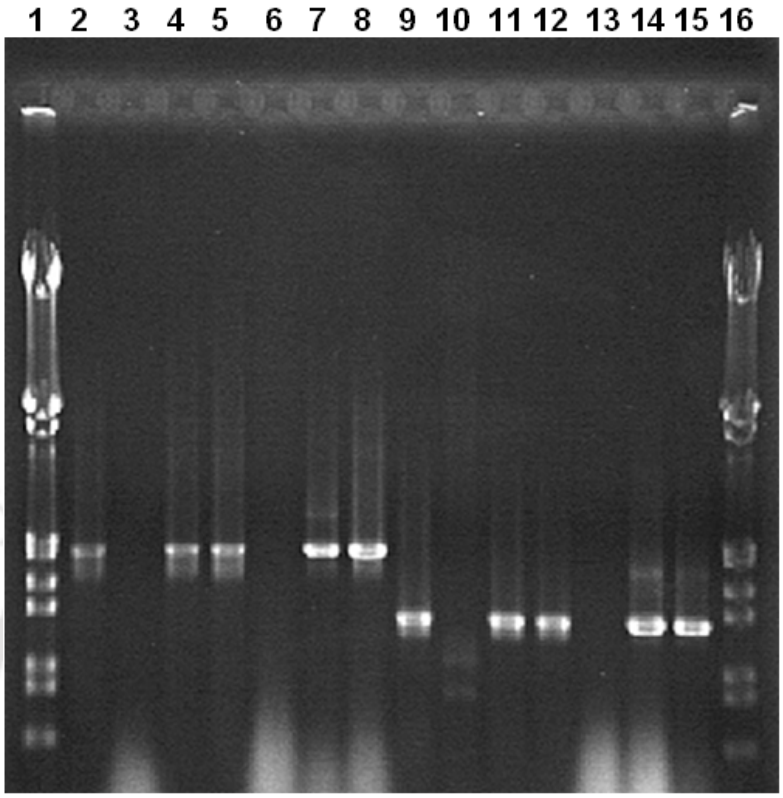

Figure 7.1: PCR and RT-PCR analysis of transfected cells. Cellular DNA & RNA extracted from the CD and CD-UPRT transfected cells were subjected to PCR (lane 2- 5 & 9-12) & RT-PCR (lane 6- 8 & 13-15) analysis. Lane 1 & 16: λ DNA/ *Eco*R I + *Hind* III marker; lane 2: 1.9kb PCR amplicon of CD-UPRT as positive control; lane 3 & 6: untransfected control BHK21 cells; lane 4 & 7: CD-UPRT transfected BHK21cells; lane 5 & 8: CD-UPRT transfected HT29 cells; lane 9: 1.2 kb PCR amplicon of CD as positive control; lane 10 & 13: untransfected control BHK21 cells; lane 11 & 14: CD transfected BHK21cells; lane 12 &15: CD transfected HT29 cells.

TH-0560_03610605

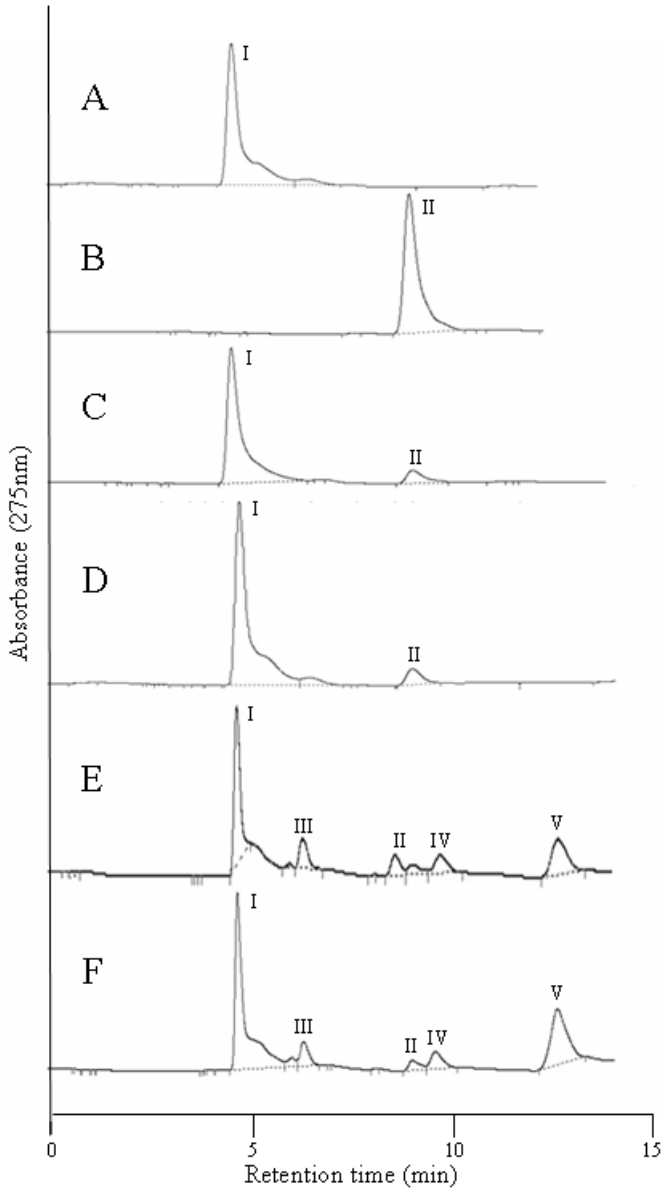

Figure 7.2: Functional activity measurement by reverse phase HPLC. Reverse phase HPLC analysis was used to determine the catabolism of the prodrug 5-FC to 5-FU and its other derivatives by CD and CD-UPRT enzymes, respectively. **(A)** the peak for 5-FC was represented by I (control) ; **(B)** for 5-FU (II) (Control); **(C)** and **(D)** showed the conversion of 5-FC (I) to 5-FU (II) by CD enzyme for BHK21 and HT29 cells, respectively; **(E)** and **(F)** showed the conversion of 5-FC (I) to 5-FU (II) derivatives (III, IV, and V) by CD-UPRT enzyme for BHK21 and HT29 cells, respectively.

TH-0560_03610605

therapeutic effect of CD and CD-UPRT gene (Rowley et al. 1996). The cell viability assay (Figure 7.3 A & B) and cell cytotoxicity assay (Figure 7.4 A & B) was used to evaluate therapeutic potential of 5-FC/CD and 5-FC/CD-UPRT suicide systems (Bernt et al., 2002; Miyagi et al., 2003) for both BHK21 and HT29 cell types. A 5-FC concentration dependent cell death was observed, where CD-UPRT showed more significant cell death as compared to CD alone. The higher therapeutic effect of CD-UPRT than CD was confirmed by conversion of 5-FU into more cytotoxic metabolites by CD-UPRT, as represented in the products analysis of HPLC (Figure 7.2).

7.4 Synergistic Effect of Curcumin on 5-FC/CD and 5-FC/CD-UPRT

The synergistic effect of curcumin on 5-FC/CD and 5-FC/CD-UPRT for apoptotic induction was quantitated by Cellular DNA fragmentation ELISA (Pan et al. 2001). The results demonstrated a significant increase of DNA fragments release for combine treatment of 5 mM & 10 mM 5-FC with 40 μM curcumin as compared to the 5-FC treatment alone and untreated control cells (Figure 7.5 A & B). In presence of curcumin, 5-FC/CD-UPRT treated cells showed more apoptosis as compared to 5-FC/CD (Figure 7.5 A, B), which also confirmed the synergistic effect of curcumin.

TH-0560_03610605

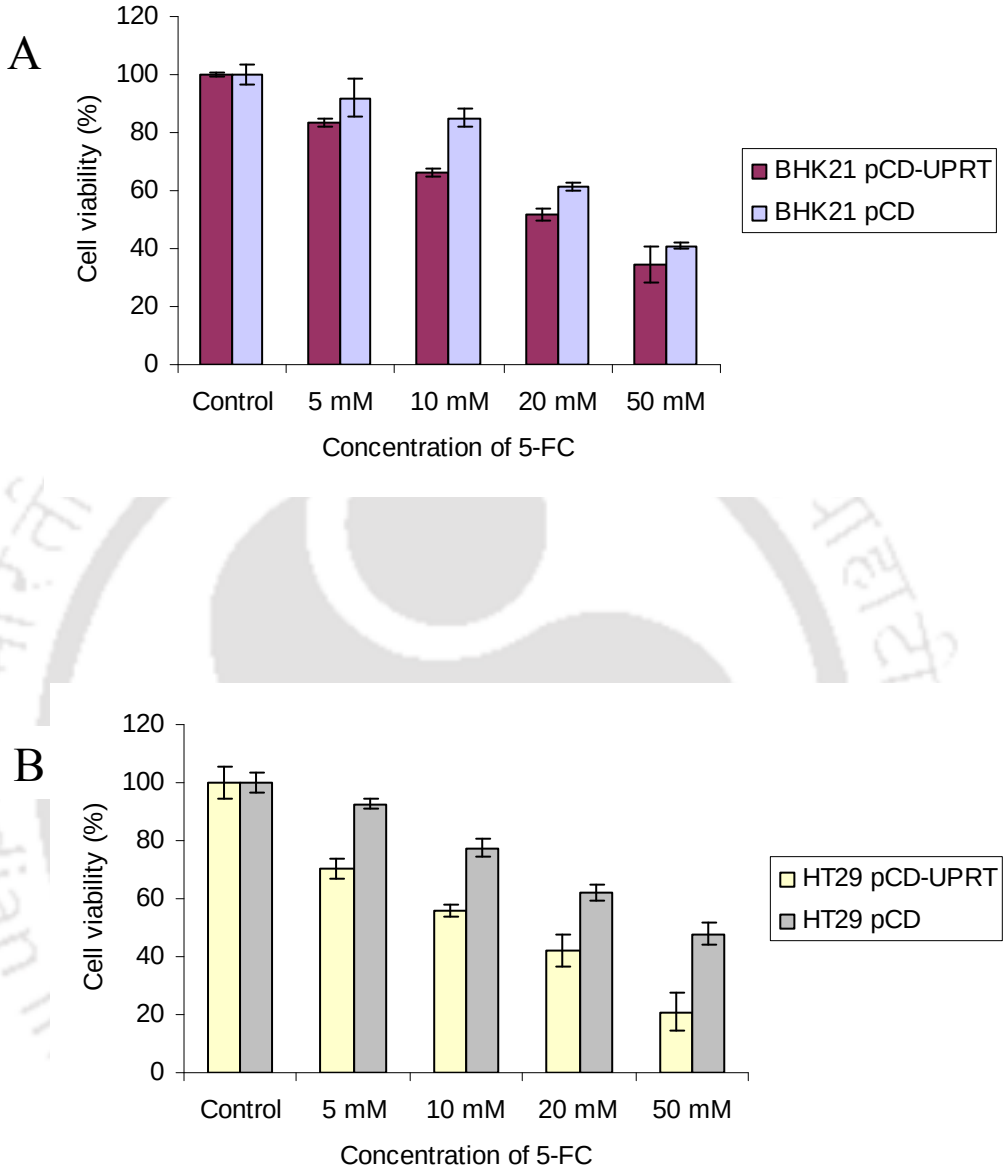

Figure 7.3: Cell viability by MTS reduction assay. BHK21 **(A)** and HT29 cells **(B)** transfected with CD and CD-UPRT were treated with different concentrations of 5-FC for 96 h.

TH-0560_03610605

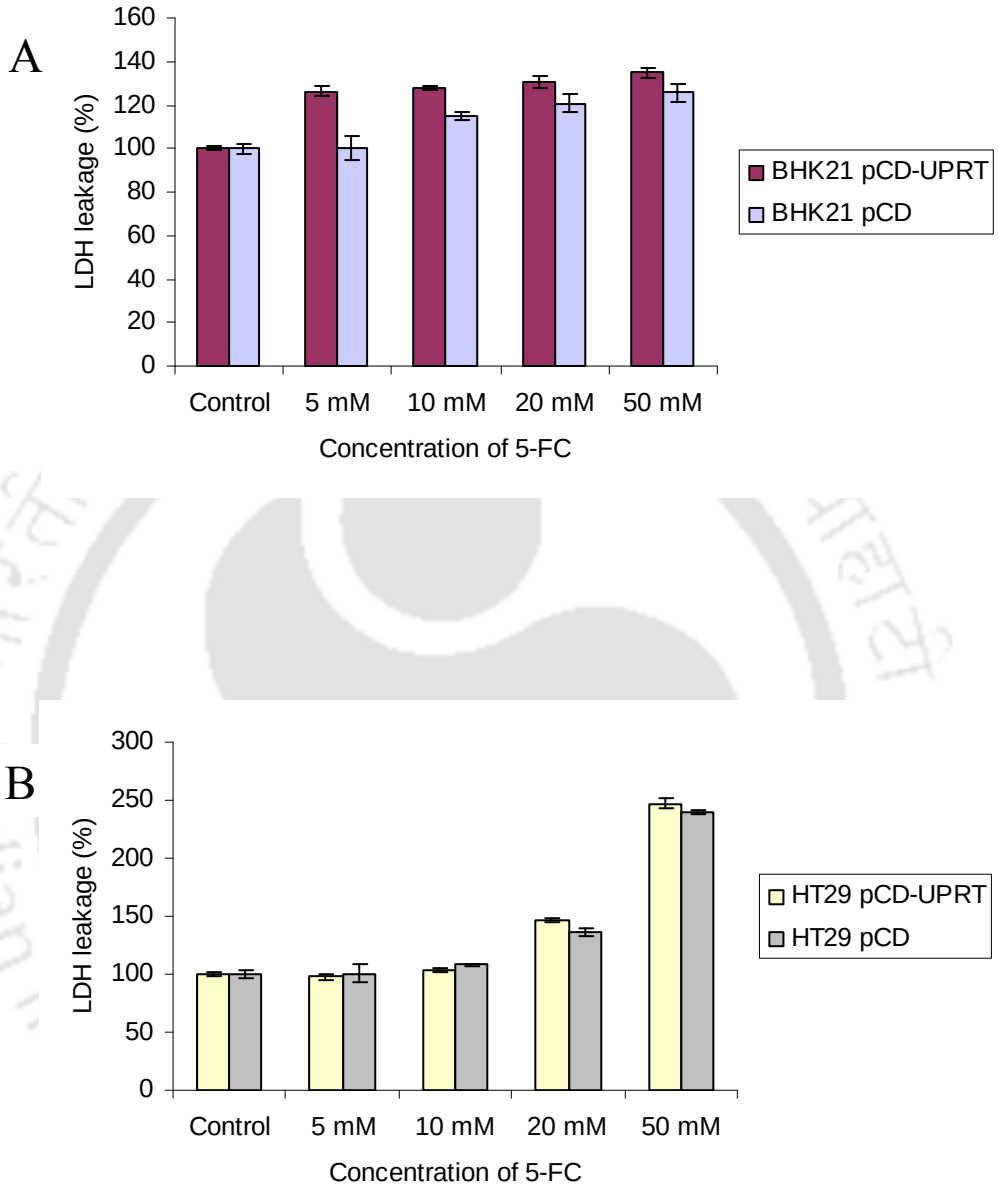

Figure 7.4: LDH assay to measure the release of LDH leakage. BHK21 **(A)** and HT29 cells **(B)** transfected with CD and CD-UPRT were treated with different concentrations of 5-FC for 96 h.

TH-0560_03610605

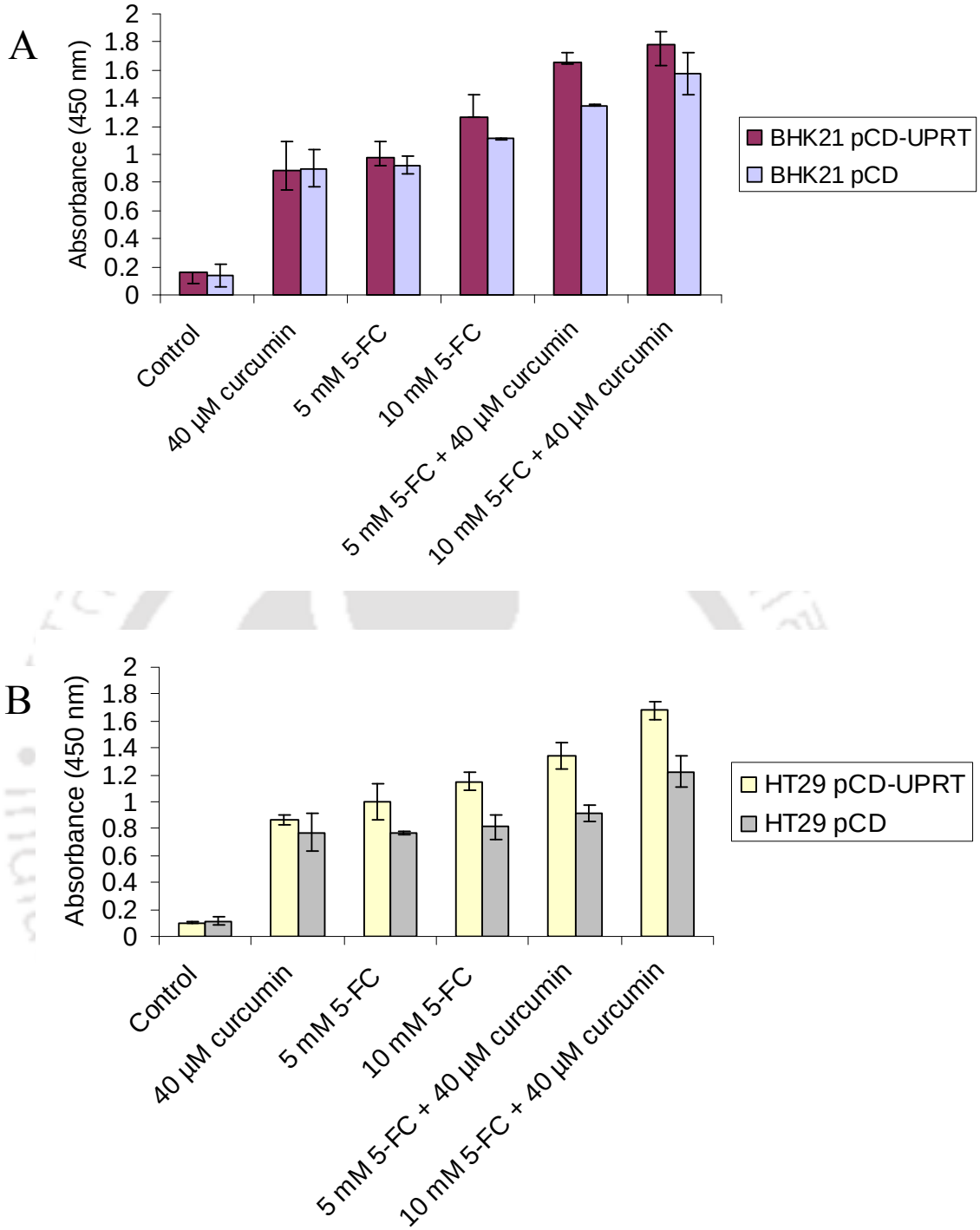

Figure 7.5: Cellular DNA fragmentation ELISA. The BrdU labeled BHK21 **(A)** and HT29 cells **(B)** were transfected with CD and CD-UPRT was treated with 5-FC alone or 5-FC in combination with curcumin (40 µM) for 72 h. DNA fragments released to cytoplasm from nuclei due to apoptosis were quantitated by recording absorbance at 450 nm.

TH-0560_03610605

In summary, the higher therapeutic efficiency of CD-UPRT than CD was established by MTS, LDH and apoptotic ELISA. Conversion of 5-FC to 5-FU and other derivatives by CD-UPRT enzyme confirmed its higher therapeutic effect. Furthermore, the therapeutic effect was potentiated with curcumin. Hence, 5-FC/CD-UPRT with curcumin would primarily be the better choice to achieve high therapeutic efficacy.

TH-0560_03610605

8

BYSTANDER EFFECT AND APOPTOSIS

Overview

Complete annihilation of tumor cells with long-term reproductive potential is a major concern in cancer therapy. Suicide gene therapy is an alternative approach for cancer treatment but limited by the inefficient gene delivery techniques. Therefore, a suicide gene with strong "bystander effects" would overcome these limitations, because very high transduction efficiency is not necessary for total killing of cancer cells if bystander effect exists, where the genetically modified tumor cells exert toxic metabolites to kill the neighboring unmodified cells in the local microenvironment. Hence, the successful eradication of cancer cells through suicide gene therapy depends on the degree of bystander effect. CD-UPRT fusion gene has been shown to have a strong therapeutic effect by inducing apoptosis *in vitro*. However, there is little data to evaluate molecular pathway of 5-FC/CD-UPRT mediated apoptosis and its strong bystander effect. A stable BHK21 cell lines expressing CD-UPRT and GFP was generated, where GFP has been used as a noninvasive probe to monitor the therapeutic effect of CD-UPRT. Dose dependent inhibition of cell growth by

TH-0560_03610605

5-FC/CD-UPRT and its strong bystander effect was investigated using MTS assay. Enzyme activity of CD-UPRT in the stable cell line was confirmed by the reverse phase HPLC analysis of the metabolic products. Atomic Force Microscopy (AFM) was used to explore the degrees of surface roughness in the 5-FC/CD-UPRT treated cells as compared to the smooth contour of the untreated cells. The involvement of apoptotic signaling genes was revealed by semi-quantitative RT-PCR.

Results and Discussions

8.1 CD-UPRT Gene Expression and its Functional Activity

CD-UPRT and GFP dual transcripts expressing BHK21 cells (BHK21 CD-UPRT::GFP) were generated by clonal selection. Confocal microscopic images of GFP (Figure 8.1 A & B) confirmed the presence of GFP unit in the stable hygromycin resistant cell lines, where as the PCR amplification of CD-UPRT confirmed the presence of CD-UPRT gene (Figure 8.1 C, Lane 3). The corresponding RT-PCR results depicted in lane 5 of the Figure 8.1 C, confirmed the presence of full length 1.9 kb RNA transcript. The functional activity of CD-UPRT enzyme was determined *in vitro* by reverse phase HPLC analysis (Khatri et al., 2006). HPLC profile of the reaction mixture shown in Figure 8.1 D, elucidated the conversion of 5-FC to 5-FU and other metabolites (possibly, 5-FUMP, 5-FdUMP and 5-FUTP) by the enzyme CD-UPRT.

8.2 Cell Viability upon 5-FC Treatment

Concentration dependent sensitization of BHK21 CD-UPRT::GFP cells upon 5-FC treatment was observed by cell viability assay at 48 h and the IC_{50} was found to be ~5 mM (Figure 8.2 A). The survival rate decreased sharply, especially at 5 mM to

TH-0560_03610605

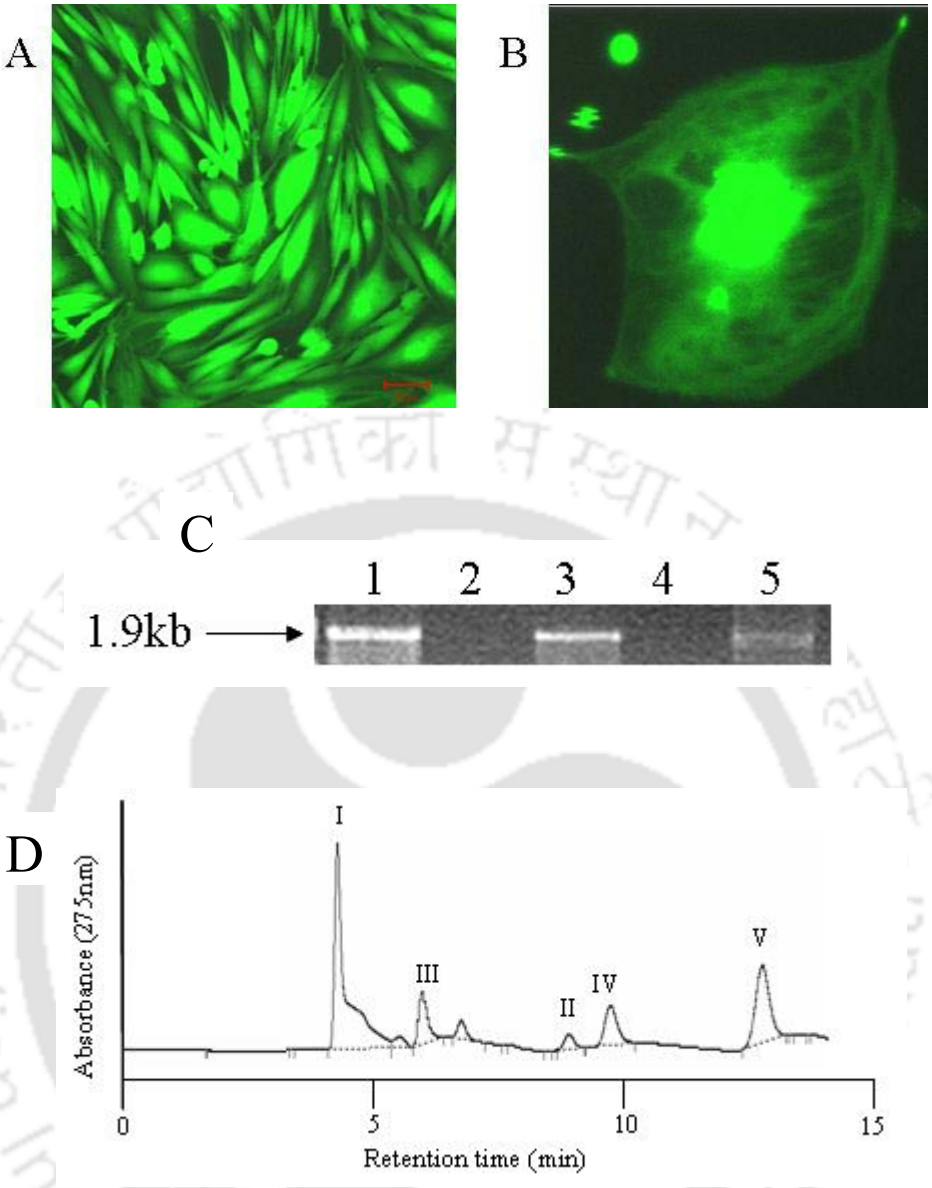

Figure 8.1: CD-UPRT expression in stable BHK21 CD-UPRT::GFP cells. **(A)** Confocal microscopic observation of GFP expression in stable BHK21 CD-UPRT::GFP cells and **(B)** Confocal micrograph of a single BHK21 CD-UPRT::GFP expressing cell. **(C)** PCR (lane 1- 3) & RT-PCR (lane 4&5) analysis. Lane 1: 1.9 kb PCR amplicon of CD-UPRT as positive control; lane 2 & 4: control BHK21 cells; lane 3 & 5: BHK21 CD-UPRT::GFP cells. **(D)** Reverse phase HPLC analysis shows the conversion of 5-FC (I) to 5-FU (II) and its derivatives (III, IV, and V) by CD-UPRT enzyme of BHK21 CD-UPRT::GFP cells.

TH-0560_03610605

50 mM 5-FC.The corresponding decrease in number of GFP expressing cells (Figure 8.2 B) correlated with the growth inhibition profile of the treated cells (Gopinath and Ghosh 2007a). The number of treated cells gradually decreased with time due to more cell death. Similarly, 5-FC concentration dependent induction of apoptotic cell death was quantitated by BrdU labeled cellular DNA fragmentation ELISA at 48 h (Figure 8.2 C). Cellular DNA obtained from 5-FC treated cells at 48 h showed characteristic DNA laddering in agarose gel electrophoresis (Lane 3 of Figure 8.2 D). There was no DNA laddering in untreated cells lane 2 of Figure 8.2 D.

8.3 Bystander Effect

BHK21 CD-UPRT::GFP clonal cells exhibited "bystander effect" when mixed with CD-UPRT negative parental cells at different ratios and treated with 5-FC. From Figure 8.3 A, the cell survival rate (SR) was 21%, 9%, and 0% when there was 25%, 50%, and 75% of BHK21 CD-UPRT::GFP cells in all, the inhibitory rate (IR=1-SR) was 79%, 91%, 100% respectively. The presence of only 10% of CD-UPRT::GFP cells led to an overall 54% decrease in cell survival after incubation with 5-FC for 96 h. Apparently the IR was much higher than the percentage of BHK21 CD-UPRT::GFP cells, which reflected the bystander effect (Wang et al., 2004). The bystander effect was also confirmed by using conditioned medium (Khatri et al., 2006), where the medium taken from the 5-FC treated CD-UPRT cells at 48 h, were mixed with an equal proportion of fresh medium and incubated with parental cells for 96 h showed bystander cytotoxic effect (Figure 8.3 B). Therefore, the bystander effect has significantly amplified the therapeutic efficacy 5-FC/CD-UPRT suicide gene therapy, which is very important for greater therapeutic implications.

TH-0560_03610605

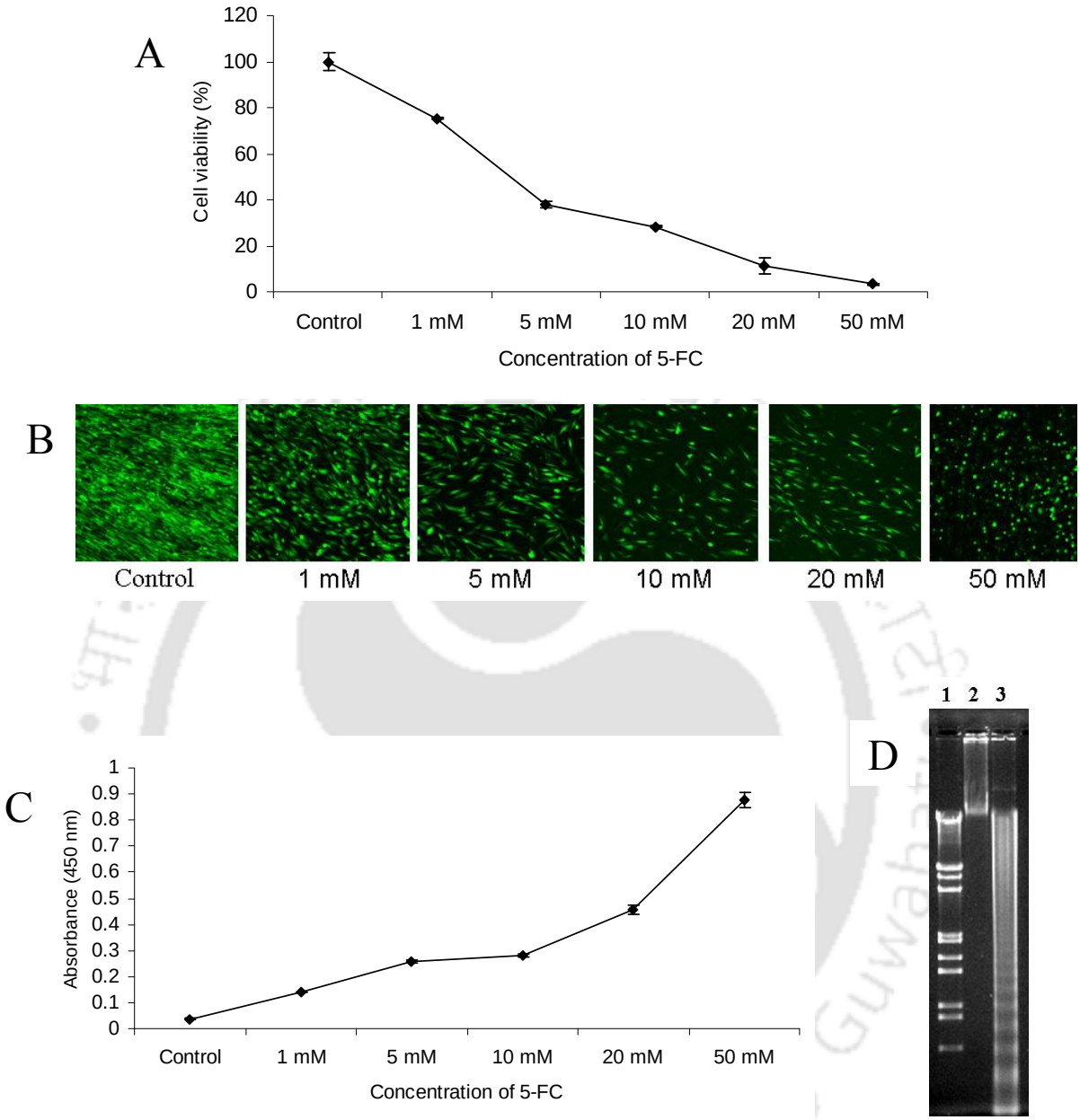

Figure 8.2: Cell viability and apoptosis of 5-FC treated BHK21 CD-UPRT::GFP cells. **(A)** Cell viability measurement by MTS. **(B)** Confocal microscopic observation of GFP upon 5-FC treatment. **(C)** Apoptotic DNA fragmentation by ELISA. **(D)** Apoptotic DNA laddering. Lane 1: λ DNA/*Eco*R I + *Hind* III marker; lane 2: untreated control BHK21 CD-UPRT::GFP cells; lane 3: BHK21 CD-UPRT::GFP cells treated with 5 mM 5-FC for 48 h.

TH-0560_03610605

8.3. Apoptosis Induction with 5-FC Treatment

8.3.1 AFM Imaging

Recent advancement of AFM as a powerful tool to investigate biological processes and topographic structures on the surface of living cells provides three dimensional molecular resolution of treated cells (Ye et al., 2006). In order to gain insight into the fine structure, BHK21 CD-UPRT::GFP cells were treated with 5-FC for 48 h and the structure of the cell surface was examined by zooming at the regions of 10 μm × 10 μm under AFM in the non contact mode. The AFM images of the cells, as represented in Figure 8.4, revealed a remarkable difference in cell surface architecture in the absence and presence of 5-FC. Cells treated with 5-FC for 48 h showed different degrees of higher surface roughness (Figure 8.4 C & D) and indentations spread over cell surfaces, while untreated cells were featured by comparatively smoother surface (Figure 8.4 A & B). The visible protruding particles were mostly the clusters of membrane proteins and the underlying gorges were possibly lipid layers (Le Grimellec et al., 1994; Parpura and Fernandez 1996). The disorganized membrane surface consisting of protruding protein clusters indicated the randomization of membrane lipid distribution in 5-FC treated cells. Taken together, these topographic AFM images provided a direct proof of membrane alteration of BHK21 CD-UPRT::GFP cells. Thus, AFM was used to characterize the membrane damage due to apoptosis induced by suicide genes.

8.3.2 Apoptosis Signaling Genes

The involvement of apoptotic signaling genes in 5-FC/CD-UPRT mediated cell death was confirmed by semi-quantitative RT-PCR. The β-actin gene expression was used as internal control for the experiment (Figure 8.5 A).

TH-0560_03610605

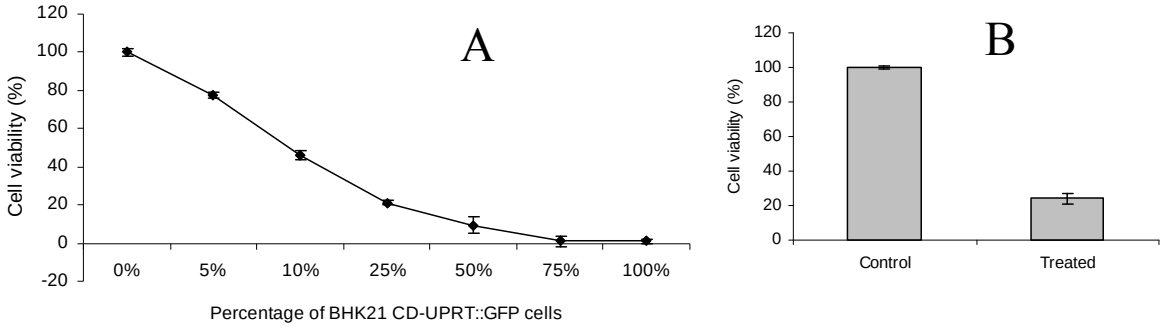

Figure 8.3: Bystander effects of BHK21 CD-UPRT::GFP cells. **A.** Co-culture method and **B.** Conditioned medium method.

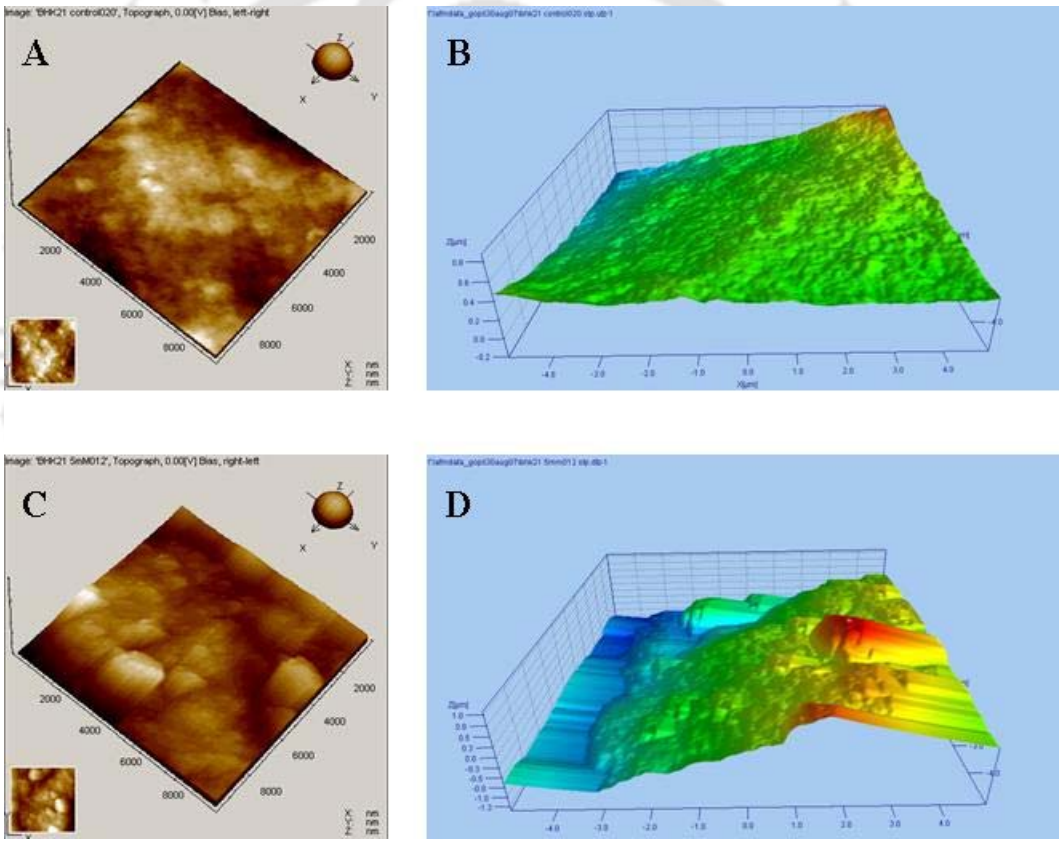

Figure 8.4: AFM analysis of 5-FC treated BHK21 CD-UPRT::GFP cells. Atomic force microscope images showing the three-dimensional surface topography of BHK21 CD-UPRT::GFP cell membrane under 10 µm × 10µm fields of view, **(A** & **B)** Control; **(C** & **D)** 5-FC treated cells. The three-dimensional images **A** & **C** and **B** & **D** were obtained using Picoscan 5.3.3 and SPIP 4.6.3 software, respectively.

TH-0560_03610605

From the Figure 8.5 A, it was clear that there was an up regulation (indicated by upward arrow) of apoptotic genes like, caspase-3, bak, bax, bad, c-myc and down regulation (indicated by downward arrow) of anti-apoptotic genes like, bcl-2 and bcl X_L. Caspases are known to be activated during apoptosis in many cells, where caspase-3 plays critical role in both the initiation and the execution of apoptosis. Activated caspases-3 cleaves the inhibitor of caspase-activated DNase (ICAD) and releases the caspases activated DNase (CAD) from the complex. CAD enters the nucleus and degrades chromatin into oligo-nucleosomal fragments (Pandey et al., 2000) leading to apoptosis, which exhibits a characteristic laddering pattern in agarose gel. This results suggested 5-FC/CD-UPRT induced apoptosis involved activation of caspase-3 and the resultant cascade of reactions there of (Cohen 1997). Bcl-2 family proteins are important regulators of apoptosis. Down regulation of anti-apoptotic bcl-2 and bcl X_L genes was observed. Bcl X_L has been already reported to be down-regulated by c-myc protein (Merino et al., 1995, Duyao et al., 1990). It was observed that c-myc expression was increased, which correlated the role of c-myc in down regulation of bcl X_L (Susin et al., 1999, Sun et al., 1999). Moreover, p53 is also known to regulate negatively cellular division by controlling a set of genes required for this process. Apoptosis induction mediated by p53 involves either stimulation of Bax and Fas antigen expression, or the repression of bcl-2 expression. The elevated expression p53 and suppression of bcl-2 upon 5-FC treatment was noted. Other apoptotic molecule such as Bad is known to dimerize selectively with Bcl X_L and inhibits the survival-promoting effects of Bcl X_L. In 5-FC treated cells, an increase in bad expression was also observed. In the presence of an appropriate stimulus, Bak is known to accelerate programmed cell death by binding to, and antagonizing α repressor of Bcl-2, which was confirmed by the elevated Bak expression in treated

TH-0560_03610605

cells. The involvement of signaling genes in apoptotic induction was represented schematically in Figure 8.5 B. It was observed that 5-FC/CD-UPRT up-regulated different pro-apoptotic genes and at the same time down-regulated anti-apoptotic genes, which revealed the involvement of apoptotic signaling genes in CD-UPRT mediated cell death.

In summary, CD-UPRT and GFP expressing BHK21 stable cell lines was generated, where GFP expression was monitored as a non invasive probe to determine therapeutic index of 5-FC/CD-UPRT. Quantitative DNA fragmentation ELISA and

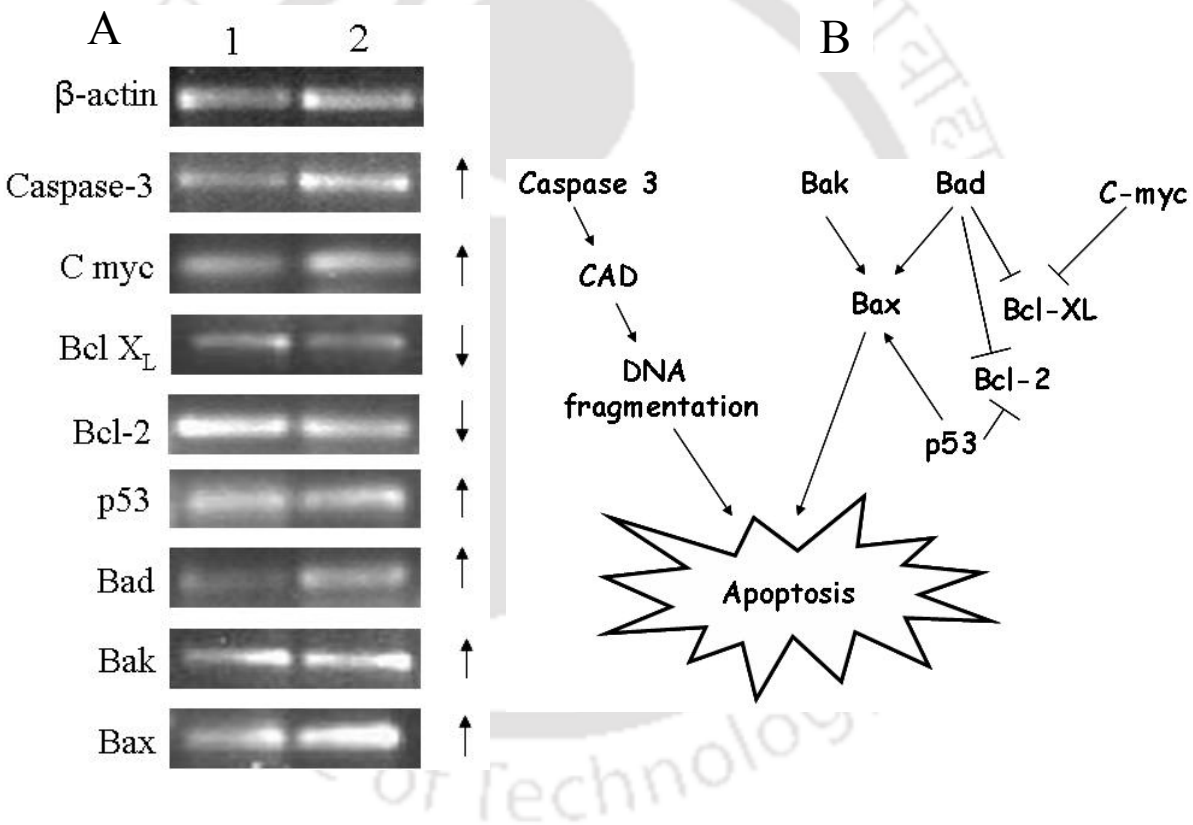

Figure 8.5: Semi-quantitative RT-PCR analysis of apoptotic signaling genes. **(A)** Expression profile of pro-apoptotic and anti-apoptotic genes. Column 1: Untreated control BHK21 CD-UPRT::GFP cells; Column 2: BHK21 CD-UPRT::GFP cells treated with 5 mM 5-FC for 12 h **(B)** Schematic representation of 5-FC/ CD-UPRT induced apoptotic pathway.

TH-0560_03610605

characteristic cell morphology changes observed by AFM confirmed the 5-FC/ CD- UPRT induced apoptosis. A strong bystander effect of CD-UPRT was demonstrated by co-culture and conditioned medium. The signaling genes were identified, which confirmed involvement of mitochondria in apoptosis. Such understanding of molecular pathways of apoptosis and determination of strong bystander effect would primarily establish CD-UPRT as a potent suicide gene for future therapeutic application.

TH-0560_03610605

9

CONCLUSIONS AND SCOPE FOR FUTURE WORK

9.1 Conclusions

The studies carried out using the suicide genes CD, UPRT and CD-UPRT along with curcumin or Ag NPs have revealed certain interesting results. From the experimental results presented in all the chapters, the following conclusions can be drawn:

- The chemotherapeutic effects of 5-FC/CD and 5-FC/CD-UPRT was established using plasmid based system, where the GFP fluorescence could be used as probe for functional detection of CD and CD-UPRT gene.
- Antibacterial property of Ag NPs studied by the application of green fluorescent protein expressing bacteria facilitated the rapid monitoring of cause-effect phenomena by microscopic techniques.
- In addition to conventional viability tests, TEM analysis, the morphological changes of the fluorescent bacteria and electrophoretic

TH-0560_03610605

analysis of cellular DNA and protein migration profiles established the effect of Ag NPs on GFP expressing bacteria.

- Ag NPs may act as a therapeutic agent. Furthermore, identification of Ag NPs induced apoptotic pathway enabled it as a representative of new chemosensitization strategy along with gene therapy. The Ag NPs induced apoptosis was mediated through caspase signaling.
- Induction of apoptosis by suicide genes CD, UPRT and CD-UPRT in both cancer and non-cancer cells was confirmed using combination of experimental methods.
- Concentration dependent induction of apoptotic pathway and synergistic apoptosis by combination of suicide gene with curcumin or Ag NPs has immense potential application in combinatorial therapy.
- The synergy in apoptosis, where the individual components used at much lower concentration than their IC_{50} values, revealed the combination of suicide gene therapy with curcumin or Ag NPs as a better choice to achieve high therapeutic efficacy.
- 5-FC/CD-UPRT showed more therapeutic potential than 5-FC/CD alone when tested on cancer cells, which was further induced with curcumin treatment.
- Involvement of apoptotic signaling genes was determined in CD-UPRT and GFP expressing stable cell line. The strong bystander effect of CD-UPRT was revealed, which established CD-UPRT as a potent suicide gene therapy system.

TH-0560_03610605

9.2 Scope for Future Work

- The apoptotic gene expressions in suicide gene therapy shall be further quantified by real time PCR analysis.
- Similarly, apoptotic signaling gene expressions in Ag NPs induced apoptosis shall be quantified by real time PCR analysis.
- Apoptosis study by FACS (Fluorescence Activated Cell Sorter) analysis would render information regarding the percentage of necrotic cells, early apoptotic cells and late apoptotic cells in a more quantitative format.
- Ag NPs and suicide genes needs to be incorporated in delivery systems such as, chitosan nanoparticles or surface modified liposomes for developing targeted delivery vehicles.
- The present findings suggest the significance of Ag NPs as novel nanomedicine for development of anticancer drug with strong therapeutic potential, which could be used in conjunction with gene therapy.
- In order to avoid the difficulties associated with the current gene delivery methods, the electroporation based suicide gene delivery could be further exploited.
- In combination therapy, the synergy in apoptosis is of great importance, especially for those cancers that are resistant to either conventional drug treatment or gene therapy, may become susceptible towards combined treatment. Thus, these combinatorial therapies have to be explored *in vivo* to achieve therapeutic efficacy.

TH-0560_03610605

BIBLIOGRAPHY

Belakavadi M and Salimath BP. (2005) Mechanism of inhibition of ascites tumor growth in mice by curcumin is mediated by NF-kB and caspase activated DNase. *Mol.Cell Biochem.* 273, 57–67.

Bernt KM, Steinwaerder DS, Ni S, Li Z, Roffler SR and Lieber A. (2002) Enzyme-activated prodrug therapy enhances tumor-specific replication of adenovirus vectors. *Cancer Res.* 62, 6089–6098.

Bielak-Zmijewska A, Koronkiewicz M, Skierski J, Piwocka K, Radziszewska E, and Sikora E. (2000) Effect of curcumin on the apoptosis of rodent and human nonproliferating and proliferating lymphoid Cells. *Nutr. Cancer* 38, 131-138.

Braydich-Stolle L, Hussain S, Schlager JJ and Hofmann MC. (2005) *In vitro* cytotoxicity of nanoparticles in mammalian germline stem cells. *Toxicol Sci.* 88, 412-419.

Bridgewater G, Springer CJ, Knox R, Minton N, Michael P and Collins M. (1995) Expression of the bacterial nitroreductase enzyme in mammalian cells renders them

TH-0560_03610605

selectively sensitive to killing by the prodrug CB1954. *Eur. J. Cancer* 31A, 2362–2370.

Cao G, Pei W, Lan J, Stetler RA, Luo Y, Nagayama T, Graham SH, Yin X, Simon RP and Chen J. (2001) Caspase-activated DNase/DNA fragmentation factor 40 mediates apoptotic DNA fragmentation in transient cerebral ischemia and in neuronal cultures. *J. Neurosci.* 21, 4678–4690.

Chung CT, Niemela SL and Miller RH. (1989) One-step preparation of competent *E. coli*: Transformation and storage of bacterial cells in the same solution. *Proc. Natl. Acad. Sci. USA.* 86, 2172-2175.

Chung-Faye GA, **Chen MJ**, **Green NK**, **Burton A**, **Anderson D**, **Mautner V**, **Searle PF and Kerr DJ.** (2001) In vivo gene therapy for colon cancer using adenovirus-mediated, transfer of the fusion gene cytosine deaminase and uracil phosphoribosyl transferase. *Gene Ther.* 8, 1547-1554.

Cohen E, Ophir I, and Shaul YB. (1999) Induced differentiation in HT29, a human colon adenocarcinoma cell line. *J. Cell Sci.* 112, 2657-2666.

Cohen GM. (1997) Caspases: the executioners of apoptosis. *Biochem. J.* 326, 1–16.

Colombo BM, Benedetti S, Ottolenghi S, Mora M, Pollo B, Poli G and Finocchiaro G. (1995) The "bystander effect": association of U-87 cell death with ganciclovir-mediated apoptosis of nearby cells and lack of effect in athymic mice. *Hum. Gene Ther.* 6, 763-772.

Denning C and Pitts JD. (1997) Bystander effects of different enzyme-prodrug systems for cancer gene therapy depend on different pathways for intercellular transfer of toxic metabolites, a factor that will govern clinical choice of appropriate regimes. *Hum. Gene Ther.* 8, 1825-1835.

TH-0560_03610605

Dezawa M, Takano M, Negishi H, Mo X, Oshitari T and Sawada H. (2002) Gene transfer into retinal ganglion cells by in vivo electroporation: a newapproach. *Micron* 33, 1–6.

Dilber MS, Abedi MR, Christensson B, Bjorkstrand B, Kidder GM, Naus CC, Gahrton G and Smith CI. (1997) Gap junctions promote the bystander effect of herpes simplex virus thymidine kinase *in vivo*. *Cancer Res.* 57, 1523-1528.

Dini L. (2005) Apoptosis induction in DU-145 human prostate carcinoma cells. *Tissue Cell* 37, 379–384.

Duyao MP, Kessler DJ, Spicer DB and Sonenshein GE. (1990) Binding of NF-KB-like factors to regulatory sequences of the c-myc gene. *Curr. Top. Microbiol. Immunol.* 166, 211–220.

El-Aneed A. (2004) An overview of current delivery systems in cancer gene therapy. *J. Control. Release* 94, 1-14.

Elion GB. (1980) The chemotherapeutic exploitation of virus-specified enzymes. *Adv.Enzyme Regul.*18, 53-66.

Fang J, Lu J, and Holmgren A. (2005) Thioredoxin reductase is irreversibly modified by curcumin A novel molecular mechanism for its anticancer activity. *J Biol. Chem.* 280, 25284–25290.

Freeman SM, Abboud CN, Whartenby KA, Packman CH, Koeplin DS, Moolten FL and Abraham GN. (1993) The "bystander effect": tumor regression when a fraction of the tumor mass is genetically modified. *Cancer Res.* 53, 5274-5283.

Freytag SO, Khil M, Stricker H, Peabody J, Menon M, DePeralta-Venturina M, Nafziger D, Pegg J, Paielli D, Brown S, Barton K, Lu M, Aguilar-Cordova E and

TH-0560_03610605

Kim JH. (2002) Phase I study of replication-competent adenovirus-mediated double suicide gene therapy for the treatment of locally recurrent prostate cancer. *Cancer Res.* 62, 4968–4976.

Freytag SO, Stricker H, Pegg J, Paielli D, Pradhan DG, Peabody J, DePeralta-Venturina M, Xia X, Brown S, Lu M and Kim JH. (2003) Phase I study of replication-competent adenovirus-mediated double-suicide gene therapy in combination with conventional-dose three-dimensional conformal radiation therapy for the treatment of newly diagnosed, intermediate- to high-risk prostate cancer. *Cancer Res.* 63, 7497–7506.

Gewies A. (2003) ApoReview - Introduction to apoptosis, 1-26.

Ghosh SS, Gopinath P and Ramesh A. (2006) Adenoviral vectors: a promising tool for gene therapy. *Appl. Biochem. Biotechnol.*133, 9-29.

Gopinath P and Ghosh SS. (2007a) Monitoring green fluorescent protein for functional delivery of *E. coli* cytosine deaminase suicide gene and the effect of curcumin *in vitro*. *Gene Ther. Mol. Biol.* 11, 219-228.

Gopinath P and Ghosh SS. (2007b) Apoptotic induction with bifunctional *E. coli* cytosine deaminase-uracil phosphoribosyl transferase mediated suicide gene therapy is synergized by curcumin treatment *in vitro*. *Mol. Biotechnol.* (doi:10.1007/s12033-007-9026-3).

Goto T, Nishi T, Tamura T, Dev SB, Takeshima H, Kochi M, Yoshizato K, Kuratsu J, Sakata T, Hofmann GA and Ushio Y. (2000) Highly efficient electro-gene therapy of solid tumor by using an expression plasmid for the herpes simplex virus thymidine kinase gene. *Proc. Natl. Acad. Sci. USA.* 97, 354–359.

TH-0560_03610605

Greco O, Folkes LK, Wardman P, Tozer GM and Dachs GU. (2000) Development of a novel enzyme/prodrug combination for gene therapy of cancer: horseradish peroxidase/indole- 3-acetic acid. *Cancer Gene Ther.* 7, 1414-1420.

Guffey MB, Parker JN, Luckett Jr WS, Gillespie GY, Meleth S, Whitley RJ and Markert JM. (2007) Engineered herpes simplex virus expressing bacterial cytosine deaminase for experimental therapy of brain tumors. *Cancer Gene Ther.*14, 45-56.

Haas K, Wun-Chey S, Javaherian A, Li Z and Cline HT. (2001) Single-cell electroporation for gene transfer in vivo. *Neuron* 29, 583–591.

Hamstra DA, Rice DJ, Pu A, Oyedijo D, Ross BD and Rehemtulla A. (1999) Combined radiation and enzyme/prodrug treatment for head and neck cancer in an orthotopic animal model. *Radiat Res.* 152, 499-507.

He S, Yao J, Jiang P, Shi D, Zhang H, Xie S, Pang S and Gao H. (2001) Formation of silver nanoparticles and self-assembled two-dimensional ordered superlattice. *Langmuir* 17, 1571-1575.

Hoganson DK, Batra RK, Olsen JC and Boucher RC. (1996) Comparison of the effects of three different toxin genes and their levels of expression on cell growth and bystander effect in lung adenocarcinoma. *Cancer Res.* 56, 1315-1323.

Hojman P, Gissel H and Gehl J. (2007) Sensitive and precise regulation of haemoglobin after gene transfer of erythropoietin to muscle tissue using electroporation. *Gene Ther.* 14, 950–959.

Holder JW, Elmore E and Barrett JC. (1993) Gap junction function and cancer. *Cancer Res.* 53, 3475-3485.

TH-0560_03610605

Hotz-Wagenblatt A and Shalloway D. (1993) Gap junctional communication and neoplastic transformation. *Crit. Rev. Oncog.* 4, 541-558.

Huang S, Tang M, Hsu K, Cheng Y and Chou C. (2002) Fas and its ligand, caspases, and Bcl-2 expression in gonadotropin-releasing hormone agonist-treated uterine leiomyoma. *J. Clin. Endocr. Metab.* 87, 4580–4586.

Hussain SM, Hess KL, Gearhart JM, Geiss KT and Schlager JJ. (2005) *In vitro* toxicity of nanoparticles in BRL 3A rat liver cells. *Toxicol. In Vitro.* 7, 975-983.

Ishihara Y and Shimamoto N. (2006) Involvement of endonuclease G in nucleosomal DNA fragmentation under sustained endogenous oxidative stress. *J. Biol. Chem.* 281, 6726–6733.

Jiang MC, Yang-Yen HF, Yen JJ and Lin JK. (1996) Curcumin induces apoptosis in immortalized NIH 3T3 and malignant cancer cell lines. *Nutr. Cancer* 26, 111-120.

Kaliberov SA, Chiz S, Kaliberova LN, Krendelchtchikova V, Manna DD, Zhou T and Buchsbaum DJ. (2006) Combination of cytosine deaminase suicide gene expression with DR5 antibody treatment increases cancer cell cytotoxicity. *Cancer Gene Ther.* 13, 203–214.

Kambara H, **Tamiya T**, **Ono Y**, **Ohtsuka S**, **Terada K**, **Adachi Y**, **Ichikawa T**, **Hamada H and Ohmoto T.** (2002) Combined radiation and gene therapy for brain tumors with adenovirus-mediated transfer of cytosine deaminase and uracil phosphoribosyl transferase genes. *Cancer Gene Ther.* 10, 840-845.

Kanai F, Lan K, Shiratori Y, Tanaka T, Ohashi M, Okudaira T, Yoshida Y, Wakimoto H, Hamada H, Nakabayashi H, Tamaoki T and Omata M. (1997) *In Vivo* gene therapy for α-fetoprotein-producing hepatocellular carcinoma by adenovirus-mediated transfer of cytosine deaminase gene. *Cancer Res.* 57, 461-465.

TH-0560_03610605

Kanai F, Kawakami T, Hamada H, Sadata A, Yoshida Y, Tanaka T, Ohashi M, Tateishi K, Shiratori Y and Omata M. (1998) Adenovirus-mediated transduction of Escherichia coli uracil phosphoribosyl transferase gene sensitizes cancer cells to low concentrations of 5-fluorouracil.*Cancer Res.* 58, 1946-1951.

Kanduc D, Mittelman A, Serpico R, Sinigaglia E, Sinha AA, Natale C, Santacroce R, Di Corcia MG, Lucchese A, Dini L, Pani P, Santacroce S, Simone S, Bucci R and Farber E. (2002) Cell death: apoptosis versus necrosis. *Int. J. Oncol.* 21, 165-170.

Khatri A, Zhang B, Doherty E, Chapman J, Ow K, Pwint H, Wilks RM and Russell PJ. (2006) Combination of cytosine deaminase with uracil phosphoribosyl transferase leads to local and distant bystander effects against RM1 prostate cancer in mice. *J. Gene Med.* 8, 1086–1096.

Kievit E, Nyati MK, Ng E, Stegman LD, Parsels J, Ross BD, Rehemtulla A and Lawrence TS. (2000) Yeast cytosine deaminase improves radiosensitization and bystander effect by 5-fluorocytosine of human colorectal cancer xenografts. *Cancer Res.* 60, 6649-6655.

Kim JA, Cho K, Shin YS, Jung N, Chung C and Chang JK. (2007) A multi-channel electroporation microchip for gene transfection in mammalian cells. *Biosens. Bioelectron.* 22, 3273–3277.

Kolber MA, Quinones RR, Gress RF and Henkart PA. (1988) Measurement of cytotoxicity by target cell release and retention of the fluorescent dye bis-carboxyethyl-carboxyfluorescein (BCECF). *J. Immunol. Methods* 108, 255-264.

Koyama F, Sawada H, Fuji H, Hamada H, Hirao T, Ueno M and Nakano H. (2000a) Adenoviral-mediated transfer of Escherichia coli uracil phosphoribosyl transferase

TH-0560_03610605

(UPRT) gene to modulate the sensitivity of the human colon cancer cells to 5-fluorouracil. *Eur. J. Cancer.* 36, 2403-2410.

Koyama F, Sawada H, Hirao T, Fujii H, Hamada H and Nakano H. (2000b) Combined suicide gene therapy for human colon cancer cells using adenovirus-mediated transfer of *Escherichia coli* cytosine deaminase gene and *Escherichia coli* uracil phosphoribosyl transferase gene with 5-fluorocytosine. *Cancer Gene Ther.* 7, 1015-1022.

Kurozumi K, Tamiya T, Ono Y, Otsuka S, Kambara H, Adachi Y, Ichikawa T, Hamada H and Ohmoto T. (2004) Apoptosis induction with 5-fluorocytosine /cytosine deaminase gene therapy for human malignant glioma cells mediated by adenovirus. *J. Neuro-Oncol.* 66, 117–127.

Kusunoki N, Yamazaki R, Kitasato H, Beppu M, Aoki H and Kawai S. (2004) Triptolide, an active compound identified in a traditional Chinese herb, induces apoptosis of rheumatoid synovial fibroblasts. *BMC Pharmacol.* 4, 2.

Lawrence TS, Davis MA and Maybaum J. (1994) Dependence of 5-fluorouracil mediated radiosensitization on DNA-directed effects. *Int. J. Radiat. Oncol. Biol. Phys.* 29, 519-523.

Lawrence TS, Rehemtulla A, Ng EY, Wilson M, Trosko JE and Stetson PL. (1998) Preferential cytotoxicity of cells transduced with cytosine deaminase compared to bystander cells after treatment with 5-flucytosine. *Cancer Res.* 58, 2588-2593.

Le Grimellec C, Lesniewska E, Cachia C, Schreiber JP, de Fornel F and Goudonnet JP. (1994) Imaging of the membrane surface of MDCK cells by atomic force microscopy. *Biophys. J.* 67, 36–41.

TH-0560_03610605

Lee KC, Hamstra DA, Bullarayasamudram S, Bhojani MS, Moffat BA, Dornfeld KJ, Ross BD and Rehemtulla A. (2006) Fusion of the HSV-1 tegument protein vp22 to cytosine deaminase confers enhanced bystander effect and increased therapeutic benefit. *Gene Ther.* 13, 127–137.

Li X, Zhang J, Xu W, Jia H, Wang X, Yang B, Zhao B, Li B and Ozaki Y. (2003) Mercaptoacetic acid-capped silver nanoparticles colloid: formation, morphology, and SERS activity. *Langmuir* 19, 4285-4290.

Li P, Li J, Wu C, Wu Q and Li J. (2005) Synergistic antibacterial effects of β-lactam antibiotic combined with silver nanoparticles. *Nanotechnology* 16, 1912-1917.

Liu J, Zou W, Lang M, Luo J, Sun L, Wang X, Qian Q and Liu X. (2002) Cancer-specific killing by the CD suicide gene using the human telomerase reverse transcriptase promoter. *Int. J. Oncol.* 21, 661-666.

Longley DB, Harkin DP and Johnston PG. (2003) 5-fluorouracil: mechanisms of action and clinical strategies. *Nat. Rev.Cancer* 3, 330-338.

Marais R, Spooner RA, Light Y, Martin J and Springer CJ. (1996) Gene-directed enzyme prodrug therapy with a mustard prodrug/carboxypeptidase G2 combination. *Cancer Res.* 56, 4735–4742.

Matono S, Tanaka T, Sueyoshi S, Yamana H, Fujita H and Shirouzu K. (2003) Bystander effect in suicide gene therapy is directly proportional to the degree of gap junctional intercellular communication in esophageal cancer. *Int. J. Oncol.* 23, 1309-1315.

Merino R, Grillot DA, Simonian PL, Muthukkumar S, Fanslow WC, Bondada S and Nunez G. (1995) Modulation of anti-IgM-induced B cell apoptosis by Bcl-xL and

TH-0560_03610605

CD40 in WEHI-231 cells. Dissociation from cell cycle arrest and dependence on the avidity of the antibody-IgM receptor interaction. *J. Immunol.* 155, 3830–3838.

Mesnil M, Piccoli C, Tiraby G, Willecke K and Yamasaki H. (1996) Bystander killing of cancer cells by herpes simplex virus thymidine kinase gene is mediated by connexins. *Proc. Natl. Acad. Sci. USA.* 93, 1831-1835.

Mir LM. (2001) Therapeutic perspectives of in vivo cell electropermeabilization. *Bioelectrochemistry* 53, 1–10.

Miyagi T, Koshida K, Hori O, Konaka H, Katoh H, Kitagawa Y, Mizokami A, Egawa M, Ogawa S, Hamada H and Namiki M. (2003) Gene therapy for prostate cancer using the cytosine deaminase/uracil phosphoribosyl transferase suicide system. *J.Gene Med.* 5, 30–37.

Moolten FL. (1986) Tumor chemosensitivity conferred by inserted herpes thymidine kinase genes: paradigm for a prospective cancer control strategy. *Cancer Res.* 46, 5276-5281.

Nakamura N and Wada Y. (2000) Properties of DNA fragmentation activity generated by ATP depletion. *Cell Death and Diff.* 7, 477- 484.

Nishihara E, Nagayama Y, Narimatsu M, Namba H, Watanabe M, Niwa M and Yamashita S. (1998) Treatment of thyroid carcinoma cells with four different suicide gene/prodrug combinations *in vitro*. *Anticancer Res.*18, 1521-1525.

Okada H and Mak TW. (2004) Pathways of apoptotic and non-apoptotic death in tumour cells. *Nat. Rev. Cancer* 4, 592-603.

Oonuma M, Sunamura M, Motoi F, Fukuyama S, Shimamura H, Yamauchi J, Shibuya K, Egawa S, Hamada H, Takeda K, and Matsuno S. (2002) Gene therapy

TH-0560_03610605

for intraperitoneally disseminated pancreatic cancers by Escherichia coli uracil phosphoribosyl transferase (UPRT) gene mediated by restricted replication-competent adenoviral vectors. *Int. J. Cancer* 102, 51-59.

Orlowski S, Belehradek Jr J, Paoletti C and Mir LM. (1988) Transient electropermeabilisation of cells in culture increase of the cytotoxicity of anticancer drugs. *Biochem. Pharmacol.* 37, 4727–4733.

Pan J, Xu G and Yeung SJ. (2001) Cytochrome C release is upstream to activation of Caspase-9, Caspase-8, and Caspase-3 in the enhanced apoptosis of anaplastic thyroid cancer cells induced by manumycin and paclitaxel. *J. Clin. Endocr. Metab.* 86, 4731–4740.

Pandey S, Smith B, Walker PR, Sikorska M. (2000) Caspase dependent and independent cell death in rat hepatoma 5123tc cells. *Apoptosis* 5, 265–275.

Park HJ, Kim YJ, Leem K, Park SJ, Seo JC, Kim HK and Chung JH. (2005) *Coptis japonica* root extract induces apoptosis through caspase3 activation in SNU- 68 human gastric cancer cells. *Phytother. Res.* 19, 189–192.

Parpura V and Fernandez JM. (1996) Atomic force microscopy study of the secretory granule lumen. *Biophys. J.* 71, 2356–2366.

Pasanen T, Hakkarainen T, Timonen P, Parkkinen J, Tenhunena, Loimas S and Wahlfors J. (2003) TK-GFP fusion gene virus vectors as tools for studying the features of HSV-TK/ganciclovir cancer gene therapy *in vivo. Int. J. Mol. Med.* 12, 525-531.

Pillai GR, Srivastava AS, Hassanein TI, Chauhan DP and Carrier E. (2004) Induction of apoptosis in human lung cancer cells by curcumin. *Cancer Lett.* 208, 163–170.

TH-0560_03610605

Porosnicu M, Mian A and Barber GN. (2003) The oncolytic effect of recombinant vesicular stomatitis virus is enhanced by expression of the fusion cytosine deaminase/uracil phosphoribosyl transferase suicide gene. *Cancer Res.* 63, 8366-8376.

Prechtel AT, Turza NM, Theodoridis AA, Kummer M and Steinkasserer A. (2006) Small interfering RNA (siRNA) delivery into monocyte-derived dendritic cells by electroporation. *J. Immunol. Methods* 311, 139–152.

Rathenberg J, Nevian T and Witzemann V. (2003) High-efficiency transfection of individual neurons using modified electrophysiology techniques. *J. Neurosci. Methods* 126, 91–98.

Reed JC. (2002) Apoptosis-based therapies. *Nat. Rev. Drug Discov.*1, 111-121.

Rhodes JD, Monckton DG, McAbney JP, Prescott AR and Duncan G. (2006) Increased SK3 expression in DM1 lens cells leads to impaired growth through a greater calcium-induced fragility. *Hum. Mol. Genet.* 15, 3559-3568.

Ribble D, Goldstein NB, Norris DA and Shellman YG. (2005) A simple technique for quantifying apoptosis in 96-well plates. *BMC Biotechnol.* 5, 12.

Richards HA, Halfhill MD, Millwood RJ and Stewart CN. (2003) Quantitative GFP fluorescence as an indicator of recombinant protein synthesis in transgenic plants. *Plant Cell Rep.* 22, 117–121.

Rols MP, Delteil C, Golzio M, Dumond P, Cros S and Teissie J (1998) *In vivo* electrically mediated protein and gene transfer in murine melanoma. *Nat. Biotechnol.* 16, 168–171.

TH-0560_03610605

Rowley S, Lindauer M, Gebert JF, Haberkorn U, Oberdorfer F, Moebius U, Herfarth C and Schackert H. (1996) Cytosine deaminase gene as a potential tool for the genetic therapy of colorectal cancer. *J. Surg. Oncol.* 61, 42-48.

Sambrook J and Russell DW. (2001) Molecular Cloning-A Laboratory Manual, 3rd ed. *Cold Spring Harbor Press: New York* 1, 1.31-1.34.

Scheerlinck JY, Karlis J, Tjelle TE, Presidente PJA, Mathiesen I and Newton SE. (2004) In vivo electroporation improves immune responses to DNA vaccination in sheep. *Vaccine* 22, 1820–1825.

Seo E, Abei M, Wakayama M, Fukuda K, Ugai H, Murata T, Todoroki T, Matsuzaki Y, Tanaka N, Hamada H and Yokoyama KK. (2005) Effective gene therapy of biliary tract cancers by a conditionally replicative adenovirus expressing uracil phosphoribosyl transferase: significance of timing of 5-fluorouracil administration. *Cancer Res.* 65, 546-552.

Somiari S, Glasspool-Malone J, Drabick JJ, Gilbert RA, Heller R, Jaroszeski MJ and Malone RW. (2000) Theory and *in vivo* application of electroporative gene delivery. *Mol. Ther.* 2, 178-187.

Sondi I and Salopek-Sondi B. (2004) Silver nanoparticles as antimicrobial agent: a case study on E. coli as a model for Gram-negative bacteria. *J. Colloid Interface Sci.* 275, 177-182.

Springer CJ and Duvaz IN. (2000) Prodrug-activating systems in suicide gene therapy. *J. Clin. Invest.* 105, 1161-1167.

Stackhouse MA, Pederson LC, Grizzle WE, Curiel DT, Gebert J, Haack K, Vickers SM, Mayo MS and Buchsbaum DJ. (2000) Fractionated radiation therapy in combination with adenoviral delivery of the cytosine deaminase gene and 5-

TH-0560_03610605

fluorocytosine enhances cytotoxic and antitumor effects in human colorectal and cholangio carcinoma models. *Gene Ther.* 7, 1019-1026.

Stegman LD, Rehemtulla A, Beattie B, Kievit E, Lawrence TS, Blasberg RG, Tjuvajev JG, and Ross BD. (1999) Noninvasive quantitation of cytosine deaminase transgene expression in human tumor xenografts with *in vivo* magnetic resonance spectroscopy. *Proc. Natl. Acad. Sci. USA.* 96, 9821–9826.

Stribbling SM, Friedlos F, Martin J, Davies L, Spooner RA, Marais R and Springer CJ. (2000) Regressions of established breast carcinoma xenografts by carboxypeptidase G2 suicide gene therapy and the prodrug CMDA are due to a bystander effect. *Hum. Gene Ther.* 11, 285-292.

Sun XM, MacFarlane M, Zhuang J, Wolf BB, Green DR and Cohen GM. (1999) Distinct caspase cascades are initiated in receptor-mediated and chemical-induced apoptosis. *J. Biol.Chem.* 274, 5053–5060.

Susin SA, Lorenzo HK, Zamzami N, Marzo I, Brenner C, Larochette N, Prévost M, Alzari PM and Kroemer G. (1999) Mitochondrial release of caspase-2 and -9 during the apoptotic process. *J. Exp. Med.* 189, 381–394.

Todorova VK, Harms SA, Kaufmann Y, Luo S, Luo KQ, Babb K and Klimberg VS. (2004) Effect of dietary glutamine on tumor glutathione levels and apoptosis-related proteins in DMBA-induced breast cancer of rats. *Breast Cancer Res. Tr.* 88, 247–256.

Tomicic MT, Thust R and Kaina B. (2002) Ganciclovir-induced apoptosis in HSV-1 thymidine kinase expressing cells: critical role of DNA breaks, Bcl-2 decline and caspase-9 activation. *Oncogene* 21, 2141-2153.

Touraine RL, Vahanian N, Ramsey WJ and Blaese RM. (1998) Enhancement of the herpes simplex virus thymidine kinase/ganciclovir bystander effect and its antitumor

TH-0560_03610605

efficacy *in vivo* by pharmacologic manipulation of gap junctions. *Hum. Gene Ther.* 9, 2385-2391.

Trinh QT, Austin EA, Murray DM, Knick VC and Huber BE. (1995) Enzyme/prodrug gene therapy: comparison of cytosine deaminase/5-fluorocytosine versus thymidine kinase/ganciclovir enzyme/prodrug systems in a human colorectal carcinoma cell line. *Cancer Res.* 55, 4808-4812.

Tsangaris GT and Tzortzatou-Stathopoulou F. (1996) Development of a quantitative method for the study of apoptosis in peripheral blood. *In Vivo* 10, 435-443.

Ueda K, Iwahashi M, Nakamori M, Nakamura M, Matsuura I, Yamaue H and Tanimura H. (2001) Carcinoembryonic antigen-specific suicide gene therapy of cytosine deaminase/5- fluorocytosine enhanced by the Cre/loxP system in the orthotopic gastric carcinoma model. *Cancer Res.* 61, 6158–6162.

Uno-Furuta S, Tamaki S, Takebe Y, Takamura S, Kamei A, Kim G, Kuromatsu I, Kaito M, Adachi Y and Yasutomi Y. (2001) Induction of virus-specific cytotoxic T lymphocytes by in vivo electric administration of peptides. *Vaccine* 19, 2190–2196.

Vanbever R, LeBoulenge E and Preat V. (1996) Transdermal delivery of fentanyl by electroporation: I. Influence of electrical factors. *Pharm. Res.* 13, 559– 565.

Verma IM and Somia N. (1997) Gene therapy-promises, problems and prospects. *Nature* 389, 239–242.

Vooijs M, Jonkers J, Lyons S and Berns A. (2002) Noninvasive imaging of spontaneous retinoblastoma pathway-dependent tumors in mice. *Cancer Res.* 62, 1862–1867.

TH-0560_03610605

Wang J, Lu X, Chen D, Li S and Zhang L. (2004) Herpes simplex virus thymidine kinase and ganciclovir suicide gene therapy for human pancreatic cancer. *World J. Gastroenterol.*10, 400-403.

Waxman DJ and Schwartz PS. (2003) Harnessing apoptosis for improved anticancer gene therapy. *Cancer Res.* 63, 8563-8572.

Wolf BB, Schuler M, Echeverri F and Green DR. (1999) Caspase-3 is the primary activator of apoptotic DNA fragmentation via DNA fragmentation factor-45/inhibitor of caspase-activated DNase inactivation. *J. Biol. Chem.* 274, 30651-30656.

Wybranietz WA, Groβ CD, Phelan A, O'Hare P, Spiegel M, Graepler F, Bitzer M, Stahler P, Gregor M and Lauer UM. (2001) Enhanced suicide gene effect by adenoviral transduction of a VP22-cytosine deaminase (CD) fusion gene. *Gene Ther.* 8, 1654–1664.

Xia K, Liang D, Tang A, Feng Y, Zhang J, Pan Q, Long Z, Dai H, Cai F, Wu L, Zhao S, Chen Z and Xia J. (2004) A novel fusion suicide gene yeast CDglyTK plays a role in radio-gene therapy of nasopharyngeal carcinoma. *Cancer Gene Ther.* 11, 790–796.

Yang M, Baranov E, Moossa AR, Penman S and Hoffman RM. (2000) Visualizing gene expression by whole-body fluorescence imaging. *Proc. Natl. Acad. Sci. USA.* 97, 12278–12282.

Yazawa K, Fisher WE and Brunicardi FC. (2002) Current progress in suicide gene therapy for cancer. *World J. Surg.* 26, 783-789.

Ye H, Gan L, Yang X and Xu H. (2006) Membrane-associated cytotoxicity induced by realgar in promyelocytic leukemia HL-60 cells. *J. Ethnopharmacol.* 103, 366–371.

TH-0560_03610605

LIST OF PUBLICATIONS

I. In Refereed Journals

1. **Gopinath P, Gogoi SK, Chattopadhyay A and Ghosh SS.** (2008) Implications of silver nanoparticle induced cell apoptosis for *in vitro* gene therapy. *Nanotechnology* (doi:10.1088/0957-4484/19/7/075104).

2. **Gopinath P and Ghosh SS.** (2008) Implication of functional activity for determining therapeutic efficacy of suicide genes *in vitro*. *Biotechnol. Lett.* (doi: 10.1007/s10529-008-9787-1).

3. **Gopinath P and Ghosh SS.** (2007) Apoptotic induction with bifunctional *E.coli* cytosine deaminase-uracil phosphoribosyl transferase mediated suicide gene therapy is synergized by curcumin treatment *in vitro*. *Mol. Biotechnol.* (doi:10.1007/s12033-007-9026-3).

TH-0560_03610605

4. **Gopinath P and Ghosh SS.** (2007) Monitoring green fluorescent protein for functional delivery of *E. coli* cytosine deaminase suicide gene and the effect of curcumin *in vitro. Gene Ther. Mol. Biol.* 11B, 219-228.

5. **Gogoi SK, Gopinath P, Paul A, Ramesh A, Ghosh SS and Chattopadhyay A.** (2006) Green fluorescent protein expressing *Escherichia coli* as a model system for investigating the antimicrobial activities of silver nanoparticles. *Langmuir* 22, 9322-9328.

6. **Ghosh SS, Gopinath P and Ramesh A.** (2006) Adenoviral vectors: a promising tool for gene therapy. *Appl. Biochem. Biotechnol.*133, 9-29.

7. **Gopinath P and Ghosh SS.** Understanding apoptotic signaling pathways in cytosine deaminase-uracil phosphoribosyl transferase mediated suicide gene therapy *in vitro*, (Under review 2008).

II. In Conferences

8. **Gopinath P and Ghosh SS.** "A comparative study of 5-flurocytosine/ cytosine deaminase and bifunctional cytosine deaminase-uracil phosphoribosyl transferase suicide gene therapy system in presence of curcumin", presented in the international conference on new horizons in biotechnology (NHBT-2007), Trivandrum, India. November 2007.

9. **Gopinath P and Ghosh SS.** "Cytosine deaminase as a prodrug/suicidal gene therapy system", presented in the 26th annual convention of Indian association for cancer research and international symposium on translational research in cancer (IACR 2007), Bhubaneswar, India, January 2007.

TH-0560_03610605